

**Molecular characterization and**  
**cytotoxicity of the outer**  
**capsid protein VP5 of**  
**African horsesickness virus**

By

IDA SOFIA WALL

A DISSERTATION SUBMITTED IN PARTIAL FULFILLMENT OF THE  
REQUIREMENTS FOR THE DEGREE

**MAGISTER SCIENTIAE**

Department of Genetics  
In the Faculty of Natural and Agricultural Sciences  
University of Pretoria  
Pretoria  
April 2006



***I can do all things through  
Christ who strengthens me.***

Philippians 4v13.

## Acknowledgements

I would like to express my heartfelt thanks and great appreciation to:

Dr Wilma Fick for all your support and exceptional guidance throughout this study

Prof. Henk Huismans for your excellent insight and inspiration

My research colleagues at the University of Pretoria, especially to:

Ms. Daria Rutkowska, I am eternally grateful for all your advice, exceptional help and friendship

Ms. Heidi Kretzmann, for all your patience and willingness to help and

Ms. Jeanne Korsman for your willingness to help in every situation.

My family, especially to:

My husband Ronald, your faith in me made it worth it.

My father Roberto, I know you are proud of me.

My aunt Erna, for your interest and uncompromising help through all my years of study.

My grandmother Cora, for all your love and continuous support.

My mother Vivienne, I know that you are smiling down on me.

To Angie and Adel, your prayers for me were heard.

The University of Pretoria and the National Research Foundation for their generous MSc bursaries.

## **Summary:**

### **The molecular characterization and cytotoxicity of outer capsid protein VP5 of African horsesickness virus.**

By

**Ida Sofia Wall**

Promoters: Doctor Wilma Fick and Professor Henk Huisman  
Department of Genetics  
University of Pretoria

#### **For the degree MSc**

African horsesickness virus (AHSV), a member of the *Orbivirus* genus in the family *Reoviridae*, is the aetiological agent of an economically important disease affecting equids. One of the outer coat proteins of the virus, VP5, has the important function of interacting with the conserved core proteins as well as adapting to facilitate changes in the major outer coat protein, VP2. VP5 plays a role in destabilizing the endosomal membrane following viral attachment to the host cell, thereby allowing access of the viral core into the host cytoplasm. Furthermore, VP5 contributes to the immune response in infected animals and has relevance to recombinant vaccine development.

The main aim of this study was to compare the genetic variation between VP5 proteins of field isolates of AHSV, isolated from dead animals, to that of laboratory strains, likely to be avirulent. This comparison was done in order to determine if any significant/common amino acid changes could be linked to the virulence phenotype. The VP5 genes of six AHSV isolates of serotypes 3, 6, 8 and 9 respectively were cloned, sequenced and the amino acid sequences deduced. This study represents the first report on the sequencing analysis of the VP5 gene and protein of an AHSV serotype 8. All sequences were aligned

and compared to those of published laboratory/vaccine strains, and other available sequence data.

Interserotype amino acid identities of between 95% and 99% were observed between isolates of serotypes 3, 6 and 9 (apart from a laboratory strain of AHSV9), indicating significant conservation between these serotypes. The VP5 protein of AHSV8 showed less homology and differed from the other serotypes by between 5.2 and 7%. The AHSV4 protein differed significantly from the rest, showing between 15 and 19% amino acid differences. The identity between the VP5 proteins of different isolates/strains of the same serotype was very high in most instances, at approximately 97% for different AHSV3 strains and 94 % for different AHSV6 strains. The VP5 protein of a laboratory adapted strain of AHSV9, however, differed from an AHSV9 field isolate by nearly 10%. In the analyses of these amino acid differences, no common amino acid change, indicative of a virulence marker, could be identified between the assumedly virulent field isolates and their respective laboratory adapted strains. Furthermore, no distinctive differences in regions supposedly involved in membrane destabilization, or particular patterns of variation were observed. The results indicate that virulence of a particular AHSV serotype is unlikely to be influenced by a common amino acid change in VP5, and more likely to be multi-faceted.

The second aim of this study was to investigate whether VP5 has a cytotoxic effect when expressed in a bacterial system, in light of similar effects reported for the analogous protein of bluetonguevirus (BTV), a related orbivirus. Computer analyses were performed and indicated that amphipatic helices found in the N-terminus of BTV VP5, proposed to be responsible for cytotoxicity, were also present in AHSV VP5. A full-length copy of the AHSV4 VP5 gene was cloned into the pET41 transfer plasmid and expression induced in bacterial cells. Optical density measurements of the bacterial cultures, indicative of cell growth, were taken at time intervals post induction. The expression of AHSV VP5 clearly had a severe negative effect on cell density (hence growth) over time, in contrast to a control where the cell density continued to increase. The results

therefore clearly indicated that expression of AHSV VP5 was cytotoxic to bacterial cells.

Lastly, a neutralizing epitope present on VP5 was expressed on the surface of a particulate display system, based on crystalline particles formed when the VP7 protein of AHSV9 is expressed in insect cells. Expression of the VP7/epitope A chimeric protein was confirmed by polyacrylamide gel electrophoresis and partially purified by sucrose gradient separation. Hexagonal crystals with a unique surface structure, but morphologically quite similar to VP7 crystals, were observed by scanning electron microscopy. The VP7 display vector could therefore tolerate insertion of the epitope without losing its ability to form crystals. The chimeric particles are now available for further evaluation as to its immunological properties. The results of this study should contribute to the development of a possible vaccine strategy against AHS in future.

## Abbreviations

AcNPV	<i>Autographa californica</i> nuclear polyhedrosis virus
AHS	African horsesickness
AHSV	African horsesickness virus
AHSV-3	African horsesickness virus serotype 3
Amp	ampicillin
AP	ammonium persulphate
$\alpha$ -helix	alpha helix
B-cells	lymphocytes that develop in the bone marrow and produce antibodies
BHK	baby hamster kidney
bp	base pairs
BSA	bovine serum albumin
BTV	bluetongue virus
$\beta$ -gal	beta-galactosidase
$\beta$ -ME	beta-mercaptoethanol
$\beta$ -sheets	beta sheets
CaCl <sub>2</sub>	calcium chloride
°C	degrees Celsius
CCD	charge coupled device
Ci	Curie
cDNA	complementary deoxyribonucleic acid
CLPs	core-like particles
cRNA	complementary ribonucleic acid
DMEM	Dulbeco's Modified Eagles Medium
DNA	deoxyribonucleic acid
dNTPs	2'-deoxy-nucleotide-5'-triphosphate
ds	double stranded
dsDNA	double stranded deoxyribonucleic acid
DTT	1,4-dithiothreitol

<i>E.coli</i>	<i>Escherichia coli</i>
EDTA	ethylenediaminetetra-acetic acid
<i>et al.</i>	<i>et alia</i> (and others)
EtBr	ethidium bromide
EHDV	epizootic hemorrhagic disease virus
FCS	fetal calf serum
HCA	hydrophobic cluster analysis
HCL	hydrochloric acid
hr	hour
IPTG	isopropyl- $\beta$ -D-thiogalactopyranoside
kb	kilobase pairs
kDA	kiloDalton
KOAc	potassium acetate
LB broth	Luria-Bertani broth
M	molar
MAb	m monoclonal antibodies
MCS	multiple cloning site
Mg	magnesium
MgCl <sub>2</sub>	magnesium chloride
mg	milligram
min	minute
ml	milliliter
mM	millimolar
MMOH	methyl-mercury hydroxide
M.O.I	multiplicity of infection
M <sub>r</sub>	molecular weight
mRNA	messenger ribonucleic acid
m/v	mass per volume
NaOAc	sodium acetate
NaCl	sodium chloride
n	nano
ng	nanogram
nm	nanometer



NS	non-structural
OD	optical density
O/N	overnight
ORF	open reading frame
PAGE	polyacrylamide gel electrophoresis
PBS	phosphate buffered saline
PCR	polymerase chain reaction
pH	measure of a solution's acid strength
pmol	picomol
PSB	protein solvent buffer
r.e.	restriction endonuclease
RNA	ribonucleic acid
r.p.m.	revolutions per minute
RT	room temperature
SEM	scanning electron microscope
SDS	sodium dodecyl sulphate
SDS-PAGE	sodium dodecyl sulphate polyacrylamide gel electrophoresis
s	second
Sf9	<i>Spodoptera frugiperda</i>
TAE	tris acetate EDTA
<i>Taq</i>	<i>Thermus aquaticus</i>
TCA	Trichloroacetic acid.
T-cells	lymphocytes that develop in the thymus and are involved in cell-mediated immunity
TE buffer	Tris hydrochloric acid and ethylenediaminetetra-acetic acid buffer
TEMED	N, N, N', N'- tetramethylethylenediamine
Tet	tetracycline hydrochloride
TGS	tris glycine sodium dodecyl sulphate buffer
Tm	melting temperature
Tris	tris-(hydroxymethyl)-aminomethane
U	units
μ	micro



$\mu\text{g}$	microgram
$\mu\text{l}$	microliter
UV	ultraviolet
V	volts
VIBs	viral inclusion bodies
VP	viral protein
VTs	viral tubules
v/v	volume per volume
wt	wild type
w/v	weight per volume
X-gal	5-bromo-4-chloro-3-indoyl- $\beta$ -D-galactopyranoside

## Table of contents

TITLE	PAGE
ACKNOWLEDGEMENTS	iii
SUMMARY	iv
ABBREVIATIONS	vii
TABLE OF CONTENTS	xi

<b>CHAPTER 1: Literature review</b>		1
1.1	Introduction	2
1.2	African horsesickness: The disease	2
1.2.1	Current vaccines	4
1.3	African Horsesickness Virus: The aetiological agent of disease	5
1.3.1	Classification	5
1.3.2	Orbivirus replication	7
1.3.3	Viral structure	9
1.3.4	Genome Segments	10
1.3.5	The protein products of AHSV	12
1.4	Vaccine development	21
1.4.1	An Overview	21
1.4.2	Vaccine Development using AHSV proteins	23
1.5	AHSV Proteins involved in virulence	25
1.5.1	Outer Capsid Protein VP5	26
1.6	Aims	29

<b>CHAPTER 2: Comparative analysis of the VP5 protein of various virulent and avirulent AHSV serotypes</b>		30
2.1	Introduction	31
2.2	Materials and Methods	36
2.2.1	Preparation of competent cells using Calcium chloride	36
2.2.2	Transformation of competent cells	37
2.2.3	Purification of plasmid DNA	38
2.2.4	Agarose gel electrophoresis	38



2.2.5	The polymerase chain reaction (PCR)	39
2.2.6	Restriction enzyme digestions	41
2.2.7	Dephosphorylation	41
2.2.8	Ligation	42
2.2.9	The bacterial pET expression system	42
2.2.10	Protein electrophoresis and Coomassie blue staining	44
2.2.11	<sup>35</sup> S -methionine labeling of expressed proteins	45
2.2.12	TCA precipitation of proteins	46
2.2.13	Preparation cDNA from dsRNA	47
2.2.14	Cloning of target genes	48
2.2.15	DNA sequencing	49
2.3	Results	52
2.3.1	Preparation of AHSV VP5 cDNA for cloning	52
2.3.2	Cloning of the purified AHSV VP5 for sequencing	53
2.3.3	Nucleotide sequence analysis	56
2.3.4	Amino acid sequence analysis	64
2.3.5	Cloning of AHSV4 VP5 into the pET expression vector	88
2.3.6	Transforming of the pET/VP5 clone into an expression host	92
2.3.7	Induction of VP5 expression	92
2.4	Discussion	97

<b>Chapter 3: The construction and expression of AHSV VP5 epitopes in a VP7 expression vector.</b>		103
3.1	Introduction	104
3.2	Materials and Methods	109
3.2.1	Amplification of AHSV VP5 epitopes	109
3.2.2	Sequencing of recombinant pFastbac vector	109
3.2.3	Bacmid transposition	110
3.2.4	Isolation of bacmid DNA	110
3.2.5	Transfection of Sf9 cells	111
3.2.6	Propagation of recombinant baculoviruses	112
3.2.7	Sucrose gradient purification by ultracentrifugation	112
3.2.8	SDS-PAGE analysis of expressed proteins	113
3.2.9	Scanning electron microscope (SEM) sample preparation	114
3.3	Results	115



3.3.1	Amplification of the VP5 epitope regions	115
3.3.2	Cloning of the VP5 epitopes into the transfer vector	119
3.3.3	Sequencing of recombinant transfer plamids	120
3.3.4	Transfections of sample and control baculoviruses	127
3.3.5	Sucrose gradient purification of baculovirus expressed proteins	128
3.3.6	Scanning electron microscopy	129
3.3.7	Hydrophilicity analysis	133
3.4	Discussion	135

<b>Chapter 4: Concluding Remarks.</b>	138
<b>References</b>	144



# Chapter 1

## Literature Review

## **1.1 Introduction**

African horsesickness (AHS) is a non-contagious but infectious equine disease that is caused by the African horsesickness virus (AHSV). The disease has an extremely high mortality rate in horses and as a result has serious implications to the horse industry by causing great economic losses and restricting international movement. Current vaccination programs also restrict export of horses, as one cannot discriminate between naturally infected and vaccinated animals. Thus, the development of appropriate vaccines is crucial to prevent this disease from occurring and spreading within the horse population.

The use of DNA recombinant technology may prove advantageous in the search and development of a safe and effective AHS vaccine strategy. Investigating and characterizing various aspects of the actual viral components at a molecular level can result in the identification of appropriate immune targets. In this study, particular focus is placed on AHSV VP5 outer capsid and the role it plays in viral virulence.

## **1.2 African horsesickness: The disease**

The AHS disease occurs widely across sub-Saharan Africa, being endemic from Senegal in the west to Ethiopia and Somalia in the east, extending as far south as South Africa (Mellor and Boorman, 1995). Sporadic cases of AHS have occurred in North America, Southern Europe and in the Middle East (Roy *et al.*, 1994).

Disease symptoms range from subclinical to severe, with mortality rates up to 100%. Morphologically and clinically distinct syndromes associated with AHSV infection was first described by Theiler in 1921 (as cited by Burrage and Laegried, 1994). The different forms of the disease include a pulmonary, cardiac and fever form, as well as a combination of the pulmonary and cardiac forms. Pulmonary AHS is the most severe with a mortality rate of close to 100%. It is characterized with symptoms such as high fever (fever can reach up to 42°C),

mild depression and anorexia in affected horses. These symptoms progress to severe respiratory distress and death. The cardiac form of the disease is subacute with a longer incubation period. Fever (39-41°C) is associated with characteristic edematous swellings of the anterior-dorsal region. The mortality rate of the cardiac form is between 50-70%, with death occurring 4-8 days after the onset of clinical signs. The fever form of AHS is a mild to sub clinical, with a variable incubation period. Signs accompanying a fever of 39-40°C may include mucous membrane congestion, anorexia and depression. All affected horses with the fever form recover.

In the field, the AHSV is transmitted between vertebrate hosts by the bites of the bloodsucking *Culicoides* midge species (Calisher and Mertens, 1998). The distribution of the virus is limited to geographical regions where competent vectors are present (Mellor, 1994). In vertebrate hosts, the virus causes viremia that lasts for a maximum period of 18 days in horses and a maximum of 27 days in zebra. In the absence of a long-term vertebrate reservoir, AHSV can only survive by continuous and uninterrupted cycles of transmission between vertebrate and invertebrate hosts. The climate in sub-Saharan Africa is conducive to continuous vector activity throughout the year and such conditions allow the cycling of virus without interruption (Mellor, 1994).

Considering the damage that can be caused, AHS is designated as a list "A" disease by the Office International des Epizooties. A description of such includes a 'Communicable disease which has the potential for very rapid spread, irrespective of national borders and has serious socio-economic or public health consequences. A disease, which is of major importance in the international trade of livestock or livestock products' (Mellor and Boorman, 1995).



## **1.2.1 Current vaccines**

Since there is no therapy for AHS, vaccination of horses is essential to protect them against the virus and avoid new outbreaks. Current vaccines include attenuated virus vaccines (Martinez-Torrecuadrada, 2001). These vaccines are effective but do not allow for differentiation of naturally infected animals from vaccinated animals. Also, the absence of such a marker vaccine affects international horse-trading. The use of attenuated vaccines could also contribute to the spread of the disease by potential reversion to virulence in vaccinated animals.

A commercial AHS vaccine currently being produced by South Africa is comprised of seven AHSV serotypes, which are attenuated through cell culture passage (Scalen *et al.*, 2002). The seven serotypes included in the vaccine are 1, 2, 3, 4, 6, 7, and 8. Serotype 9 is not included as this serotype rarely occurs in Southern Africa and serotype 6 was found to offer some cross-protection against serotype 9. The attenuated AHSV serotype 5 was discontinued in 1990 as safety problems occurred with this particular strain. The absence of these two serotypes in the AHS vaccine, as well as the general disadvantages of live attenuated vaccines, makes the development of a new recombinant AHS vaccine more credible (Scalen *et al.*, 2002). Thus, the production of a recombinant or subunit vaccine may be more desirable in avoiding most of these concerns (Martinez-Torrecuadrada, 2001).

## **1.3 African horsesickness virus: the aetiological agent of disease**

### **1.3.1 Classification**

Viruses with double stranded RNA genomes occur in all living species and there are basically two distinct virus groups that comprise this featured structure. These two family groups, known as *Reoviridae* and *Birnaviridae*, are recognized by morphological structure and RNA content. *Reoviruses* (derived from the respiratory-enteric orphan virus, which persists in nature by infecting respiratory and enteric epithelia) have unique genomic organizations and replicative properties and occur in mammals, plants, many vertebrates and insects (Levy *et al.*, 1994). All members of the *Reoviridae* family share the same overall pattern of virion organization such as having multi-segmented dsRNA genomes and multiple icosahedral capsids (Urbano and Urbano, 1994; see Table 1.1). *Birnaviridae*, on the other hand, do not occur in mammalian species, but rather in lower species and contain fewer gene segments.

Members of the *Reoviridae* family can be clustered into subgroups/genera on the basis of minor structural differences and major extrinsic properties (Urbano and Urbano, 1994; see Table 1.1). The morphological structures of the various genera played a role in the classification process. For instance, the genus rotaviruses (rota derived from the Latin word for “wheel”) have wheel-like capsids and the genus orbiviruses (derived from the Latin word "orbis", meaning "ring/circle") have ring-shaped capsomeres on the surface of their cores (Levy *et al.*, 1994). There are many differences between the orbiviral members and other *Reoviridae* family members (such as reo- and rota- viruses) despite shared/common morphological and physiological properties. For instance, orbiviruses are vectored to vertebrate hosts by certain arthropods and can replicate in both hosts. Proteins contained in the *Orbivirus* structure are structurally unique when compared to reo- and rota- virus proteins, with no primary sequence similarities (Roy *et al.*, 1996).

**Table 1. 1 Physical and Biological properties of some *Reoviridae* family members (adapted from Levy *et al.*, 1994).**

Genus	Prototype	Diameter of virion nm (S)	Number of gene segments and mass (Da)	Hosts
<i>Orthoreovirus</i>	Reovirus type I	76 (630)	10, 15 x 10 <sup>6</sup>	Vertebrates
<i>Rotavirus</i>	Human rotavirus	70 (525)	11, 12 x 10 <sup>6</sup>	Mammals
<i>Orbivirus</i>	Blue-tongue virus	63 (550)	10, 12 x 10 <sup>6</sup>	Insects, mammals
<i>Phytoreovirus</i>	Rice dwarf virus	70 (510)	12, 17 x 10 <sup>6</sup>	Leafhoppers, grasses
	Wound tumour virus	70 (514)	12, 15 x 10 <sup>6</sup>	Leafhoppers, dicotyledons
<i>Fijivirus</i>	Fiji disease virus	75	10	Sugarcane, insects
<i>Cypovirus</i>	Cytoplasmic polyhedrosis	55 (440)	10, 13 x 10 <sup>6</sup>	Insects

The AHSV serogroup, along with BTV, is classified within the *Orbivirus* genus of *Reoviridae* viruses. General properties of the *Orbivirus* members include: viral particles with diameters of 65-80nm, sensitivity to acidic conditions and high temperatures and a bi-shelled structure with an inner shell composed of 32 capsomers. Orbiviruses have a dsRNA genome comprised of 10 gene segments, each having a single open reading frame, which generally gives rise to a single translation product (Verwoerd *et al.*, 1972). Mature virus particles contain seven structural proteins (designated VP1-VP7) and three non-structural proteins (NS1-NS3). The biological host range of orbiviruses includes both insects and other arthropods. Vertebrate hosts include man, horses, monkeys, rabbits, cattle, deer, and suckling mice, whilst vectors of orbiviruses include culicoides, mosquitoes, phlebotomines and ticks.

The *Orbivirus* genus is comprised of 12 serogroups, which are further subdivided into serotypes based on serological neutralization tests (Gould and Hyatt, 1994). The best-studied serogroup of the *Orbivirus* genus is the prototype Bluetongue virus (BTV) (Roy *et al.*, 1990b). BTV is an economically important pathogen of various domestic ruminants such as sheep, cattle and goats. For almost a century, BTV has been associated with disease and mortality in its vertebrate host species. There are at least 24 different BTV serotypes, having been identified from different parts of the world (Roy *et al.*, 1990a).

The AHSV serogroup of orbiviruses are subdivided into nine virus serotypes. These serotypes have been defined on the basis of serum cross-neutralization

tests, which mainly depend on the specific outer capsid proteins found in the virus coat/capsid (Calisher and Mertens, 1998).

### **1.3.2 Orbivirus replication**

The major events in *Orbivirus* replication are described by Gould and Hyatt (1994), as being i) adsorption and penetration, ii) uncoating and formation of replicative complexes, iii) formation of viral tubules (VTs) and viral inclusion bodies (VIBs) and lastly iv) movement of virus to and release from the cell's surface.

#### **1.3.2.1. Adsorption and penetration:**

The infection cycle of orbiviruses begins with the attachment of virions to host cell surfaces. Attachment proteins (such as the outer capsid proteins) interact with complementary sites (receptors) on the host cell. Binding of the virus to new host receptor sites is facilitated by evolution/alteration of protein domains on the virus coat (Iwata *et al.*, 1992b). Once the virus binds to receptors on the cell surface (adsorption), the virus is subsequently taken up by endocytotic vesicles, which penetrate the cell's plasma membrane (Gould and Hyatt, 1994). There is evidence indicating that the VP2 coat protein is involved in cellular attachment, as the selective removal of the outer capsid layer is associated with a lack of infectivity (Verwoerd *et al.*, 1972). Immunofluorescence assays investigating direct cell binding of VP2 and subsequent internalization of viruses also support the role of VP2 being involved in cell attachment and entry (Hassan and Roy, 1999).

Endocytotic vesicles are transported to a juxta-nuclear position by cytoskeleton components and fuse together to form endosomes. Translocation of the viral core into the cytoplasm after cell entry has been the suggested role for the VP5 coat protein, considering its position in the BTV capsid (Hassan *et al.*, 2001).

#### 1.3.2.2 Uncoating and formation of replicative complexes:

The virus coat is disrupted within the endosomes, as VP2 is removed in acidic conditions. Once the virus is uncoated of one or both outer shell proteins, the core-like particle is released into the cytoplasm as vesicle membranes are destabilized. A matrix comprised of mRNA and translated viral proteins are formed around the core particles. These structures are known as virus inclusion bodies (VIBs) and are characteristic orbiviral structures that are formed from parental viral particles (Gould and Hyatt, 1994).

#### 1.3.2.3. Formation of viral tubules (VTs) and viral inclusion bodies (VIBs):

Viral tubules form part of the 'insoluble' phase of the cell and are composed of the non-structural protein NS1. Although the function of the tubules is still unknown, it is postulated that they associate with the cell's cytoskeleton and prevent mitosis by disrupting the formation of mitotic spindle in orbiviral-infected cells (Gould and Hyatt, 1994).

Viral inclusion bodies (VIBs) are viral factories in which the virions mature. These entities contain single stranded and double stranded RNA binding proteins (VP6 and NS2) (Hyatt *et al.*, 1991) and the three different types of viral particles, namely; subcores, cores and virus-like particles. Structural (VP3, VP5 and VP7) and non-structural (NS1 and NS2 proteins), of which NS2 is the major constituent is also present (Thomas *et al.*, 1990). Within these structures, BTV subcores develop into cores, which then further develop into mature virions with double shells. These virions are subsequently released into the cytoplasm, where they associate with the intermediate filaments of the cells' cytoskeleton. Incomplete development of viruses results in their incorporation into the matrix of the inclusion bodies (Gould *et al.*, 1988).

#### 1.3.2.4. Movement of orbiviruses to and release from the cell surface:

The non-structural NS3/NS3A protein of BTV is responsible for the release of BTV from infected cells (Gould and Hyatt, 1994). NS3/NS3A proteins are associated with the cell membrane and aid to transport BTV across the cytoplasm and out of the cell by budding or extrusion. The interaction of these

NS3/NS3A containing vesicles with the plasma membrane facilitates both these forms of virus release from cells. Upon release of new viral progeny, more cells can subsequently be infected (Gould and Hyatt, 1994).

### **1.3.3 Viral structure**

The morphology of AHSV is essentially identical to that of bluetongue virus (BTV). Three morphologically distinct types of BTV particles can be found within infected cells; namely virions, core and subcore particles (Huisman and Van Dijk, 1990). In virus-infected cells, BTV virions are converted to core particles by the loss of capsid proteins, VP2 and VP5. Later in the infection cycle, core particles are uncoated further to subcore particles, which lack the VP7 protein (Huisman *et al.*, 1987a). Negatively stained core particles exhibit icosahedral symmetry with distinct capsomeric units clustered into distinct penta- and hexameric fashion, whilst the outer shell of the virion has an obscure, non-structured morphology (Roy, 1996).

Subcore particles are mainly unstable and are composed of only 25% of the original protein content of virions. These particles consist of the VP3 core protein and smaller quantities of the minor structural proteins, VP1, VP4 and VP6 (Huisman *et al.*, 1987a). BTV virions are most stable at a high pH of between 8 and 9 and lowering of the pH allows for the disruption of the BTV particles (Verwoerd *et al.*, 1972).

AHSV particles, like BTV, have double capsids that are comprised of seven discrete structural proteins (VP1-VP7) in specific but non-equimolar ratios (see Figure 1.1). The outer capsid of the mature virion is composed of the two major capsid proteins VP2 and VP5, whilst the inner capsid/core contains the major core proteins VP3 and VP7 and the minor proteins VP1, VP4 and VP6 (Roy *et al.*, 1989; Roy *et al.*, 1994). The two outer capsid proteins (VP2 and VP5) form a continuous layer of 86nm in diameter around the core and is removed to yield a transcriptionally active core once the virus is uncoated after cell entry (Verwoerd and Huisman, 1972). The VP3 protein of the inner capsid acts as a



scaffold for the VP7 trimers and together these two proteins encapsulate the three minor proteins and the viral genome (Roy *et al.*, 1994).

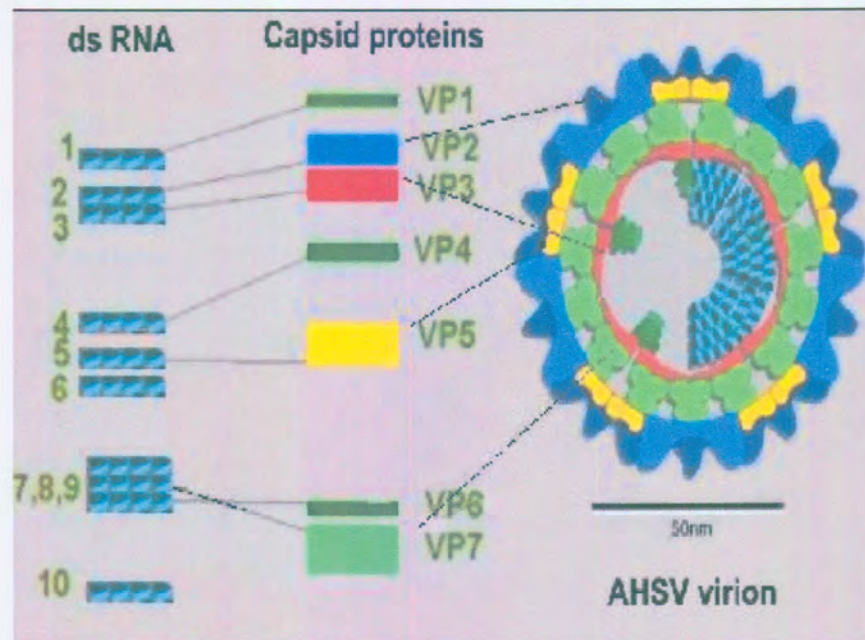


**Figure 1.1** Schematic diagram of the AHSV virion showing the dsRNA genome (located in the AHSV core particle) encoding the capsid proteins. The diagram shows the two outer capsid proteins, VP2 and VP5 surrounding the VP7 trimers on the core surface. VP3 forms a scaffold for VP7 trimers and encloses the three minor proteins and the 10 dsRNA segments (Mertens *et al.*, 2000).

### 1.3.4 Genome Segments

The AHSV genome, which is also comparable to that of BTV, is composed of 10 double-stranded RNA segments. These segments are numbered 1-10 in the order of their electrophoretic migration on a polyacrylamide gel. The segments are grouped as large (L1-3), medium (M4-6) and small segments (S7-10). The mobility's of the various segments may vary between serotypes (Roy *et al.*, 1989; Roy *et al.*, 1994).

The dsRNA genome segments serve as templates for the synthesis of single-stranded mRNA species by the core particle associated RNA polymerase or transcriptase. The different mRNA species are transcribed in a specific molar ratio throughout the infection cycle. Transcription of these segments is initiated when the transcriptase enzyme is activated by the removal of the outer capsid of the virus. The BTV transcriptase was found to have optimal activity at 28°C, as opposed to the 45°C optimal temperature of Reovirus transcriptase (Verwoerd and Huismans, 1972). This temperature difference may likely be due to the fact that BTV is transmitted and can replicate in its intermediate insect host, whilst Reoviruses only replicate in mammalian hosts.

Important common features of all dsRNA segments are that their 5' noncoding regions are relatively short (between 8 and 34 nucleotides long), whilst the 3' non-coding regions are generally longer (from 31-116 nucleotides long) (Roy, 1989). Rao *et al.*, 1983 (as cited by Huismans and Van Dijk, 1990), found a conserved six-nucleotide sequence located at both the 5' and 3' ends of all double-stranded RNA segments. The different genome segments can be classified as either being highly variable, moderately conserved or highly conserved. Highly conserved genome segments (such as VP3 and NS1) show little sequence evolution and can be considered as suitable serogroup-specific genomic probes. A highly variable segment, such as segment 2 (VP2) is considered the best serotype-specific probe (Huismans and Van Dijk, 1990).

**Table 1.2 AHSV4 proteins and genome coding assignments (adapted from Grubman and Lewis, (1992).**

<b>Viral Protein</b>	<b>Molecular weight (Da)</b>	<b>Genome segment</b>	<b>Location</b>
VP1	128,500	1	Core
VP2	107,000	2	Outer capsid
VP3	88,500	3	Core
VP4	69,000	4	Core
VP5	65,000	6	Outer capsid
NS1	62,500	5	Non-structural
VP6	60,500	6	Core
NS2	54,000	8	Non-structural
VP7	42,000	7	Core
NS3	27,500	9	Non-structural
NS4	26,000	10	Non-structural
NS4a	25,000	10	



In the study by Grubman and Lewis, (1992) the authors determined the coding assignments of the ten genome segments of AHSV 4 (Table 1.2) The segments coding the viral structural and nonstructural proteins were assigned by comparing synthetic proteins (produced by in vitro translation of dsRNA in a cell-free system) to actual viral proteins. Most segments coded for only one protein, except for segments 10. The two low molecular nonstructural proteins, NS3 and NS3A, are transcribed from two different initiation sites in the same ORF of segment 10.

### **1.3.5 The protein products of AHSV**

Of the AHSV gene products, the four major capsid proteins (VP2, VP5, VP3 and VP7) are the best studied, whilst relatively less information is available for the three minor proteins (VP1, VP4 and VP6). Sequence comparisons between the four major capsid proteins of BTV, EHDV and AHSV show that all three viruses have comparable primary sequences for their capsid components.

The innermost VP3 core protein is the most conserved, whilst the outermost VP2 outer core protein is the most variable in all of these *Orbivirus* serogroups. Based on data obtained from BTV, the 3 minor proteins are involved in the virus transcription-replication process. This role is ascribed considering the minor proteins have a close association with the dsRNA genome of the virus (Roy *et al.*, 1994). In addition to the 7 structural proteins, there are 4 virus specified non-structural proteins namely NS1, NS2, NS3 and NS3A (see Table 1.3).

**Table 1.3 BTV genes, gene products and possible function. Adapted from Roy and Sutton (1998).**

Genome Segment	Number of base pairs	Encoded Protein(s)	Predicted mass (Da)	Location	Function
1	3954	VP1	149,588	Inner core	RNA polymerase
2	2926	VP2	111,112	Outer Shell	Type specific structural protein
3	27772	VP3	103.344	Core	Structural protein, forms scaffold for VP7 trimers
4	2011	VP4	76,433	Inner core	Capping enzyme, guanylyltransferase
5	1639	VP5	59,163	Outer Shell	Structural Protein
6	1769	NS1 tubules	64,445	Non Structural	Unknown, may be involved in morphogenesis
7	1156	VP7	38,548	Core Surface	Group specific structural protein
8	1123	NS2 VIBs	40,999	Non Structural	Binds mRNA
9	1046	VP6	35,730	Inner core	Helicase, ATPase, binds ss +dsRNA
10	822	NS3 NS3A	25,572 24,020	Non structural Non Structural	Glycoprotein, aids virus release Glycoprotein, aids virus release

#### 1.3.5.1 The two outer capsid proteins: VP2 and VP5.

Of the four outer capsid proteins, VP2 is the most variable. The differences reflect the immune pressures of the host upon this outer coat protein. Since VP2 constitutes the major target for host immune responses, the surface of the protein functions to evade immune responses by presenting a unique structure which might give VP2 an evolutionary advantage whilst preserving its 3D structure (Roy, 1989).

VP2 proteins are sail-shaped and they protrude as spikes above 180 of the VP7 trimers (Hewat *et al.*, 1992b). The VP2 spikes, together with the VP7 trimers, form 60 triskelion type motifs, which cover all but 20 of the VP7 trimers. In addition, these VP2 spikes project 4nm beyond the globular VP5 molecules, making VP5 less exposed. It is postulated that these spikes contain the VP2 hemagglutinating and neutralizing antibodies (Roy, 1996). Many authors (Mertens *et al.*, 1989, Burrage *et al.*, 1993, Martinez-Torrecuadrada *et al.*, 1994; Roy *et al.*, 1996) have demonstrated the direct involvement of the VP2 protein in determining virus serotype and the generation of neutralizing antibodies.

VP2 is a large protein encoded for by genome segment L2 (Grubman and Lewis, 1992). The calculated molecular size ( $M_r$ ) of VP2 (Martinez-Torrecuadrada *et al.*, 1994) is in the region of 115kDa, whilst other authors estimate VP2's  $M_r$  as being 124kDa and 107kDa (Iwata *et al.*, 1992a; Grubman and Lewis, 1992). Amino acid comparisons between VP2 proteins of related orbiviruses (in particular BTV 10, EDHV 1 and AHSV 4) show only 19-24% identical shared amino acids (Iwata *et al.*, 1992a).

The second coat protein VP5 is globular in shape and 120 molecules of VP5 are located on each of the six-membered rings of VP7 trimers (Hewat *et al.*, 1994). In contrast to VP2, VP5 is more conserved and shares 43-45% amino acid identity between BTV and EHDV VP5 proteins. The homology value rises to 64% when amino acids of similar character are considered (Iwata *et al.*, 1992b). The higher degree of conservation of VP5 relative to VP2 indicates a higher degree of restraint on the structural variability of VP5 (Huisman and Van Dijk, 1990). VP5 is more closely associated with the core particle than VP2, considering that VP2 can be removed from the outer capsid without removing VP5 (Verwoerd *et al.*, 1972 and Huisman *et al.*, 1987a).

The M6 dsRNA gene segment of AHSV encodes for the VP5 outer capsid protein. The  $M_r$  of this protein is approximately 56,7kDa and is smaller than its BTV and EHDV counterpart that is approximately 59kDa (Iwata *et al.*, 1992b). The AHSV VP5 protein contains at least three hydrophobic domains (which includes the carboxy terminus) and is less exposed than VP2 on the outer capsid (Roy, 1989; Roy *et al.*, 1994). It has been suggested that the M6 mRNA may synthesize a truncated version of the VP5 protein by in-frame initiation at a downstream start codon (Martinez-Torrecuadrada *et al.*, 1994), although to date, the experimental data is still lacking.

#### 1.3.5.2 The major core proteins VP3 and VP7

Cryo-electron micrographs of BTV core-like particles reveal that the core is an icosahedral structure with an arrangement of 260 triangular spikes (made up of VP7 trimers) and that the subcore is composed of 60 copies of VP3 molecules

(Hewat *et al.*, 1992a). VP3 molecules are closely bonded to each other in a pentameric fashion to form a sphere. The spaces between the VP3 molecules form the pores observed in the inner shell. The pores are likely to allow for passage of metabolites and mRNA into and out of the core particle (Hewat *et al.*, 1992a; Prasad *et al.*, 1992). When VP7 is expressed independently of VP3 in baculoviruses, the VP7 molecules do not form icosahedral structures, indicating that VP3 and VP7 molecules interact closely to form the inner shell structure (French and Roy, 1990).

The L3 dsRNA gene segment encodes for the 103kDa VP3 protein in AHSV (Grubman and Lewis, 1992; Iwata *et al.*, 1992b). The VP3 protein is highly conserved between different orbiviruses; BTV and EHDV VP3 being more closely related than AHSV VP3, sharing 79% and 58% identical amino acids respectively. When homologous substitutions in the VP3 sequences are considered, the percentage of similar amino acids rise to 75-90% (Roy, 1996). This degree of homology indicates the conserved nature of this inner core protein. The conserved regions within VP3 between *Orbivirus* serogroups may reflect regions that are essential for core formation. The VP3 protein has a low content of charged amino acids and has high hydrophobic amino acid content. This is not unexpected, considering its innermost location within the core (Iwata *et al.*, 1992b).

Sequence analysis of the VP3 gene segment and its translated protein has provided insight into the relationships between BTV serotypes and related orbiviruses. It was found that for each serogroup, the VP3 sequence was virtually identical and so aided to unequivocally assign an *Orbivirus* to a particular serogroup (Gould and Hyatt, 1994). VP3 sequence analysis is also important when studying the epidemiological inter-relationships of orbiviruses. The probable geographic origin of *Orbivirus* "incursion" can also be determined by VP3 sequence analysis.

Louden and Roy (1992) investigated the interaction of nucleic acids with BTV purified VP7 and VP3. Binding activity was shown to reside on VP3. The RNA binding domain on VP3 was suggested to be involved and function in assembly. Alternatively, VP3 was also suggested to function as a nucleocapsid protein and hold the genomic dsRNA in the correct conformation for packaging.

The S7 dsRNA gene segment encodes for the structural core protein VP7. This protein is the major component of the inner core and specifically makes up the capsomeric unit (Huisman *et al.*, 1987a). The shape and location of these capsomeres on the axes of the BTV core particles indicates trimer aggregation. Since there are 260 capsomeres on the BTV particle, there are a total of 780 molecules of VP7 per virion (Prasad *et al.*, 1992).

The estimated molecular size of AHSV VP7 is 38kDa, which is slightly smaller than the VP7 of BTV (Roy *et al.*, 1991). Like VP3, VP7 is rich in hydrophobic amino acids and is conserved between orbiviruses, albeit less conserved than VP3. Sixty-four percent identical amino acids are shared between VP7 proteins of BTV and EHDV, with AHSV exhibiting only 44-46% amino acid identity to BTV and EHDV respectively (Iwata *et al.*, 1992a). VP7 has a low occurrence of charged amino acids and is rather rich in hydrophobic amino acids, such as alanine, methionine and proline. The highest homology between VP7 of AHSV-4 and BTV-10 was discovered to be in both the amino and carboxy terminal regions (Roy *et al.*, 1991).

The carboxy terminus of VP7 is critical for inner core formation, as the last 50 amino acids are hydrophobic and is involved in intra and/or inter molecular protein interactions important for particle formation (Roy, 1996). Two conserved cysteine residues are found within *Orbivirus* serogroups and appear to be essential for VP7 trimer formation or VP7/VP3 interactions. Considering that VP7 is the most exposed of the two major core proteins, it is subjected to immunological pressure, which results in additional variation between serotypes (Huisman and Van Dijk, 1990).

### 1.3.5.3 The minor structural proteins: VP1, VP4 and VP6.

It is likely that the minor virion proteins of AHSV, like BTV, are involved in transcription and replication of AHSV (Roy *et al.*, 1994). BTV core particles that were purified and studied by Verwoerd and Huismans (1972) contained a RNA-directed RNA polymerase activity. VP1 is considered to be the RNA polymerase, as its size, location and amino acid sequence is comparable to other polymerases (Vreede and Huismans, 1998). The VP1 protein, which is encoded by gene segment L1, is the largest BTV protein, being 150kDa in size.

The M4 gene product VP4 is considered to have guanylyl transferase activity, which implicates VP4 in being involved in mRNA capping (Roy *et al.*, 1994). The VP4 protein of BTV has a high content of charged amino acids, such as histidine and tryptophan. The 5' non-coding region of segment M4 is relatively short (8bp) when compared to the other RNA segments. Hybridization data implies that BTV M4 is highly conserved (Roy *et al.*, 1994).

The 38kDa VP6 protein of BTV, encoded for by the small gene segment S9, is a hydrophilic protein and has the most basic and charged amino acids per length among all BTV gene products (Fukusho *et al.*, 1989). Roy *et al.*, (1990b), demonstrated the nucleic acid binding affinity of VP6, showing that VP6 can bind both single- and double- stranded RNA and other nucleic acid species. It is suggested that VP6 chaperones the incorporation of RNA into virion particles (Roy, 1996). This role for VP6 is plausible as Roy *et al.*, (1990a) demonstrated that the VP6 is present within the VIB-matrix. Within this matrix, VP6 can bind the BTV RNA during viral morphogenesis. The VP6 amino acid sequence is relatively conserved between BTV serotypes and the sequence contains a motif common to helicases. The helicase motif suggests that VP6 is responsible for the unwinding of dsRNA prior to cRNA synthesis (Roy *et al.*, 1994).

#### 1.3.5.4 The non-structural AHSV proteins: NS1, NS2, NS3 and NS3A:

Two morphologically distinct structures characterize the cytoplasm of *Orbivirus*-infected cells and are known as tubules and virus inclusion bodies (VIBs). Both these virus-specific entities are believed to be involved in virus morphogenesis. VIBs are also referred to as 'viral factories' or 'inclusion bodies' and are characterized as dense, fibrillar structures that are associated with the infected cell's cytoskeleton (Lecatsas, 1968; Cromack *et al.*, 1971). These inclusion bodies are recognized as the sites of viral assembly and contain dsRNA, virus-specific polypeptides and both complete and incomplete viral particles (Thomas *et al.*, 1990).

Extensive studies on tubule formation have been done for BTV and they indicate that tubules are formed from helically coiled ribbons of non-structural protein NS1 (Hewat, 1992). Within *Orbivirus* infected cells, NS1 is synthesized in large amounts and is rapidly converted to these high molecular tubular structures (Huisman and Van Dijk, 1990). These tubules are synthesized continuously throughout the infection cycle, initially associated with VIB's and mature viral particles and later the tubules become dispersed through the cytoplasm (Huisman and Els, 1979).

Lecatsas (1968) discovered that the tubules attach to the intermediate filaments of the cell's cytoplasm, indicating a role in virus transportation within infected cells. Huisman and Els, (1979) compared the tubule formation between *Orbivirus* groups and found that BTV and EHDV tubules are more similar in morphology than the AHSV tubules. The BTV and EHDV tubules have a ladder-like surface, whilst the smaller AHSV tubules have a less clearly defined structure with no linear periodicity.

Grubman and Lewis (1992) found the 63kDa NS1 protein of AHSV to be encoded by the M5 dsRNA gene segment. The gene segment encoding NS1 in BTV is highly conserved between serotypes, whilst AHSV NS1 protein shares approximately 31% identical amino acids and 71% similar amino acids with that of BTV serotypes. Certain cysteine residues within NS1 are conserved in



orbiviruses, indicating the existence of a highly ordered structure (Roy *et al.*, 1994). BTV NS1 has a low content of charged amino acids and hydrophobic domains, especially near the C-terminus (Roy, 1989).

The NS2 protein, encoded by the small dsRNA segment S8, is the only viral phosphorylated protein found in virus-infected cells. NS2 of BTV bind single-stranded RNA and this activity may indicate a role of condensing RNA into subviral particles during viral morphogenesis (Lymeropoulos *et al.*, 2003, Markotter *et al.*, 2004, Thomas *et al.*, 1990). The NS2 protein is rich in charged and hydrophilic amino acids, making interaction with nucleic acids possible. The amino terminus of the NS2 protein (and to a lesser extent, the carboxy terminus) contains hydrophobic residues, whilst the middle region contains many charged residues (Fukusho *et al.*, 1989). The NS2 protein also associates with VIBs and it is thought that NS2 is the major component of these large and dense inclusion bodies (Brookes *et al.*, 1993, Eaton *et al.*, 1987). The NS2 protein of AHSV has a molecular size of 41 kDa with a sequence variation of 33-45% when compared to the NS2 of BTV (Roy *et al.*, 1994).

The smallest dsRNA gene segment, the S10 segment, encodes the two colinear NS3 proteins, NS3 and NS3A from two in-phase overlapping reading frames (Van Staden and Huisman, 1991; Mertens *et al.*, 1984). In contrast to NS1 and NS2 expression, NS3 and NS3A are synthesized in small amounts in infected cells. Both proteins were shown to be N-linked glycosylated and associated with lipid membranes (Hyatt *et al.*, 1993; Van Staden *et al.*, 1998). NS3 is the second most variable AHSV protein. There is approximately 36% amino acid variation between different serotypes and as much as 27% within serotypes (Van Niekerk *et al.*, 2001b).

NS3 was demonstrated to mediate the release of virus particles from cells and is thus implicated in the final stages of viral morphogenesis and release (Hyatt *et al.*, 1993). NS3 expressed from recombinant baculoviruses was found to be cytotoxic in *Spodoptera frugiperda* cells (Van Staden *et al.*, 1998). Cytotoxicity of



NS3 has been shown to be dependant on two hydrophobic domains, which are responsible for membrane anchoring (Van Niekerk *et al.*, 2001a).

Beaton *et al.*, (2002) demonstrated that BTV NS3 facilitated viral release by interacting with specific host trafficking proteins at the plasma membrane. NS3 is suggested to function as a bridge by linking progeny virions to cellular export machinery. Han and Harty, (2004) demonstrated that NS3 possess properties associated with viroporins. Viroporins compose a small group of hydrophobic transmembrane proteins that can form hydrophilic pores through lipid bilayers.

## 1.4. Vaccine development

### 1.4.1 An Overview

The aim of vaccine development is to modify a pathogen or its antigens, so that the vaccine is innocuous (a loss of pathogenicity), but still antigenic enough to elicit an effective immune response. Thus, altered preparations of microbes or its antigens can be used to generate enhanced immunity against the virulent organism. From an immunological perspective, the antigen(s) of a vaccine must induce clonal expansion of specific T and/or B cells and be able to leave a host of memory cells for future challenges with the real pathogen. This enables the organism to mount a more rapid and effective secondary immune response, as the primary response is often too slow to prevent serious disease (Roitt *et al.*, 1998), also see Table 1.4.

**Table 1.4** Main antigenic preparations used as vaccines (adapted from Roitt *et al.*, 1998)

TYPE OF ANTIGEN		VACCINE EXAMPLES
Living organisms	Natural	Vaccinia (for small pox) Vole bacillus (for TB; historical)
	Attenuated	Polio (Sabin; oral polio vaccine), Measles, mumps, rubella, yellow fever, varicella-zoster (human herpes virus 3) BCG (for TB)
Intact but non-living organisms	Viruses	Polio (Salk), rabies, influenza, hepatitis A, typhus
	Bacteria	Pertussis, typhoid, cholera, plague
Subcellular fragments	Capsular polysaccharides	Pneumococcus Meningococcus <i>Haemophilus influenza</i>
	Surface antigen	Hepatitis B
Toxoids		Tetanus, diphtheria
Recombinant DNA based	Gene cloned and expressed	Hepatitis-B (yeast derived)
	Genes expressed in vectors	Experimental
	Naked DNA	Experimental
Anti-idiotypic		Experimental

Two types of viral vaccines are mostly used in vaccination programs; namely inactivated whole virus vaccines or attenuated forms (mild forms) of a live virus (Roy *et al.*, 1990a).

Inactivated vaccines comprise viruses that have lost their infectivity due to a chemical/physical process. Generally, these vaccines elicit antibodies directed against the coat proteins of the virus. The disadvantages associated with this type of vaccine include the need to ensure complete inactivation and booster inoculations, as these vaccines only confer limited or brief immunity.

Passaging virulent virus strains through cell culture generates attenuated live vaccines. The process results in strains with lower virulence. These viruses behave as natural viruses, by still being able to replicate within the hosts and still able to confer both humoral and cellular immunity. Generally, tissue culture adapted vaccines for AHS are effective and were successfully used to control outbreaks in various European countries. However, these attenuated live vaccines are less desirable for use outside enzootic areas for numerous reasons. These include: failure to prevent viraemia, variable immunogenicity, potential reversion to virulence or vector transmission and the inability to readily differentiate between vaccinates and naturally exposed horses (House *et al.*, 1998). With the current BTV vaccine, possible fetal infection lowers the immunogenicity in lambs as passive colostral immunity neutralizes these strains more readily. Also, the use of polyvalent vaccines may confer incomplete immunity due to interference between component serotypes (Roy *et al.*, 1990a).

Such problems are not associated with inactivated vaccines. Inactivated vaccines however, require the culturing of large amounts of virus and are subject to biocontainment outside enzootic regions, as well as ensuring complete inactivation (Stone-Marshat *et al.*, 1996). Subunit vaccines could potentially circumvent many of the above-mentioned difficulties. Subunit vaccines involve gene expression of virus subunits or known antigens in a vector, where the subunit/antigen is derived from infectious material or is genetically engineered. Production of these vaccines allows for its preparation

without having to grow and propagate the pathogenic organism. A variety of vectors are available for such gene expression including bacterial, yeast, viral, and other cellular systems (Roy *et al.*, 1990a). Subunit vaccines made with recombinant proteins are regarded as the safest means of inducing immunity, as these vaccines are not subject to reversion or vector transmission (Burrage and Laegried, 1994).

Synthetic peptides have also been considered for vaccine purposes, but their efficacy is generally lower than conventional vaccines. The reason for this is that B-cell epitopes are usually in a specific conformation, which is difficult to reproduce, especially if the peptides are short. Anti-peptide antibodies have been shown to be protective in certain diseases (Martinez-Torrecuadrada, 2001) making a peptide vaccine feasible in the case of AHS.

Since there are nine AHSV serotypes, horses require immunity to all serotypes to be fully protected in the event of a viral challenge. Good AHSV vaccines should be safe and elicit a rapid and enduring protective immune response in vaccinated horses. Preferably, the vaccine should not induce viraemia and prevent secondary viraemia following infection, in order to prevent infecting insect vectors. Vaccines should be produced following high international standards, with additional data informing the user of efficacy, safety and duration of immunity in all domestic equids (Mellor *et al.*, 1998).

### **1.4.2 Vaccine Development using AHSV proteins**

Generally speaking, the neutralizing antibody titre is of importance when determining the horse's immune status (Scalen *et al.*, 2002). There is a strong association between the production of neutralizing antibodies and the protection of horses against AHS (Burrage and Laegried, 1994). Given the important role of neutralizing antibodies for protection against AHS, an effective subunit/vectored vaccine should express epitopes that elicit neutralizing antibodies in horses (Burrage and Laegried, 1994).

It is of value to identify antigenic and neutralizing regions of the virus and subsequently test the corresponding synthetic peptides for induction of an immune response. Immunogenic epitopes are expected to be exposed on the surface of the AHSV capsid so that neutralizing antibodies can effectively bind to these regions and prevent virus attachment and/or cell entry. Thus, the development of an effectual peptide vaccine against AHSV lies in the determination of the exact location of antigenic determinants, which are thought to exist mostly on VP2 (Martinez-Torrecuadrada, 2001).

In the case of BTV vaccine development, purified VP2 (Huisman *et al.*, 1987a) or VP2 expressed from a recombinant baculovirus expression vector (Inumara and Roy, 1987) was shown to induce serotype-specific neutralizing antibodies. These VP2 preparations were used to raise neutralizing antibodies and block cell attachment of BTV, as immunized sheep were subsequently protected from BTV infection. Significantly higher titres of BTV neutralizing antibodies against baculovirus expressed VP2 were raised when a combination of VP2 and VP5 antigens within the baculovirus expression vector was used (Roy *et al.*, 1990a). Protection conferred by this combination of proteins lasted longer than 15 months. These results suggest that VP5 indirectly enhances the immune response by interacting with VP2, which in turn affects VP2 conformation and serological properties.

Burrage *et al.*, (1993) demonstrated that like BTV, the VP2 coat protein of AHSV bears the neutralizing epitopes. Antibodies directed against these epitopes were shown to be protective in a neonatal mouse model. This suggests that recombinant VP2, which bears these neutralizing epitopes, may be effective in a vaccine strategy against AHS. Results obtained by Vreede and Huisman, (1994) and Martínez-Torrecuadrada *et al.*, (1994) also confirm that VP2 carries neutralizing specific epitopes. Stone-Marshat *et al.*, (1996) demonstrated that neutralizing antibodies induced by AHSV4 VP2/vaccinia virus recombinants fully protected horses against disease with no clinical signs or viraemia observed.

Martínez-Torrecedrada *et al.*, (1996), like Roy *et al.*, (1990a) with vaccination studies on BTV showed that the simultaneous expression of VP2 and VP5 in vaccination strategies enhanced the induction of neutralizing antibodies against AHSV. Additionally, a combination of non-purified VP2, VP5 and VP7 was able to confer full protection against a lethal challenge in horses. It was suggested that the best conformation of VP2 (i.e. the exposure of immunodominant neutralizing epitopes) was achieved when VP5 and VP7 was coexpressed in a baculovirus system. The search for antigenic regions and choice of adjuvants (Scalen *et al.*, 2002) remain critical factors for increasing the efficacy and reproducibility of AHSV vaccines.

A novel approach in presenting epitope regions to the immune system is currently being investigated in our laboratories, namely the use of a VP7 particulate protein presentation system. The VP7 protein of AHSV is a highly insoluble protein that forms crystals when expressed by baculoviruses in insect cells (Chuma *et al.*, 1992; Burroughs *et al.*, 1994; Maree *et al.*, 1998). Various hydrophilic regions within the AHSV9 VP7 protein have been modified to allow for insertion and expression of antigenic peptides (Maree, 2000). This system is currently being investigated as a display vector for AHSV peptides and it is anticipated to have the ability to induce strong epitope-specific neutralizing immune responses. All features of the display system have not been fully explored and the immunological response that insertion of epitopes may have, cannot be predicted but have to be tested on an individual basis.

## **1.5 AHSV Proteins involved in virulence**

Notably, certain AHSV proteins seem predominantly responsible for virulence. Virulence of a particular virus infecting its host is generally attributed to the efficacy of its entry into the cell, its ability to replicate within the cells and its subsequent successful release from the cell. The VP2 protein as previously mentioned (1.3.2.1) is responsible for viral attachment and entry (Eaton and Crameri 1989; Hassan and Roy 1999). Although VP5 is not responsible for internalization (Hassan *et al.*, 2001) it is suggested that inherent cytotoxicity is

responsible for core access into the cytoplasm. Similarly, the NS3 protein has also been shown to be highly cytotoxic and aid in viral release from infected cells (Roy 1996). Viral proteins involved in these functions are thus of great importance as major targets in vaccine development.

### **1.5.1 Outer capsid protein VP5**

The AHSV protein of interest in this study is the outer capsid protein VP5. The VP5 protein has an approximate molecular weight of 56,9KDa and ranges in size from 504 to 505 amino acids in length (Williams *et al.*, 1998; Du Plessis and Nel, 1997). Williams *et al.*, (1998) found the VP5 protein to be rich in non-polar amino acids such as isoleucine and alanine. It has a hydrophobic central region suggestive of a “hinge”, which can separate the protein into an N and C terminal.

Several of the VP5 genes of AHSV has been cloned and characterized by various authors. Williams *et al.*, (1998) cloned the M6 gene of AHSV6 (Gen Bank accession number: AF 021237) and found the length of VP5 to be two base pairs shorter than the 1566 bp long AHSV4 VP5 gene sequenced by Iwata *et al.*, (1992). Du Plessis and Nel (1997) cloned the M6 gene segment of AHSV9. Comparison of AHSV9 VP5 with AHSV4 VP5 showed that the base composition was virtually identical.

AHSV VP5 sequence comparisons to related orbiviruses such as BTV and EHDV show definite conserved regions, which are likely to be responsible for structural maintenance (Du Plessis and Nel, 1997; Williams *et al.*, 1998). The VP5 proteins between these serogroups are structurally similar (Oldfield *et al.*, 1991; Iwata *et al.*, 1992; Du Plessis and Nel, 1997) with variable regions likely to be exposed on virion surfaces where important T-cell epitopes are thought to reside. Such T cell epitopes would in theory enhance immune responses if included in a recombinant vaccine. Thus, VP5 has the important function of interacting with more conserved core proteins as well as adapting to facilitate changes in VP2 (Williams *et al.*, 1998).

Hassan and Roy (2001) used hydrophobic cluster analysis (HCA) to predict the structural organization of BTV10 VP5 based on its amino acid sequences. VP5 residues can be divided into two regions, an amino terminal region (residues 1-240) with a coiled-coiled feature and a carboxy terminal region (residues 260-526). A hinge region rich in flexible alanine and glycine residues separates the amino- and carboxy- terminals (see Figure 1.2).

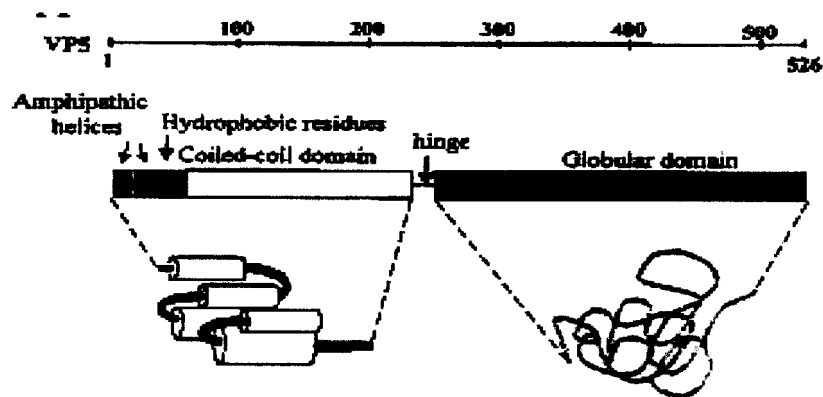


**Figure 1.2** Structural features and domains of BTV10 VP5 identified using computer-assisted 2D hydrophobic cluster analysis as well as “coils” and “learn coil” programs. Taken from Hassan *et al.*, (2001).

Two amphipathic helices were identified within the first 40 N-terminal residues of BTV10 VP5, followed by hydrophobic residues, which are likely to be unexposed (Hassan *et al.*, 2001). Both helices have a net positive charge, which would allow them to bind to negative phospholipids during membrane attachment. Considering that the N-terminal is responsible for membrane destabilization and conferred cytotoxicity, this amphipathic structure supports the notion that insertion into lipid bilayers can generate pores for the destabilization of membrane potential. The coiled-coiled region behind the helices is thought to act as molecular connectors by allowing oligomerization. VP5 was seen to exist as a trimer in solution, a finding that is consistent with cryoelectron microscopy and image analysis predictions. In order to investigate



whether these amphipathic helices could play a role in this suggested cytotoxicity, Hassan *et al.*, (2001) constructed deletion mutants of both the N- and C- terminal regions of BTV VP5, which was later expressed in a baculovirus expression system. The presence of these helices correlated with cell cytotoxicity and damage. In addition, the expressed peptides representing the first and second amphipathic helices showed the highest levels of LDH release, indicating their ability to destabilize the cellular plasma membrane.

When Martinez-Torrecuadrada *et al.*, (1999) expressed the AHSV4 VP5 protein in insect cells (alone or in combination with VP2), AHSV specific neutralizing antibodies were induced. Specifically, two monoclonal antibodies (MAb) were found to neutralize the virus in a plaque reduction assay. Although these neutralizing antibodies were able to elicit a response, titres were found to be much less than those induced by VP2.

Two antigenic sites recognized by these MAbs were found on the VP5 protein and are likely to become exposed after protein denaturation. These two sites were mapped to the N-terminal region of VP5 (Martinez-Torrecuadrada *et al.*, 1999), which was also shown to be extremely toxic when expressed in bacterial cells. No antigenic regions were detected in the C-terminal region, which is conserved between all the VP5s compared. This indicates that the C-terminal is likely to be buried within the core and to function in virus structure preservation.

The first MAb recognized a highly conserved epitope in orbiviruses located between amino acid residues 83-120, whilst the lesser-conserved second epitope was found to reside between residues 151-200. Prior to this study, it was assumed that antibodies elicited against orbiviral and specifically BTV VP5 does not neutralize infectivity (Roy *et al.*, 1990). This seems contrary to the findings in AHSV (Martinez-Torrecuadrada *et al.*, 1999) where AHSV VP5 elicited significant neutralization activity. The study provided the first evidence of such an activity associated with an *Orbivirus* VP5.

## **1.6 Aims**

From the literature survey, it is clear that the use of VP2 and VP5 in a recombinant *Orbivirus* vaccine development strategy is of great importance. A crucial step in the initial stages of vaccine development involves the cloning and characterization of the relevant genes. In South Africa, we are privileged to have access to AHSV field strains and furthermore, all AHSV serotypes occur in this country. Using genes from viruses that are currently in circulation makes their use in vaccine development preferable over laboratory-adapted strains that are likely to be avirulent. At present, it is a priority to produce clones of the various outer capsid proteins using genes from serotypes 3, 4, 6, 8 and 9 for subsequent characterization and immunological testing. Once the clones are available, it may be used in various vaccine development strategies. These include the VEE system and/or particulate delivery systems being investigated in our laboratories.

### **In this study it was aimed to:**

- Compare the genetic variation between VP5 proteins of a number of AHSV field isolates likely to be virulent to that of laboratory adapted strains likely to be avirulent and identify possible virulence markers.
- Investigate whether AHSV VP5 displays a cytotoxic effect when expressed in bacterial cells.
- Display epitope regions of AHSV4 VP5 in a particulate display system based on the VP7 protein of AHSV and evaluate its ability to form crystals.

**Chapter 2:**  
**Comparative analysis of the VP5**  
**protein of various field and**  
**laboratory adapted strains of**  
**various AHSV serotypes.**

## **2.1. Introduction**

In order to ascribe particular functions and properties to the VP5 protein, the actual DNA sequence with its corresponding protein sequence must be elucidated. Comparisons between VP5 sequences of various serotypes and/or groups can reveal important regions necessary for the integrity and functioning of the VP5 protein. Sequence analysis data can also reveal certain evolutionary relationships between such viruses, depending on the variability of the actual sequence analyzed.

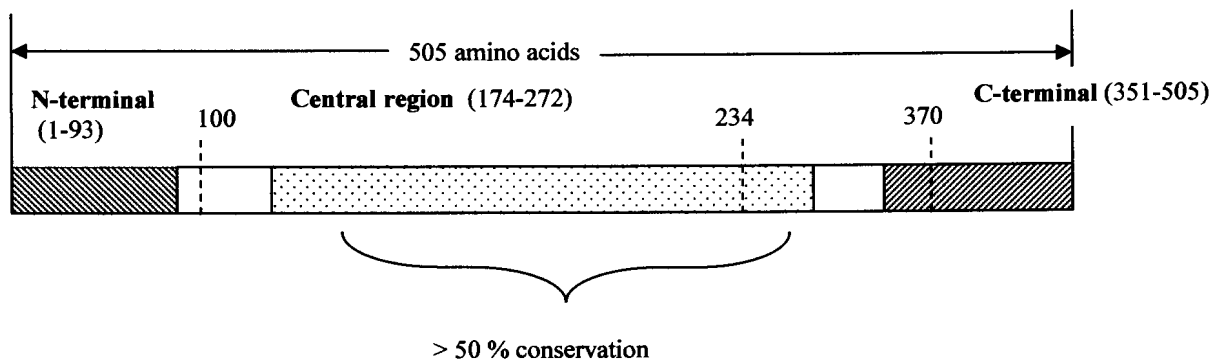
Since VP5 is thought to play a role as one of the proteins contributing to the virulency of a specific AHSV strain, comparative analysis between field and laboratory adapted strains within a serotype may give insight to possible indicators of virulence/ antigenicity. Such defined virulent regions in the viral proteins involved in antigenicity are also vital for the development of vaccines. Interactions of different viral proteins within the structure of the virus as well as with host cell components can give insight to various questions regarding the replication efficiency and spread of the pathogen within host cell organisms.

Table 2.1.1 summarizes the basic properties of VP5 as elucidated with various independent studies based on sequencing data from a number of orbiviruses.

From BTV VP5 studies, Oldfield *et al.* (1991) showed 79 amino acids in the N-terminal, 200-270 amino acids in the central region and 45 amino acids the C-terminal regions to be conserved between BTV serotypes. Du Plessis and Nel (1997) described the central region of AHSV9 VP5 to be highly conserved, with hydrophobic profiles resembling that of BTV and EHDV. Figure 2.1.1 depicts the three different regions within the AHSV9 VP5 from du Plessis and Nel (1997).

**Table 2.1.1** Summary of the basic properties of the VP5 gene segment elucidated by various authors.

Sequence	Author (s) and accession number in GENBANK	Number of Base-pairs	Mr (kDa)	Number of Amino acids	% Amino acid identities-similarities between serotypes	% Amino acid identities-similarities between serogroups
AHSV9 M6 gene segment	du Plessis and Nel (1997) U74489	1566	56,737	505	81-90	39-50
AHSV6 M6 gene segment	Williams <i>et al.</i> , (1998) AF021237	1564	56,9	505	83-92	42-65
AHSV4 M6 gene segment	Sakamoto <i>et al.</i> , (1994) D26571 Iwata <i>et al.</i> , (1992) M947311	1566	56,793	505	98	46-58
		1566	56,780	505	81-90	43-64
EHDV1 M5 gene segment	Iwata <i>et al.</i> , (1992) X55782	1566	59	527	59-62	62-76
BTV1 SA M5 gene segment	Wade-Evans <i>et al.</i> , (1988) P33475	1635	59,195	526		



**Figure 2.1.1** Diagram depicting the three different regions of AHSV9 VP5, as described by Du Plessis and Nel (1997). A hydrophilic domain exists between amino acids 100 and 234, whilst a conserved cysteine residue exists in position 370 (which is normally found at position 383 in BTV and EHDV).

Williams *et al.*, (1998) confirmed that the VP5 protein of AHSV6 had three definite conserved regions when compared to the AHSV4, BTV10 and EHDV1 VP5 sequences. These conserved regions are thought to be important for maintaining the structural integrity of the virus core. Hassan *et al.*, (2001) used hydrophobic cluster analysis (HCA) to predict the structural organization of BTV VP5 based on its amino acid sequence. This analysis showed that the VP5 residues are divided into two domains; the N-terminal (with a coiled-coiled feature) and the C-terminal (with a globular structure) separated by an alanine - glycine rich hinge region.

Considering that the VP5 proteins of AHSV, BTV and EHDV are structurally similar (although BTV and EHDV are more closely related), the VP5 protein does seem to play a supportive role to VP2 in enhancing the immune response (*see Chapter 1*). The variable regions within VP5 are likely to be exposed on the virion surface and are not involved in inner core interactions. The important T-cell epitopes are thought to occur in these variable regions, which could potentially enhance the immune response if included in a recombinant vaccine.

In this current study, in contrast to those VP5 sequence studies published to date, an investigation of AHSV field strains will be undertaken. Most of the sequence data generated thus far has been done on laboratory adapted vaccine strains and a need exists to investigate whether field strains isolated from dead animals (assumed to be virulent) are significantly different from their laboratory-adapted counterparts, likely to be avirulent. In addition, the M6 gene segment of a previously unpublished serotype will also be presented here. Various sequencing analysis tools will be utilized to clarify the differences and similarities between those published and those presented here. Studies by various authors have provided insight into the possible functions of the outer capsid VP5 protein of certain orbiviruses. For instance (as mentioned in Chapter 1), Mertens *et al.*, (1989) showed that in bluetongue virus, VP5 together with VP2, is involved in virus serotype determination. It has been suggested that VP5 may interact indirectly with the VP2 outer capsid protein and affect the virus serotype by changing its conformational structure and hence influence

its serological properties. Roy *et al.*, (1990a), showed that baculovirus expressed BTV VP5, together with VP2, induced higher neutralizing antibodies in sheep than immunization with VP2 alone. Similarly, Martinez-Torrecuadrada *et al.*, (1996) showed that AHSV VP5 also induced higher titres of neutralizing antibodies in horses when expressed together with VP2 in a baculovirus expression system. These studies reveal that VP5 may be responsible for the preservation of VP2's natural conformation and so aids to enhance the immune response with its subsequent interaction with VP2.

Hassan *et al.*, (2001) showed that BTV VP5 can bind to cell surfaces, but does not play a role in internalisation of the virus. VP5 is suggested to play a role in membrane destabilization, which is required for subsequent core access into the cytoplasm. This membrane binding function of VP5 is suggested to be facilitated by the amphipatic structure found in the first 40 residues of the N-terminal region, by allowing membrane disruption by insertion and affecting membrane potential. This destabilization of the membrane potential allows for the formation of pores, which facilitates core access into the cytoplasm. This membrane binding function of VP5, with its consecutive role in membrane disruption, can explain the cytotoxic nature of VP5.

Both Martinez-Torrecuadrada *et al.*, (1994) and du Plessis and Nel, (1997) observed that the expression of AHSV VP5 seemed to be detrimental to the growth of cells in which it was expressed, indicating that this protein is quite cytotoxic to host cells. In the study of Martinez-Torrecuadrada *et al.*, 1999, various truncated mutants containing different lengths and regions of the VP5 protein were generated for the purpose of identifying epitopes that occur on VP5. Low levels of expression of some of these mutants were observed, especially those containing N-terminal regions of VP5. It seemed as if expression of these truncated proteins were toxic to the *E.coli* host cells and caused a significant decrease in their growth rate, which lead to a rapid lysis of cells after IPTG induction. In a study of Hassan *et al.*, (2001), it was shown that the expression of BTV VP5 is indeed cytotoxic to insect cells, that the VP5- induced cytotoxicity is dose-dependant and that it varied little between BTV serotypes.

In this study, expressing the protein in bacterial cells and quantifying the effects on cell growth will investigate the apparent cytotoxic nature of AHSV VP5. The pET expression system (Novagen), a very powerful inducible bacterial system developed for the cloning and expression of recombinant proteins in *E.coli*, was chosen in order to selectively express the VP5 protein. The system is especially well suited for the expression and characterisation of toxic proteins. Cytotoxicity of expressed VP5 proteins will be analysed by inducing expression and measuring the optical density of bacterial cultures at various time intervals post induction. Optical density will be used as an indication of cell growth. Values will be compared to the expression and cell growth of known non-cytotoxic proteins.

In the pET expression system, the gene of interest is first cloned into a suitable pET vector and is then placed under the control of a strong bacteriophage T7 promoter. Transcription of the cloned gene is selectively induced when T7 RNA polymerase is present, which is usually produced by the host cell line. When fully induced, the T7 RNA polymerase causes very high levels of gene expression, such that the desired protein comprises up to 50% of the total expressed protein for the cell within a few hours. Modulation of the amount of gene expression is of great importance when dealing with proteins assumed to be cytotoxic. In addition, this system is able to maintain target genes transcriptionally silent in the uninduced state, increasing the chances of vector and cell-line stability and survival.

Initial cloning of the gene is done in hosts that do not contain the T7 RNA polymerase enzyme. This initial step eliminates plasmid instability when the expressed protein is potentially toxic to the host cell. Once the recombinant plasmid vector is established in a non-expression host, expression of the target gene can be initiated by transferring the plasmid into an expression host. This host cell line contains the T7 RNA polymerase gene under lacUV5 control, allowing induced expression by the addition of IPTG (isopropyl- $\beta$ -D-thiogalactopyranoside) to the bacterial culture.



## **2.2 Materials and Methods**

### **2.2.1 Preparation of competent cells using calcium chloride**

Mandel and Higa (1970) first described the calcium chloride procedure for preparing competent bacterial cells. The procedure allows for the exposure of cells to calcium ions at a low temperature, which in renders these cells able to internalize foreign DNA after a heat shock treatment. This method has been utilized to make *XL1*-blue bacterial cells, DH10BAC cells as well as and BL-21 (DE3) bacterial cells competent. This procedure promotes the efficient uptake (transformation) of both recombinant and non-recombinant plasmid DNA (Sambrook *et al.*, 1989).

A 2ml overnight culture of Luria-Bertani (LB) broth<sup>1</sup> (containing the appropriate antibiotics that the cell line is resistant to) was used to inoculate a larger 100ml culture. The bacterial cell line was allowed to grow by shaking at 37°C until growth is indicative of one in logarithmic (log) phase. The log phase is reached at an optical density (OD) reading at a wavelength of 550 of between 0.45 and 0.5. Cells were then incubated on ice for a period of 10 minutes to inhibit mitosis. Some of the cells were collected by centrifugation (2000r.p.m for 10 minutes at 4°C) and resuspended in half the original volume of solution containing ice-cold and freshly prepared 50mM CaCl<sub>2</sub>. These cells in solution were collected by centrifugation (as above) and resuspended in 1/20<sup>th</sup> of the original volume of CaCl<sub>2</sub> solution. Cells were kept on ice for at least an hour before use or were stored in 15% glycerol at -70° C for later use. Transforming the competent cells with a standard plasmid vector can assess the competency of cells.

---

<sup>1</sup> Luria-Bertani broth: 1% bactotryptone (m/v), 0.5% bacto yeast (m/v), 1% NaCl (m/v).

### 2.2.2 Transformation of competent cells

This procedure allows for the uptake of plasmid DNA into competent cells. According to Sambrook *et al.*, (1989) the transformation efficiency is improved by harvesting the bacterial cell cultures at the optimum growth phase (log phase), keeping the cells on ice throughout the procedure and by prolonging the CaCl<sub>2</sub> exposure time.

Approximately 250ng of plasmid DNA (or half of a ligation mix) was added to 100-200µl of competent cells placed within glass test tubes. The glass tubes were incubated on ice for 30 minutes to allow for DNA adsorption. Consequently, the cells were subjected to heat shock for 90 seconds at 42°C, which facilitates the uptake of DNA into the competent cells (Brown, 1986). Placing the tubes on ice for a further 2 minutes then rapidly cools the mixture. The addition of LB broth to a final volume of 1ml allowed for cell growth by shaking for an hour at 37°C. Approximately one tenth of the transformation mixture was plated out onto 1.2% (m/v) LB agar plates containing the advised concentration of appropriate antibiotics. The plates were further incubated at 37°C overnight to allow for growth of transformed bacterial colonies (Ausabel *et al.*, 1989).

### 2.2.3 Purification of plasmid DNA

The most commonly used plasmid purification protocols from liquid cultures of bacterial cells are adaptations of the alkaline lysis method of Birnboim and Doly, (1979) and Ish-Horowicz and Burke, (1981), as described by Sambrook *et al.*, (1989). The alkaline lysis method allows for the purification of plasmid DNA from chromosomal DNA by first destabilizing and then disrupting bacterial cell walls by the addition of an alkaline/SDS (sodium dodecyl sulphate) buffer. Separation of genomic and plasmid DNA is achieved by adjusting the pH of the mixture, which in turn alters the conformation of the different DNA species. Genomic DNA is easily removed by centrifugation when it reverts to its native conformation and forms an insoluble network. Plasmid DNA is recovered upon the addition of ethanol, which in turn precipitates the plasmid DNA. Variations of this method (in mini- and large-scale preparations) as well as plasmid

purification using the High Pure plasmid purification kit (Roche biochemical's) were utilized according to the manufacturer's instructions.

Basically, for small-scale plasmid purification, LB broth containing the appropriate antibiotics was inoculated with a single bacterial colony and allowed to grow to saturation by incubation at 37°C with shaking. Cultured cells were collected by centrifugation (5000r.p.m for 10 minutes) and resuspended in ice-cold solution I (25mM Tris-HCL at pH 8, 50mM glucose and 10mM EDTA<sup>2</sup>). Bacterial cells were gently lysed and proteins, chromosomal and plasmid DNA were denatured by the addition of solution II (0.2M NaOH-1% SDS pH 7.4). The cells were kept on ice for a period not exceeding 5 minutes before adding 3M NaOAc (pH4.8) and vortexing vigorously. Genomic DNA and bacterial proteins were precipitated and collected by centrifugation (13000r.p.m for 10 minutes). The supernatant containing the renatured plasmid DNA was transferred to a new tube and precipitated by adding 96% ethanol at -20°C. After an hour, the DNA pellet was collected by centrifugation (13000rpm for 20 minutes) and washed with 70% ethanol. The pellet was allowed to dry before resuspending in water of TE buffer<sup>3</sup>. A sample was analyzed on agarose gel in order to determine if plasmid DNA was extracted.

Plasmid DNA was stored in TE buffer or distilled water at 4°C for short time periods or at -20/70°C for longer time periods in the presence of 15% sterile glycerol (at -70°C) (Ausubel *et al.*, 1989).

#### 2.2.4. Agarose gel electrophoresis

Electrophoresis is the migration of charged particles under the influence of an electric field, which is created by attached electrodes (Brown, 1986). Agarose, the support media through which negatively charged DNA molecules migrate, dissolves in aqueous buffer (1x TAE; 40mM Tris-HCL, 20mM NaAc and 1mM EDTA, pH8.5) to set and form a gel. After electrophoresis, the DNA was

---

<sup>2</sup> EDTA: ethylenediamine tetraacetate: functions to inactivate nucleases by binding  $mg^{2+}$  co-factors and so promotes the destabilization of bacterial cell walls (Brown, 1986).

<sup>3</sup> TE buffer: 10mM Tris-HCL, 1mM EDTA, pH 8.0

visualized under UV light by staining with the intercalator, ethidium bromide (0.5µg/ml) and compared to a standard marker (Old and Primrose, 1994). Ethidium bromide was visualized as fluorescent orange bands under the UV transilluminator (Hackett *et al.*, 1988). Mostly 1 or 2% (w/v) agarose gels were used to separate and analyze the various DNA samples.

### 2.2.5 The polymerase chain reaction (PCR):

The polymerase chain reaction is an easily performed procedure for the *in vitro* enzymatic amplification of a specific sequence of DNA (Ausabel, 1989). The principle involves the use of two oligonucleotide primers (forward and reverse), which are homologous to the flanking regions one would like to amplify. Under the correct reaction conditions, the template DNA is denatured and the single stranded primers allowed to hybridize. DNA polymerase, co-factors and dNTPs amplify the target region. Repetitive cycles allow for the exponential amplification of the target sequence (Old and Primrose, 1995). The thermal stable Taq DNA polymerase<sup>4</sup> is the preferred PCR catalyzer, because of its high optimal temperature of polymerization (75°-80°C) allowing for more specific hybridization of primers to complementary DNA (Ausabel, 1989). Automation of the PCR reaction is accomplished with the aid of a thermocycler, which can accurately and reproducibly maintain a range of incubation temperatures.

The primers utilized in this study to amplify certain regions of the template DNA are described below in Tables 2. 2. 1 and 2. 2. 2.

A master mix was made to contain all the necessary components of a 50µl PCR reaction and included (50-200ng) template DNA, 100pmol of each specific primer, 1.5mM MgCl<sub>2</sub> (Promega), 0.2mM of each dNTP (Promega), 1x 10 Mg-free thermophilic DNA Polymerase buffer (Promega), *Taq* DNA polymerase enzyme (Promega) and Sabax water to adjust the final reaction volume. A negative control, containing no template DNA, was always prepared to ensure no aberrant amplification of contaminant DNA. All PCR reactions for this study were performed in a Hybaid thermocycler using the appropriate reaction

---

<sup>4</sup> Isolated from the *Thermus Aquaticus* bacterial species found in hot springs

conditions. The PCR products were analyzed electrophoretically on a 1% agarose gel in comparison to a DNA Molecular weight marker II ( $\lambda$ II) (Roche). PCR products were purified using the High Pure PCR product purification kit (Roche) in accordance to the manufacture's instructions.

**Table 2.2.1** Primer set designed to amplify the VP5 gene of AHSV4 in order to facilitate directional cloning into a pET 41b expression vector.

Primer name	Sequence	Features:	Template	PCR conditions
HS4M6FowNde (Forward primer)	5'- GCACCGCA↓TATGG GAAAGTTCACATC – 3'	Contains an <i>Nde</i> I restriction enzyme site (underlined) to facilitate directional cloning into pET vector DNA.	5' terminal of AHSV4 segment 6	95°C, 2 min. X 1 [95°C, 1 min., 58°C, 45 s 72°C, 2 min] X30 72°C, 10 min
HS4M6EcoRev (Reverse Primer)	5'- CGG↓AATTCGTATG TGTTTTCTCCGCG- 3'	Contains an <i>Eco</i> RI restriction enzyme site (underlined) to facilitate directional cloning into pET vector DNA.	3' terminal of AHSV4 segment 6	

**Table 2.2.2** Custom primers (Invitrogen) designed for this study to produce cDNA transcripts from the AHSV VP5 gene segment.

Name of Primer	Sequence of Primer	T <sub>m</sub> 4(G+C) <sub>n</sub> + 2(A+T) <sub>n</sub>	Target Region	PCR conditions
Forward Primer: HS4VP5Fow	5' GTTAATTTTTCCAGA AGCCATGGGAAG 3'	66.26°C	Upstream non-coding region of first ATG start codon of the VP5 gene of AHSV4.	95°C, 2 min. X 1 [95°C, 45s. 56°C, 45 s. 72°C, 2 min] X30 72°C, 10 min
Reverse Primer: HS4VP5Rev	5' GTATGTGTTTTCTCCG CGCCGTGAG 3'	61.9°C	Non-coding region downstream of the AHSV4 VP5 gene termination codon.	

### 2.2.6. Restriction enzyme digestions

Type II endonucleases can recognize and cleave double stranded DNA in a sequence specific manner. In general, one unit of restriction enzyme will digest 1 $\mu$ g of DNA at 37°C within one hour. Some enzymes have different kinetic properties and require other reaction conditions (Perbal, 1988), i.e. *Pst* I requires 2 hours incubation at 37°C for complete digestion in buffer H. Optimising the enzyme concentration and increasing the reaction volume to allow for the dilution of potential inhibitors, increase restriction enzyme digestion efficiency. Increasing the incubation time also influences efficiency of the enzyme digesting the DNA template in question.

Roche supplied most of the enzymes used in this study and the digestions were carried out in the recommended salt buffer supplied with the enzyme under the conditions described.

### 2.2.7. Dephosphorylation

Dephosphorylation of linearised plasmid vector is necessary to prevent self-ligation and to ensure that only the DNA insert (which is phosphorylated) is able to ligate to the plasmid vector (Hackett *et al.*, 1988). Previously digested DNA was first placed in a water bath at 65°C in order to inactivate residing endonucleases before proceeding with dephosphorylation. According to the manufacturer's instructions, 1 $\mu$ mol of linearised DNA was incubated with 1U Alkaline Phosphatase<sup>5</sup> enzyme (Roche) and 1x 10-dephosphorylation buffer (50mM Tris-HCL, 0.1mM EDTA, pH8.5) to a final reaction volume of 50 $\mu$ l. The reaction was incubated at 37°C for 30 minutes to an hour. Dephosphorylated DNA was consequently purified using the High Pure PCR purification Kit (Roche) prior to ligation.

---

<sup>5</sup> Alkaline phosphatase catalyzes the hydrolysis of the 5' phosphate residues on either side of the linear molecule (Ausabel *et al.*, 1989).

### 2.2.8. Ligation

This procedure allows for the formation of phospho-diester bonds between adjacent 3' hydroxyl and 5' phosphate groups on the ends of the linearised plasmid and insert DNA (Blackburn and Gait, 1996). Both DNA species are required to have compatible sticky ends before ligation can be facilitated. The ligation reaction is catalyzed by the bacteriophage T4 DNA ligase (supplied by Roche).

The procedure involves the addition of DNA fragments to a linearised plasmid vector and incubation with the T4 DNA ligase and the ligation buffer (660mM Tris-HCL, 10mM DTT, 50mM MgCl<sub>2</sub>, 10mM ATP, pH 7.5) at 16°C overnight. The recommended insert to vector molar ratio used was in excess of 3:1. A control reaction, containing only linearised vector DNA was included to determine whether complete endonuclease digestion and dephosphorylation occurred.

### 2.2.9 The bacterial pET expression system

The pET expression system (Novagen) was used to clone and express target genes of interest within this study. The most recent pET vectors designed by Novagen are developed with enhanced features to permit easier subcloning, detection and purification of proteins. These are translation vectors designed to contain the efficient phage T7 ribosome-binding site, which the target gene lacks. Subcloning of foreign DNA (containing the protein-encoding region) into a pET vector is achieved by cloning the insert in a specific orientation using two different unique restriction sites within the multiple cloning region. Specifically, the pET-41b (+) vector was used in this study and it contains the selective marker kan<sup>+</sup> for kanamycin resistance (see Figure 2.2.1 below of pET-41a (+)). The suffix following the name of the pET vector denotes the reading frame relative to the Bam HI cloning recognition site.

Suitable bacterial hosts for cloning include the *E.coli* K12 strains such as Novablue, JM109 and DH5 $\alpha$ . For target gene expression, the recombinant pET vector is transferred to an *E.coli* host strain that contains a chromosomal copy of the T7 RNA polymerase, such as BL21 (DE3), a general-purpose expression

host. This RNA polymerase gene is under *lacUV5* control and expression is allowed by the addition of IPTG<sup>6</sup> to the bacterial culture. Thus, the inducer IPTG tightly controls protein expression from the foreign gene. BL21 strains are *E.coli* B strains, which are deficient in the *lon* protease and lacks the *omp* outer membrane protease that can degrade proteins during purification.

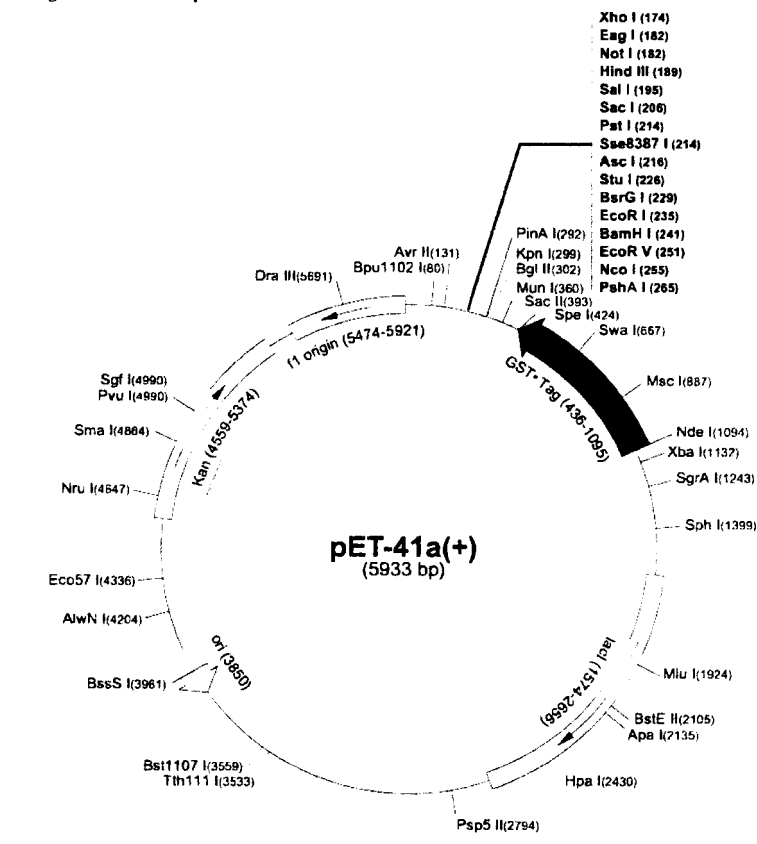


**Figure 2.2.1:** Diagrammatic representation of the pET expression vector (supplied by Novagen). The vector pET-41b (+) is a derivative of the above containing the phage T7 ribosome-binding site and kanamycin resistance selective marker was used in this study.

<sup>6</sup> IPTG: Isopropyl-β-D-thiogalactopyranoside, induces the expression of the T7 RNA polymerase gene under *lacUV5* control within an expression host cell line.



#### 2.2.9.1 Expression of recombinant pET clones:

A recombinant pET construct was used to transform the expression host cell line, BL21 (DE3). Resulting colonies on 50µg/ml kanamycin (kan<sup>+</sup>) (Roche) agar plates were picked and grown in a small volume of kan<sup>+</sup> LB broth, until an OD reading of between 0.6-1.0 was reached. The culture was then incubated at 4°C overnight. A portion of this overnight culture (750µl) was used to inoculate a tube containing 20ml LB broth (kan<sup>+</sup>) and allowed to grow at 37°C with shaking, until an OD reading of between 0.5-0.6 was reached.

For induction of protein expression, freshly prepared 1mmol/ml IPTG (Boehringer Mannheim) was added to the transformed BL21 (DE3) cell cultures and allowed to shake at 37°C. The OD measurements, as well as a 1ml sample for SDS PAGE analysis, of each induced sample was taken at the various time intervals. Before induction, a small aliquot (1ml) of each 20ml culture was retained as uninduced samples for later analysis by SDS-PAGE. All the 1ml samples for later analysis were prepared by first centrifuging at 10000rpm for 1 minute, washing once with PBS and then resuspending the resulting pellet in 30µl of PBS. Each preparation was stored at -20°C for later analysis by SDS PAGE.

#### 2.2.10 Protein electrophoresis and Coomassie blue staining

Electrophoresis of protein samples was facilitated on a denaturing polyacrylamide gel, which allows for the separation of proteins based on molecular size. Before electrophoresis, the mixture of proteins was first dissolved in a sodium dodecyl sulphate (SDS) solution, which is an anionic detergent that disrupts the non-covalent interactions between the proteins (Laemmli, 1970). Addition of β-mercaptoethanol or dithiothreitol (DTT) reduces the disulphide bonds and so aids in the disruption of the proteins' secondary structure. Following electrophoresis, staining with a suitable dye facilitated the visualization of separated proteins (Strachan and Read, 1996). The SDS-PAGE gel consists of a lower resolving (separating) gel and an upper stacking gel that aids to concentrate the sample before its entry into the separating gel

(Rodriguez and Tait, 1983). Mostly 10% separating gels with the standard 5% stacking gels were used in this study, unless stated otherwise.

The separating gel contained the separating buffer (0.375 M Tris-HCl, pH 8.8 and 0.1% SDS), whilst the stacking gel contained the stacking buffer (0.125M Tris-HCl, pH 6.8 and 0.1% SDS). Both gels were prepared from a stock solution of 30% acrylamide and 0.8% bisacrylamide. The gels are chemically polymerized by the addition of 0.008% (v/v) TEMED<sup>7</sup> (Promega) and 0.08% (m/v) ammonium Persulphate (AP).

Prior to electrophoresis on a mini-gel Hoefer electrophoresis system, protein samples were denatured by the addition of an equal volume of 2X Protein Solvent Buffer<sup>8</sup> (PSB) and incubation at 95°C for 5-10 minutes. A Rainbow marker (Amersham) and the appropriate control samples were always included. The samples were electrophoresed between 90 and 120V for approximately 2-3 hours in 1X TGS<sup>9</sup> buffer. The polyacrylamide gel was subsequently stained with Coomassie brilliant blue staining solution (0.125% Coomassie blue, 50% methanol and 10% acetic acid) for 30 minutes at RT. The stained gel was then destained in 5% ethanol and 5% acetic acid, to allow for the reduction in background stain and the visualization of protein bands.

### 2.2.11. <sup>35</sup>S -methionine labeling of expressed proteins

An adapted protocol of the *in vitro* labeling of translation products was used. The experimental procedure as for the expression of pET cloned genes (see 2.2.9.1) was followed, with a few exceptions as follows: After the 20ml transformed expression host cell line reaches an O.D. measurement of 0.5-0.6, 300µl of the culture was retained as an uninduced sample. 5µCi<sup>10</sup> of <sup>35</sup>S-methionine was added to each 300µl sample and incubated for 30 minutes at

---

<sup>7</sup> TEMED: N, N, N', N' tetramethylethylene diamine, catalyzer of polymerizing reaction.

<sup>8</sup> PBS: 125mM Tris-HCL pH6.8, 4% SDS, 0.2% bromophenol blue, 10 % β-mercaptoethanol and 20% glycerol

<sup>9</sup> TGS: 25 mM Tris-HCL pH8.3, 192 mM glycin and 0.1% SDS.

<sup>10</sup> The Curie (Ci) measures the number of radioactive disintergrations occurring each second in a sample. One Ci is the decay rate of 1g of Radium, which is 3.7X10<sup>10</sup> disintergrations per second (McMurry and Castellion, 1996)

37°C with shaking, which consequently labeled the translation products within the cell. The sample was then centrifuged and prepared (as described in 2.2.9.1) for storage at -20°C, until later use in SDS-PAGE analysis.

The remaining culture was induced (as described in 2.2.9.1) with 1mM IPTG and left shaking at 37°C for 30 minutes. The induced culture was divided into two  $\pm$  10ml cultures. 200 $\mu$ g/ml rifampicin<sup>11</sup> antibiotic was added to 1x 10ml culture, in order to inhibit bacterial host cell gene expression and so aid to eliminate background bacterial protein expression. The 1x 10ml culture containing the rifampicin, as well as the culture without was left to shake for a further 30 minutes at 37°C before 300 $\mu$ l was removed and 5 $\mu$ Ci of <sup>35</sup>S-methionine was added. The culture was allowed to shake for a further 15-45 minutes at 37°C to allow for incorporation of the labeled methionine. The labeled samples were centrifuged and prepared as described (2.2.9.1) for storage at -20°C, until later use in SDS-PAGE analysis. Instead of staining the polyacrylamide gel after electrophoresis with Coomassie blue, the gel was dried in a DrygelSr- Slab gel dryer, model SE1160 (Hoefer Scientific Instruments) for at least two hours before exposing to a phosphorus screen used for visualization in a BIORAD gel doc system. Both the gel and screen were loaded into a cassette to allow for exposure upon contact. Depending on the concentration of the samples electrophoresed on the acrylamide gel, the length of exposure time needed was determined. Approximately 12-24 hours of exposure was utilized to allow for sufficient radioactive signal to be detected by the CCD camera within the apparatus.

### 2.2.12 TCA precipitation of proteins

In order to obtain the proteins from the cell culture supernatant, the proteins were precipitated by the addition of Trichloroacetic acid (TCA). For every 100 $\mu$ l of supernatant, 10 $\mu$ l of 100% TCA was added. The solution was mixed well and then incubated on ice for 1 hour. The mixture was centrifuged at 15000r.p.m

---

<sup>11</sup> Rifampicin: is a potent inhibitor of transcription by interacting directly with one of the subunits of RNA polymerase and inhibits initiation of RNA synthesis (Blackburn and Gait, 1996).

for 20 minutes at 4°C. All traces of the supernatant were removed and the pellet was resuspended in 15µl 2x PBS for further analysis by SDS-PAGE.

### 2.2.13 Preparation cDNA from dsRNA

#### 2.2.13.1 Virus isolates and viral dsRNA

The Onderstepoort Veterinary Institute or Equine Research Centre, Onderstepoort provided various AHSV field isolates. Viruses were originally isolated from the blood/organs of horses that had died of the disease, and cultivated between four and six times on cultured Baby Hamster Kidney cells to ensure that the viral progeny remained genetically as close as possible to the original field viruses. For the purposes of this study, the viral stocks were assumed to be virulent. The viruses included the following serotypes and isolates: AHSV3 M322/97 (AHSV3vir1), AHSV3 E73/02 (AHSV3vir2), AHSV6 6/98 (AHSV6vir1), AHSV6 E1/02 (AHSV6vir2), AHSV8 7/98 (AHSV8vir), AHSV9 E41/02 (AHSV9vir). The names indicated in brackets will be used throughout this study.

Double stranded RNA of viral stocks were isolated using Trizol® (Life Technologies) and were provided by Dr Wilma Fick (University of Pretoria).

#### 2.2.13.2 Denaturation of dsRNA

Trizol® purified (Life Technologies) double-stranded RNA (dsRNA) was denatured by the addition of Methyl-Mercury Hydroxide (MMOH) and β-mercaptoethanol. Basically, 5µl of dsRNA and an equal volume of MMOH were mixed and incubated at 25°C for 10 minutes. Consequently, 2µl β-mercaptoethanol and 2µl RNAsin (Promega), which aids to inhibit RNases, was added and incubated at the same temperature for a further 5 minutes.

#### 2.2.13.3 Generation of cDNA species

To 4µl of denatured dsRNA, 100pmol of both the forward and reverse gene-specific oligonucleotide primers, one-fifth-reaction volume 10mM dNTPs (Promega), 5X Reverse transcriptase buffer (Invitrogen), 2µl 0.1M DTT (Invitrogen) and 1µl high fidelity Superscript™ II RNase H- Reverse

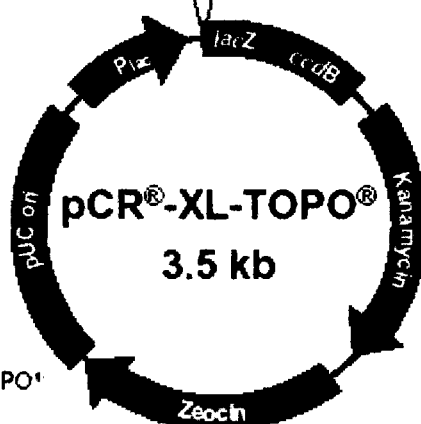
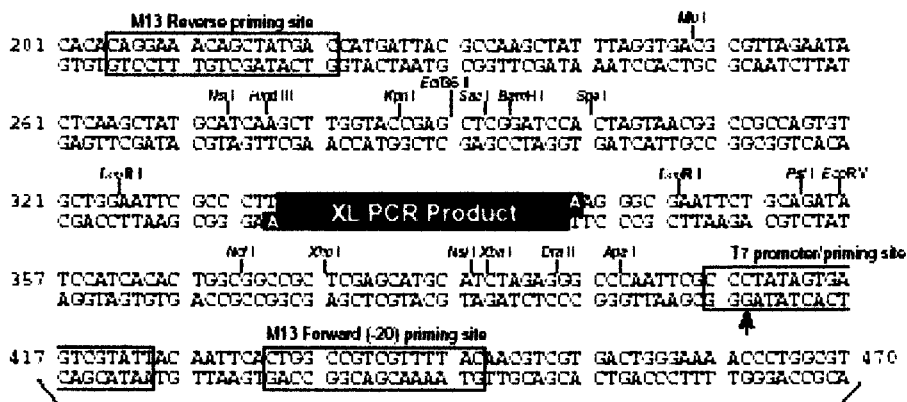
Transcriptase (Invitrogen) was added. The reaction was mixed and incubated at 42°C for 1 hour. In most cases, the cDNA obtained was diluted one-tenth in Sabax water and amplified by PCR (*as described in 2.2.5*).

#### 2.2.14 Cloning of target genes

The cloning strategy of choice was to use the TOPO® XL PCR cloning kit (Invitrogen). Long PCR products are cloned very efficiently by this 5-minute, one-step cloning strategy without the use of DNA ligase or specific primers.

In order to clone these PCR products, it was preferable to first gel purify the amplified DNA species. With traditional ethidium bromide staining of agarose gels, large DNA molecules can be damaged when exposed to UV light and thus can significantly decrease cloning efficiency. Hence, the visualization and purification of PCR products by agarose gel electrophoresis using crystal violet (provided for in the S.N.A.P™ UV-free Gel purification kit utilized by Invitrogen) was done. Crystal violet is non-mutagenic and DNA can be visualized under normal light as thin violet bands after electrophoresis. The PCR product bands within the agarose gels were excised and gel-purified using the S.N.A.P™ UV-free Gel purification kit (Invitrogen) according to the manufacturer's instructions and eluted in 40µl sterile water or T.E Buffer.

The purified genes were cloned into the plasmid vector pCR®-XL-TOPO® according to the manufacture's instructions and transformed into chemically competent TOP10F cells provided in the kit. The pCR®-XL-TOPO® vector (see Figure 2.2.2) is kanamycin (kan+) resistant and so 20-150µl of each transformation reaction was plated out on pre-warmed LB plates containing 50µg/ml kan+ and incubated at 37°C overnight. Colonies were picked with sterile toothpicks and allowed to grow O/N in kan+ LB broth for subsequent plasmid purification. Purified plasmid preparations were digested with specified enzyme (s) to confirm the correct cloning of the targeted gene into the plasmid vector. Once the presence of the cloned gene was confirmed, plasmid preparations were purified with the High Pure PCR kit (Roche) for sequencing analyses.



Comments for pCR<sup>®</sup>-XL-TOPO<sup>®</sup>  
3519 nucleotides

Lac promoter/operator region: bases 95-216  
 M13 Reverse priming site: bases 205-221  
 Lac Za ORF: bases 217-576  
 Multiple Cloning Site: bases 248-399  
 TOPO<sup>®</sup> Cloning site: bases 336-337  
 T7 promoter priming site: bases 406-425  
 M13 Forward (-20) priming site: bases 433-448  
 Fusion joint: bases 577-585  
 ccdB lethal gene ORF: bases 586-888  
 Kanamycin resistance ORF: bases 1237-2031  
 Zeocin resistance ORF: bases 2238-2612  
 pUC origin: bases 2680-3393

**Figure 2.2.2** Diagrammatic representation of the PCR<sup>®</sup>-XL-TOPO<sup>®</sup> vector map. Features of the vector as well as sequences surrounding the TOPO TA Cloning<sup>®</sup> site are shown. The arrow indicates the start of transcription for T7 polymerase.

### 2.2.15. DNA sequencing:

DNA polymerase is utilized in the Sanger dideoxy method of DNA sequencing by enzymatically elongating DNA molecules in one chemical reaction. A series of single stranded DNA molecules of differing lengths are generated by the incorporation of a dideoxy chain terminator by DNA polymerase. The DNA fragments are labeled with four different fluorescent dyes that can be detected

by automated DNA sequencers. The labeled DNA fragments are loaded into a single lane of a vertical gel made from polymerized acrylamide and separated by electrophoresis in lengths differing by as little as one nucleotide (Klug and Cummins, 1997). As the DNA fragments pass through the lower gel region, a scanning laser results in the excitement of the fluorescent dyes. Light wavelengths specific for each dye is emitted and collected into channels that are consequently separated by a spectrograph on a charge coupled device (CCD) camera. The light intensities are collected from the CCD camera by DATA collection software and stored on a Macintosh PC as digital signals for processing (ABI prism DNA sequencing Chemistries).

Sequencing reactions were performed using the ABI Prism BigDye® Terminator cycle sequencing Ready Reaction Kit version 3.1 (Applied Biosystems). Approximately 350ng of template DNA, together with 3.2pmol of a specified primer (all the primers used in sequencing reactions are described in Table 2.2.3) as well as 4µl of Terminator Ready Reaction mix (supplied in the kit) were added to the 0.2µl PCR tube and mixed well before placing on ice for subsequent cycle sequencing.

#### 2.2.15.1. Cycle Sequencing:

All reactions were cycle sequenced in a Perkin Elmer GeneAmp PCR 9600 system, according to the following cycling parameters: 25 cycles of denaturation (by rapid thermal ramp to 96°C for 10 seconds), primer annealing (by rapid thermal ramp to 50°C for 5 seconds) and primer extension (by rapid thermal ramp to 60°C for 4 minutes). After 25 cycles, a rapid ramp to 4°C was initiated to keep the samples cold until removed. The unincorporated dye terminators were removed by ethanol/NaOAc precipitation.

#### 2.2.15.2 Ethanol precipitation of cycle sequence products:

To each cycle-sequenced reaction, 2µl of 3M Sodium acetate (NaOAc), pH 4.6 and 50µl 99.9% ethanol was added and incubated on ice for 10 minutes. This step allowed for the precipitation of the extension products, which was subsequently collected by centrifugation at 13000r.p.m for 20 minutes. The



supernatant containing the unincorporated dye products was aspirated and discarded. The pellet was washed with freshly prepared 70% Ethanol and centrifuged again for 10 minutes. The pellet was air-dried and left at -20°C before sequencing. Each pellet was resuspended in 6µl loading buffer (deionised formamide, 25mM EDTA, pH 8 and 50mg/ml blue dextran). The sample was denatured at 95°C for 2 minutes and placed on ice prior to loading onto a sequencing gel. All samples were separated by electrophoresis in an ABI Prism 377 DNA sequencer.

**Table 2.2.3 Oligonucleotide primers used in this study to amplify and sequence various regions of the AHSV VP5 gene.**

Primer name	Primer sequence	Target
M13 Forward (Invitrogen)	5' CATTTCGCTGCCGGTC 3'	M13 Forward (-20) priming site: bases 433-448 on pCR®-XL-TOPO® vector.
M13 Reverse (Invitrogen)	5' GTCCTTTGTCGATACTG 3'	M13 Reverse priming site: bases 205-221 on pCR®-XL-TOPO® vector.
VP5HS3/8 INT Internal forward primer	5' GAACTTCAGACGAGACGAGGAT 3'	VP5HS3/8INT binding site: bases 569 - 590 on the coding strand of the VP5 gene from AHSV serotypes 3 and 8.
VP5IF3/9 Internal forward primer	5' AGGAAGATCGTGTGATTG 3'	Binds approximately 380bp downstream of the ATG start codon in the VP5 gene of AHSV3 and 9.
VP5IR3/9 Internal reverse primer	5' TGGGGTATGCTCTGAATG 3'	Binds approximately 1160bp downstream of the ATG start codon in the VP5 gene of AHSV3 and 9.



## **2.3 Results**

### **2.3.1 Preparation of AHSV M6 cDNA for cloning purposes.**

Trizol® purified (Life Technologies) double-stranded RNA (dsRNA) from AHSV3vir2, AHSV6vir2 and AHSV9vir field isolates [section 2.2.13.1] were provided by Dr Wilma Fick (University of Pretoria). These strains, originally isolated from horses that had died of AHS, were cultivated for a minimal number of passages in BHK cells and therefore assumed to be virulent.

AHSV4 VP5 specific primers (Table 2.2.2) were used to generate M6 cDNA by reverse transcription and then amplified by PCR (see 2.2.5). It was anticipated that these primers would allow reverse transcription and amplification of the M6 gene across the different serotypes, given that enough homology existed in the 5' and 3' non-coding regions of the gene. Samples from each reaction was analyzed on an agarose gel (Figure 2.3.1) and showed an amplified product of the expected size, approximately 1.6 Kb in length, for AHSV3vir2 (lane 3), AHSV6vir2 (lane 4) and AHSV9vir (lane 5). Amplification from AHSV4 M6 cDNA (Figure 2.3.1, lane 2) was used as a positive control to ensure that the correct sized products were amplified from the other isolates. A substantial amount of non-specific amplification evident in lanes 3-5 (Fig 2.3.1) indicated that the primers were not 100% homologous across the serotypes, and that cDNA synthesis and/or PCR conditions were not fully optimized.

Since the M6 segments represented the majority of amplified products in the respective samples, it was decided to excise and purify the desired fragments from agarose in order to obtain enough for cloning purposes. A large scale preparation of reverse transcribed and amplified product from each viral isolate was prepared, separated on a preparative gel (results not shown) and the correct sized band (approximately 1.6 Kb) representing the amplified M6 product was excised from the gel and purified using the S.N.A.P™ UV-free gel purification kit (see 2.2.14).

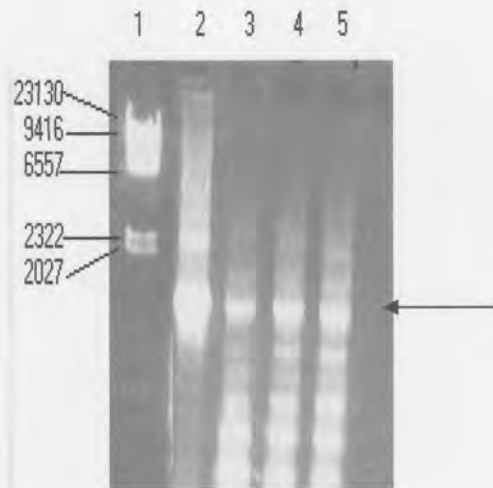


**Figure 2.3.1:** 1% Agarose gel of electrophoresed cDNA species amplified by PCR with AHSV4 VP5 specific primers. Lane 1: Molecular weight marker II (MWII), lane 2: PCR product from AHSV4 (positive control) sample lane 3: PCR product from AHSV3vir2, lane 4: PCR product from AHSV6vir2 and lane 5: PCR product from AHSV9vir. Arrow indicates the size of the M6 PCR product.

Other viral M6 gene samples were obtained in the form of purified M6 PCR products from AHSV3vir1, AHSV6vir1 and AHSV8vir field isolates, as prepared via reverse transcriptase PCR by Dr. Fick (University of Pretoria). Large scale PCR products of these were also prepared and excised from preparative gels as mentioned above, with the purpose of cloning and including these genes in further analyses.

### 2.3.2: Cloning of AHSV M6 gene segments

Purified PCR products of the M6 gene segment prepared from dsRNA in this study (from AHSV3vir2, AHSV6vir2 and AHSV9vir), as well as those provided as PCR products (from AHSV3vir1, AHSV6vir1 and AHSV8vir) were cloned into the pCR®-XL-TOPO® vector as described in 2.2.14. A kanamycin-resistant gene present on the plasmid vector allowed for the selection of recombinants. Following transformation, cells were plated onto kan<sup>+</sup> agar plates and a number of colonies selected for further analyses. For most of the cloning procedures, large numbers of colonies, i.e. in the excess of 150, were obtained after cloning. For some however, for example AHSV6vir1 M6, cloning was not as efficient and a total of 4 colonies were obtained. Representative samples of some of the

plasmids purified from these colonies were taken and analyzed by agarose gel electrophoresis, Figures 2.3.2 A and B. Size comparisons using two known Topo /AHSV4M6 recombinants from a colleague (Fig 2.3.2B -compare lanes 5, 6 with lanes 3, 4 and 7-14) suggested that some plasmids were recombinant, while the size of others (see lanes 8 and 9) were too small and probably represented non-recombinant vector.

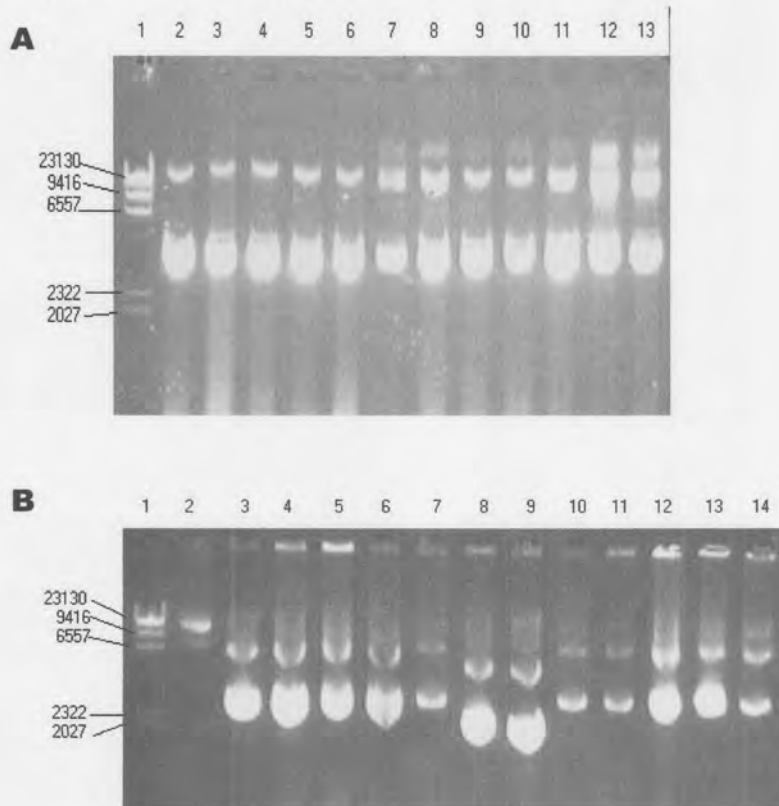


**Figure 2.3.2** 1% Agarose gel electrophoretic analysis of some plasmids obtained after cloning into the PCR®-XL-TOPO® vector.

- A.** Lane 1: MWII, lane 2-7: Plasmids from the cloning of AHSV3vir1 M6, Lanes 8-13: Plasmids from the cloning of AHSV8vir M6
- B.** Lane 1: MWII, lane 2, 5, 6: Plasmids from cloning AHSV4vir M6 (J. Korsmann, UP), lanes 3 and 4: Plasmids from cloning AHSV3vir2 M6, lanes 7-10: Plasmids from the cloning of AHSV6vir2 M6 and lanes 11-14: Plasmids from the cloning of AHSV9vir2 M6.

Putative recombinants were then analyzed by restriction enzyme digestion with *Eco* RI. Since two *Eco* RI sites flank the cloning site in the pCR®-XL-TOPO® vector, digestion allows for the excision of the cloned gene segment. Some of the plasmids with the correct sized insert of approximately 1.6 Kb are shown (Fig



2.3.3 A and B). *Eco* RI digestion of the Topo/AHSV8vir M6 recombinants resulted in the insert being excised as two fragments of approximately 1.2Kb and 400bp in length (Fig 2.3.3 B lanes 8-12), indicating that the M6 gene of AHSV8 has an internal *Eco* RI restriction enzyme site.

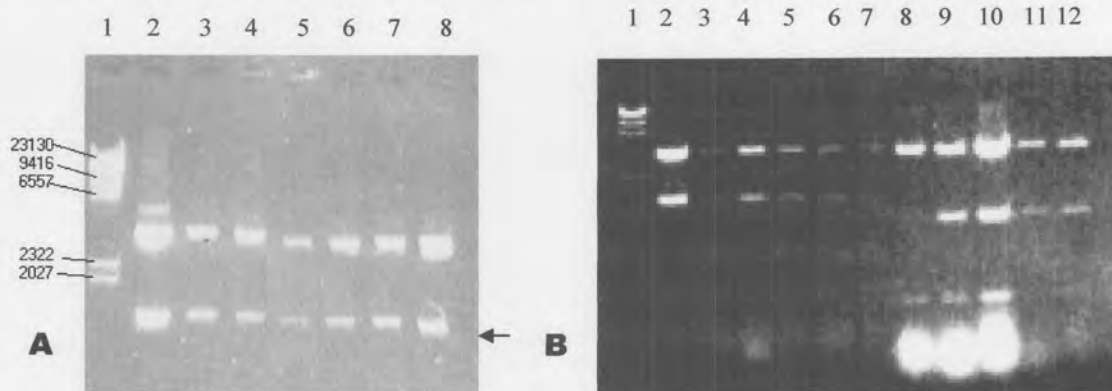


**Figure 2.3.3** 1% Agarose gel electrophoretic analysis of putative AHSV M6 recombinants by *Eco* RI digestion.

- A** Lane 1: MW II; lane 2: Topo/AHSV4vir M6, lanes 3, 4: Topo/AHSV3vir2 M6; lanes 5, 6: Topo/AHSV6vir2 M6; lanes 7, 8: Topo/AHSV9virM6. Arrow indicates the excised M6 gene segment.
- B** Lane 1: MW II; lane 2: Topo/AHSV6vir1 M6, lanes 3-7: Topo/AHSV3vir1 M6; lanes 8-12: Topo/AHSV8vir M6

Identification of recombinants containing the full-length M6 gene segment was aided by amplification by PCR using the same AHSV4 VP5 specific primer set used to amplify the M6 gene segment from the cDNA (HS4VP5Fow and HS4VP5Rev).



**Figure 2.3.4** 1% Agarose gel electrophoretic analysis of PCR products amplified with AHSV4 VP5 specific primers to confirm the sizes of gene inserts. Lane 1: MWII, lane 2: Insert of Topo/AHSV4vir M6 recombinant representing full-length gene of 1.6Kb (positive control), lane 3-7: Inserts of selected Topo/AHSV3vir2 M6 recombinants.

As seen in Figure 2.3.4, some recombinants showed the correct size product (lane 3) and others not (lanes 4-7) when compared to a positive control and measured against the included molecular marker. Consequently, only correct clones were chosen for each serotype and purified on large scale for use in sequencing analysis.

### 2.3.3 Nucleotide sequence analysis

The complete nucleotide sequence of the various AHSV M6 gene segments was determined and is shown in Figures 2.3.5 (AHSV3vir1 field M6 gene segment); 2.3.6 (AHSV3vir2 field M6 gene segment); 2.3.7 (AHSV6vir1 field M6 gene segment); 2.3.8 (AHSV6vir2 field M6 gene segment); 2.3.9 (AHSV8vir field M6 gene segment) and 2.3.10 (AHSV9vir field M6 gene segment). The entire M6 gene segment of each serotype was sequenced in both directions using all the primers mentioned in Table 2.2.3. As of yet, no AHSV8 VP5 gene sequences have been published.

All the genes were 1566bp long, similar to other M6 genes sequenced to date (see Table 2.1.1, pg 33) with non-coding regions of 19 nucleotides at the 5' terminal region and 29 nucleotides at the 3' terminal region. The sizes of the non-coding regions also correlate to that of AHSV9, as reported by Du Plessis and Nel (1997).

All the conserved 5' and 3' hexanucleotides of the M6 genes are underlined in the accompanying Figures and were determined to be GTTAAT and ACATAC respectively. These hexanucleotide sequences are found to be in agreement with the AHSV terminal sequences published by Mizukoshi *et al.*, (1993) as being 5' GTT (A/T) A (A/T) and (C/A) C (T/A) TAC 3' on the RNA level. The longest open reading frame (ORF) was defined by the ATG start codon immediately adjacent to the 19 nucleotide long non-coding region at the 5' terminus and ends with a TGA stop codon, 29 nucleotides from the 3' terminus. The nucleotide composition (as determined with the computer program DNAssist, version 2.0) of all the serotypes sequenced is tabulated in Table 2.3.1 and shows that VP5 is AT rich (~58%) across all the genes analyzed.

ttgttaaatttttccagaagccATGGGAAAGTTCACATCCTTCTTGAAGCGTGCGGGTAGCGCAACCAAGAAAGCACTAACTTCAGATGCG 23  
 90  
 A K R M Y K M A G K T L Q K V V E S E V G S A A I D G V M Q 53  
 GCTAAAAGGATGTATAAGATGGCTGGTAAAACGTTACAGAAAAGTCGTAGAAAAGTGGGTAAGCGCGCGGATAGATGGAGTAATGCAA 180  
 G T I Q S I I Q G E N L G D S I K Q A V I L N V A G T L E S 83  
 GGAACAATTTCAGAGCATAATACAGGGTGAATAATTTGGGGGACTCAATCAAACAAGCAGTAATTTTGAACGTAGCTGGCACGTTAGAGTCG 270  
 A P D P L S P G E Q L L Y N K V S E I E R A E K E D R V I E 113  
 GCTCCAGACCCATTAAGCCCAGGTGAACAATATTATATAATAAAGTATCTGAAATCGAAAGAGCGGAGAAGGAAGATCGTGTGATTGAG 360  
 T H N K K I V E K Y G E D L L K I R K I M K G E A E A E Q L 143  
 ACACATAATAAAAAGATTGTCGAAAAGTATGGGGAAGATTTATTGAAGATCCGGAAAATAATGAAGGGAGAGGCTGAAGCAGAGCAGCTC 450  
 E G K E M E Y V E K A L R G M L K I G K D Q S E R I T R L Y 173  
 GAAGGAAAAGAAATGGAATATGTCGAAAAGCGCTAAGGGGCATGCTGAAAATCGGAAAAGATCAATCTGAGCGTATTACACGGTTGTAC 540  
 R A L Q T E E D L R T S D E T R I I S E Y R E K F D A L K Q 203  
 CGCGCTCTCAAACGGAGGAGGATTTAAGAACTTCGGATGAGACGAGGATCATCAGCGAGTATAGAGAAAAATTTGATGCATTGAAACAG 630  
 A I E L E Q Q A T H E E A V Q E M L D L S A E V I E T A A E 233  
 GCGATTGAACCTTGAACAGCAGGCAACGCATGAAGAAGCTGTGCAGGAAATGTTGGATTTAAGTGCCGAGGTCATCGAAACGGCGGCTGAG 720  
 E V P V F G A G A A N V V A T T R A I Q G G L K L K E I I D 263  
 GAGGTGCCAGTCTTTGGCGCAGGCGCAGCAATGTTGTTGCGACGACCGCGCAATCCAAGGAGGCCTAAAGCTGAAGGAGATAATAGAT 810  
 K L T G I D L S H L K V A D I H P H I I E K A M L K D K I P 293  
 AAACCTCACAGGGATCGATCTCTCCATTTGAAAGTAGCAGATATTCATCCTCACATAATTGAGAAAAGCAATGTTAAAGGATAAAAATCC 900  
 D N E L A M A I K S K V E V V D E M N T E T E H V I E S I M 323  
 GACAACGAGTTAGCGATGGCGATAAAGTCAAGGTTGAGGTTGTCGATGAGATGAATACGGAGACGGAACACGTTATAGAGTCCATCATG 990  
 P L V K K E Y E K H D N K Y H V N I P S A L K I H S E H T P 353  
 CCTCTAGTGAAGAAAGAAATACGAAAAGCATGATAACAAATACCATGTAATATACCAAGTGCCTTGAAAATACATTCAGAGCATACGCCA 1080  
 K V H I Y T T P W D S D K V F I C R C I A P H H Q Q R S F M 383  
 AAGGTACACATATACTACACCGTGGGACTCTGATAAAGTTTTTATATGCAGATGCATTGCGCCACATCACCAGCAGAGGAGTTTTATG 1170  
 I G F D L E I E F V F Y E D T S V E G H I M H G G A V S I E 413  
 ATTGGATTTGATTTAGAGATTGAATTTGTCTTCTATGAAGATACCTCGGTTGAGGGTCACATTTATGCATGGGGGAGCGGTGTCGATTGAG 1260  
 G R G F R Q A Y S E F M N A A W S M P S T P E L H K R R L Q 443  
 GGACGAGGATTTAGACAGGCTTATAGTGAGTTCATGAACCGGCTTGGTCTATGCCTCGACTCCAGAGCTACATAAGAGAAGGTTACAA 1350  
 R S L G S H P I Y M G S M D Y T I S Y E Q L V S N A M K L V 473  
 CGTAGTCTGGGCTCACATCCGATTTATATGGGATCGATGGATTATACCATAAGTTATGAACAGCTCGTTTCGAACCGCATGAAGTTAGTC 1440  
 Y D T D L Q M H C L R G P L K F Q R R T L M N A L L F G V K 503  
 TATGACACGGACCTACAGATGCACTGTTTACGTGGACCACTGAAATTCCAAAGGCGCACCTGATGAACGCGCTTCTCTTTGGTGTGAAA 1530  
 V A \* 505  
 GTAGCTTgaaagcctcacggcgcgagaaaaacatac 1568

**Figure 2.3.5** The complete nucleotide and deduced amino acid sequence of the AHSV3vir1 M6 gene. The conserved 5' and 3' hexanucleotides are underlined and the termination codon is marked with a \*.

M G K F T S F L K R A G S A T K K A L T S D A 23  
ttgtaatttttccagaagccATGGGAAAGTTCACATCCTTCTTGAAGCGTGCGGGTAGCGCAACCAAGAAAGCACTAACTTCAGATGCG 90  
 A K R M Y K M A G K T L Q K V V E S E V G S A A I D G V M Q 53  
 GCTAAAAGGATGTATAAGATGGCTGGTAAAACGTTACAGAAAGTCGTAGAAAGTGAGGTGGGAAGCGCGCGATAGATGGAGTAATGCAA 180  
 G T I Q S I I Q G E N L G D S I K Q A V I L N V A G T L E S 83  
 GGAACAATTCAGAGCATAATACAGGGTAAAATTTGGGGACTCAATCAAACAAGCAGTAATTTTGAACGTAGCTGGCACGTTAGAGTCG 270  
 A P D P L S P G E Q L L Y N K V S E I E R A E K E D R V I E 113  
 GCTCCAGACCCATTAAGCCAGGTGAACAACCTATTATATAATAAAGTATCTGAAATCGAAAGAGCGGAGAAGGAAGATCGTGTGATTGAG 360  
 T H N K K I V E K Y G E D L L K I R K I M K G E A Q A E Q L 143  
 ACACATAATAAAAAGATTGTGAAAAGTATGGGGAAGATTTATTGAAGATCCGAAAATAATGAAGGGAGAGGCTCAAGCAGAGCAGCTC 450  
 E G K E M E Y V E K A L G G L L K I G K D Q S E R I T R L Y 173  
 GAAGAAAAGAAATGGAATACGTCGAAAAGCGCTAGGGGGCTTCTGAAAATCGGGAAAGATCAATCTGAGCGTATTACACGGTTGTAC 540  
 R A L Q T E E D L R T S D E T R I I S E Y R E K F D A L K Q 203  
 CGCGCTCTCCAACGGAGGAGGATTTAAGAACTTCGGATGAGACGAGGATCATCAGCGAGTATAGAGAAAAATTTGATGCATTGAAACAG 630  
 A I E L E Q Q A T H E E A V Q E M L D L S A E V I E T A A E 233  
 GCGATTGAACCTGAACAGCAGGCAACGCATGAAGAAGCTGTGCAGGAAATGTTGGATTTAAGTGCCGAGGTCATCGAAACGGCGGCTGAG 720  
 E V P V F G A G A A N V V A T T R A I Q G G L K L K E I I D 263  
 GAGGTGCCAGTCTTTGGCGCAGGCGCAGCAAATGTTGTTGCGACGACACGCGCAATCCAAGGAGGCCTAAAGCTGAAGGAGATAATAGAT 810  
 K L T G I D L S H L K V A D I H P H I I E K A M L K D K I P 293  
 AAACCTCACAGGGATCGATCTCTCCATTTGAAAGTAGCAGATATTCATCCTCACATAATTGAGAAAGCAATGTTAAAGGATAAAAATCC 900  
 D N E L A M A I K S K V E V V D E M N T E T E H V I E S I M 323  
 GACAACGAGTTAGCAATGGCGATAAAGTCGAAGGTTGAGGTTGTGATGAGATGAATACGGAGACGGAACACGTTATAGAGTCCATCATG 990  
 P L V K K E Y E K H D N K Y H V N I P S A L K I H S E H T P 353  
 CCTCTAGTGAAGAAAGAATACGAAAAGCATGATAACAAATACCATGTAAATATACCAAGTGCCTTGAAAATACATTACAGACATACGCCA 1080  
 K V H I Y T T P W D S D K V F I C R C I A P H H Q Q R S F M 383  
 AAGGTACACATATACTACACCGTGGGACTCTGATAAAGTTTTTCATATGCAGATGCATTGCCACATCACCAGCAGAGGAGTTTTATG 1170  
 I G F D L E I E F V F Y E D T S V V G H I M H G G A V S I E 413  
 ATCGGATTTGATTTAGAGATTGAATTTGCTTCTATGAAGATACCTCGGTTGTGGGTCACATTATGCATGGGGAGCGGTGTCGATTGAG 1260  
 G R G F R Q A Y S E F M N A A W S M P S T P E L H K R R L Q 443  
 GGACGAGGATTTAGACAGGCTTATAGTGAGTTCATGAACGCGGCTTGGTCTATGCCCTCGACTCCAGAGCTACATAAGAGAAGGTTACAA 1350  
 R S L G S H P I Y M G S M D Y T I S Y E Q L V S N A M K L V 473  
 CGTAGTCTGGGCTCACATCCGATTTATATGGGATCGATGGATTATACCATAAGTTATGAACAGCTCGTTTCGAACGCGATGAAGTTAGTC 1440  
 Y D T D L Q M H C L R G P L K F Q R R T L M N A L L F G V K 503  
 TATGACACGGACCTACAGATGCACTGTTTACGTGGACCACTGAAATTCAAAGGCGACCCTGATGAACGCGCTTCTCTTTGGTGTGAAA 1530  
 V A \* 505  
 GTAGCTtgaagcctcacggcgaggagaaaacacatac 1568

**Figure 2.3.6 The complete nucleotide and deduced amino acid sequence of AHSV3vir2 M6 gene. The conserved 5' and 3' hexanucleotides are underlined and the termination codon is marked with a \*.**

```

M G K F T S F L K R A G S A T K K A L T S D A 23
ttgttaattttttccagaagccATGGGAAAGTTCACATCCTTCTTGAAGCGTGCGGGTAGCGCAACCAAGAAAGCACTAACTTCAGATGCG 90

A K R M Y K M A G K T L Q K V V E S E V G S A A I D G V M Q 53
GCTAAAAGGATGTATAAGATGGCTGGTAAAACGTTACAGAAAGTCGTAGAAAGTGAGGTGGGAAGCGCGGCGATAGATGGAGTAATGCAA 180

G T I Q S I I Q G E N L G D S I K Q A V I L N V A G T L E S 83
GGAACAATTTCAGAGCATAATACAGGGTAAAATTTGGGGGACTCAATCAAACAAGCAGTAATTTTGAACGTAGCTGGCACGTTAGAGTCG 270

A P D P L S P G E Q L L Y N K V S E I E R A E K E D R V I E 113
GCTCCAGACCCATTAAGCCCAGGTGAACAACCTATTATATAATAAAGTATCTGAAATCGAAAGAGCGGAGAAGGAAGATCGTGTGATTGAG 360

T H N K K I V E K Y G E D L L K I R K I M K G E A E A E Q L 143
ACACATAATAAAAAGATTGTCGAAAAGTATGGGGAGATTTTATGAAGATCCGAAAATAATGAAGGGAGAGGCTGAAGCAGAGCAGCTC 450

E G K E M E Y V E K A L R G M L K I G K D Q S E R I T R L Y 173
GAAGGAAAAGAAATGGAATACGTCGAAAAGCGCTAAGGGGCTGCTGAAAATCGGGAAAGATCAATCTGAGCGTATTACACGGTTGTAC 540

R A L Q T E E D L R T S D E T R I I S E Y R E K F D A L K Q 203
CGCGTCTCCAAACGGAGGAGGATTTAAGAAGTTCGGATGAGACGAGGATCATCAGCGAGTATAGAGAAAAATTTGATGCATGAAACAG 630

A I E L E Q Q A T H E E A V Q E M L D L S A E V I E T A A E 233
GCGATTGAACCTGAACAGCAGGCAACGCATGAAGAAGCTGTGCAGGAAATGTTGGATTTAAGTCCGAGGTCATCGAAACGGCGGCTGAG 720

E V P V F G A G A A N V V A T T R A I Q G G L K L K E I I D 263
GAGGTGCCAGTCTTTGGCGCAGGCGCAGCAAATGTTGTTGCGACGACCGCAATCCAAGGAGGCCTAAAGCTGAAGGAGATAATAGAT 810

K L T G I D L S H L K V A D I H P H I I E K A M L K D K I P 293
AAACTCACAGGGATCGATCTCTCCCATTTGAAAGTAGCAGATATTCATCCTCACATAATTGAGAAAGCAATGTTAAAGGATAAAATTCCC 900

D N E L A M A I K S K V E V V D E M N T E T E H V I E S I M 323
GACAACGAGTTAGCAATGGCGATAAAGTGAAGGTTGAGGTTGTCGATGAGATGAATACGGAGACGGAACACGTTATAGAGTCCATCATG 990

P L V K K E Y E K H D N K Y H V N I P S A L K I H S E H T P 353
CCTCTAGTGAAGAAAGAATACGAAAAGCATGATAACAAATACCATGTAATATAACCAAGTGCCTGAAAATACATTTCAGAGCATACGCCA 1080

K V H I Y T T P W D S D K V F I C R C I A P H H Q Q R S F M 383
AAGGTACACATATACTACACCGTGGACTCTGATAAAGTTTTTCATATGCAGATGCATTGCGCCACATCACCAGCAGAGGAGTTTTATG 1170

I G F D L E I E F V F Y E D T S V E G H I M H G G A V S I E 413
ATCGGATTTGATTTAGAGATTGAATTTGCTTCTATGAAGATACCTCGGTTGAGGGTCACATTATGCATGGGGGAGCGGTGTCGATTGAG 1260

G R G F R Q A Y S E F M N A A W S M P S T P E L H K R R L Q 443
GGACGAGGATTTAGACAGGCTTATAGTGAGTTCATGAACGCGGCTTGGTCTATGCCTCGACTCCAGAGCTACATAAGAGAAGGTTACAA 1350

R S L G S H P I Y M G S M D Y T I S Y E Q L V S N A M K L V 473
CGTAGTCTGGGCTCACATCCGATTTATATGGGATCGATGGATTATACCATAAGTTACGAACAGCTCGTTTCGAACGCGATGAAGTTAGTC 1440

Y D T D L Q M H C L R G P L K F Q R R T L M N A L L F G V K 503
TATGACACGGACCTACAGATGCACTGTTTACGTGGACCACTGAAATTCCAAAGGCGCACCTGATGAACGCGCTTCTCTTTGGTGTGAAA 1530

V A * 505
GTAGCTtgaagcctcacggcgcgagaaaacacatac 1568

```

**Figure 2.3.7** The complete nucleotide and deduced amino acid sequence of AHSV6vir1 M6 gene. The conserved 5' and 3' hexanucleotides are underlined and the termination codon is marked with a \*.



M G K F T S F L K R T G S A T K K A L T S D A 23  
ttgtaatttttccagaagccATGGGAAAGTTCACATCCTTCTTGAAGCGTACGGGTAGCGCAACCAAGAAAGCACTAACTTCAGATGCG 90  
 A K R M Y K M A G K T L Q K V V E S E V G S A A I D G V M Q 53  
 GCTAAAAGGATGTATAAGATGGCTGGTAAAACGTTACAGAAAGTCGTAGAAAGTGAGGTGGGAAGCGCGGCGATAGATGGAGTAATGCAA 180  
 G T I Q S I I Q G E N L G D S I K Q A V I L N V A G T L E S 83  
 GGAACAATTCAGAGCATAATACAGGGTAAAATTTGGGGGACTCAATCAAACAAGCAGTAATTTTGAACGTAGCTGGCACGTTAGAGTCCG 270  
 A P D P L S P G E Q L L Y N K V S E I E R A E K E D R V I E 113  
 GCTCCAGACCCATTAAGCCAGGTGAACAACACTATTATATAATAAAGTATCTGAAATCGAAAGAGCGGAGAAGGAAGATCGTGTGATTGAG 360  
 I H N K K I V E K Y G E D L L K I R K I M K G E A E A E Q L 143  
 ATACATAATAAAAAGATCGTCGAAAAGTATGGGGAAGATTTATTGAAGATCCGAAAATAATGAAGGGAGAGGCTGAAGCAGAGCAGCTC 450  
 E G K E M E Y V E K A L R G M L K I G K D Q S E R I T R L Y 173  
 GAAGGAAAAGAAATGGAATACGTCGAAAAGCGCTAAGGGGCATGCTGAAAATCGGGAAAGATCAATCTGAGCGTATTACACGGTTGTAC 540  
 R A L Q T E E D L R T S D E T R I I S E Y R E K F D A L K Q 203  
 CGCGCTCTCCAAACGGAGGAGGATTTAAGAACTTCGGATGAGACGAGGATCATCAGCGAGTATAGAGAAAAATTTGATGCATTGAAACAG 630  
 A I E L E Q Q A T H E E A V Q E M L D L S A E V I E T A A E 233  
 GCGATTGAACCTGAACAGCAGGCAACGCATGAAGAAGCTGTGCAGGAAATGTTGGATTTAAGTGCCGAGGTCATCGAAACGGCGGCTGAG 720  
 E V P V F G A G A A N V V A T T R A I Q G G L K L K E I I D 263  
 GAGGTGCCAGTCTTTGGCGCAGGCGCAGCAAATGTTGTTGCGACGACACGCGCAATCCAAGGAGGCCATAAGCTGAAGGAGATAATAGAT 810  
 K L T G I D L S H L K V A D I H P H I I E K A M L K V K I P 293  
 AAACCTCACAGGGATCGATCTCTCCCATTTGAAAGTAGCAGATATTCATCCTCACATAATTGAGAAAGCAATGTTAAAGGTTAAAAATCC 900  
 D N E L A M A I K S K V E V V D E M N T E T E H V I E S I M 323  
 GACAACGAGTTAGCGATGGCGATAAAGTCGAAGGTTGAGGTTGTCGATGAGATGAATACGGAGACGGAACACGTTATAGAGTCCATCATG 990  
 P L V K K E Y E K H D N K Y H V N I P S A L K I H S E Q T P 353  
 CCTCTAGTGAAGAAAGAATACGAAAAGCATGATAACAAATACCATGTAAATATACCAAGTGCGTTGAAAATACATTAGAGCAAACGCCA 1080  
 K V H I Y T T P W D S D K V F I C R C I A P H H Q Q K S F M 383  
 AAGGTACACATATACTACACCGTGGGACTCTGATAAAGTTTTTCATATGCAGATGCATTGCGCCACATCACCAGCAGAAGAGTTTTATG 1170  
 I G F D L E I E F V F Y E D T S V E G H I M H G G A V S I E 413  
 ATTGGATTTGATTTAGAGATTGAATTTGTCTTCTATGAAGATACCTCGGTTGAGGGTCACATTATGCATGGGGGAGCGGTGTGCGATTGAG 1260  
 G R G F R Q A Y S E F M N A A W S M P L T P E L H K R R L Q 443  
 GGACGAGGATTTAGACAGGCTTATAGTGAGTTCATGAACGCGGCTTGGTCTATGCCCTTGACTCCAGAGCTACATAAGAGAAGATTACAA 1350  
 R S L G S H P I Y M G S M D Y T I S Y E Q L V S N A M K L V 473  
 CGTAGTCTGGGCTCACATCCGATTTATATGGGATCGATGGATTATACCATAAGTTATGAACAGCTCGTTTCGAACGCGATGAAGTTAGTC 1440  
 Y D T D L Q M H C L R G P L K F Q R R T L M N A L L F G V K 503  
 TATGACACGGACCTACAGATGCACGTGTTTACGTGGACCACTGAAATTCAAAGGCGCACCTGATGAACGCGCTTCTTTGGTGTGAAA 1530  
 V A \* 505  
 GTAGCTtgaagcctcacggcgcgagaaaacacatac 1568

**Figure 2.3.8 The complete nucleotide and deduced amino acid sequence of AHSV6vir2 M6 gene. The conserved 5' and 3' hexanucleotides are underlined and the termination codon is marked with a \*.**

```

M G K F T S F L K R A G S A T K K A L T S D T      23
ttgtaaatttttccagaagccATGGGAAAGTTCACATCCTTTCTGAAGCGCGCGGGAAGCGCCACGAAGAAAGCGTTGACTTCTGATACA 90

A K R M Y K M A G K T L Q K V V E S E V G S A A I D G V M Q      53
GCAAAAAGGATGTATAAAATGGCAGGGAAAACATTGCAAAGGTCGTGAAAGCGAAGTtGGTAGCGCGGCTATCGATGGAGTGATGCAA 180

G T I Q S I I Q G E N L G D S I R Q A V I L N V A G T L E S      83
GGTACGATACAAAGCATAATACAAGGAGAAAACCTTGGGAGATTCAATCAGACAGGCAGTGATTTTAAATGTTGCAGGGACTTTGGAGTCA 270

A P D P L S P G E Q L L Y N K V A E L E R A E K E D R V I E      113
GCGCCAGATCCGTTAAGTCCGGGCGAGCAGCTTCTGTATAATAAGGTGGCTGAGTTGGAGAGAGCGGAGAAGGAGGATCGCGTGATTGAA 360

T H N E K I I Q E Y G K D L L K I R K I M K G E A K A E Q L      143
ACGCACAATGAAAAGATAATTCAAGAATATGGTAAGGACCTTTTGAAGATTGGAAAATAATGAAGGGAGAGGCTAAGCGGAACAGCTT 450

E G K E I E Y V E M A L K G M L K I G K D Q S E R I T Q L Y      173
GAGGGGAAAGAGATTGAATATGTTGAGATGGCATTGAAAGGGATGTTAAAGATTGAAAGGATCAATCAGAACGTATCACCCAACATATAT 540

R A L Q T E E D L R T S D E T R M I N E Y R E K F D A L K Q      203
CGCGCTTTACAGAcAGAGGAGGATCTGAGAACTTCAGACGAGACGAGGATGATAAATGAGTATAGAGAAAAATTTGACGCACTAAAACAA 630

A I E L E Q Q A T H E E A V Q E M L D L S A E V I E T A A E      233
GCAATGAACTCGAACAGCAAGCGACGCATGAAGAGGAGTGCAGGAGATGTTGGACCTAAGCGCAGAGGTCATTGAGACAGCAGCGGAG 720

E V P I F G A G A A N V V A T T R A V Q G G L K L K E I I D      263
GAGGTGCCAATTTTGGCGCAGGGGCTGCAAACGTTGTCGAAACACGCGCGCAGTTTCAAGGAGGTTTGAAGCTTAAGGAAATTATAGAT 810

K L T G I D L S H L K V A D I H P H I I E K A I L K D K I P      293
AAGCTCACAGGAATCGATCTCTCCCATTTAAAGGTAGCGGATATCCACCCACATATCATTGAAAAAGCCATATTAAGATAAGATTCCA 900

D S E L A M A I K S K V E V I D E M N T E T E H V I K S I M      323
GATAGTGAGTTAGCTATGGCGATAAAATCAAAGGTTGAGGTGATCGATGAAATGAATACGGAAACAGAGCATGTGATTAAATCAATTATG 990

P L V K K E Y E K H D N K Y H V N I P S V L K I H S E H T P      353
CCATTAGTGAAGAAAGAGTACGAGAAGCATGATAATAAATATCACGTGAATATACCAAGTGTCTGAAGATACATTGAGAACACACACCG 1080

K V H I Y T T P W D S D K V F I C R C I A P H H Q Q K S F M      383
AAAGTTCATATATATACGACGCCCTGGGATTCCGACAAAGTCTTTATATGTAGGTGCATTGGCCCGCATCACCAACAGAAGAGTTTTATG 1170

I G F D L E I E F V F Y E D T S V E G H I M H G G A V S I E      413
ATAGGTTTCGaTCTGGAGATCGAATTCGTTTTTTATGAGGATACATCGGTAGAGGGACACATAATGCACGGGGGAGCTGTGTCAATTGAG 1260

G R G F R Q A Y S E F M N A A W S M P S T P E L H K R R L Q      443
GGACGGGGTTTTAGACAaGCTTATAGTGAATTTATGAAtGCAGCTTGGTCGATGCCCTCCACTCCAGAGTTACATAAGaGGAGATTGCAA 1350

R S L G S H P I Y M G S M D Y T V S Y D Q L V S N A M K L V      473
CGTAGCTTAGGATCtCATCCAATCTACATGGGATCAATGGATTACACCGTTAGTTATGATCAGCTCGTTTCTAACGGGATGAAATTAGTT 1440

Y D T E L Q M H C L R G P L K F Q R R T L M N A L L F G V K      503
TATGATACTGAATTACAAATGCaTTGCTTACGAGGACCATTGAAGTTTCAAAGACGCACTTTAAATGAATGCGCTTCTATTTGGTGTGAAA 1530

I A *                               505
ATAGCTtgaaagcctcacggcgcggagaaaaacatac 1568

```

**Figure 2.3.9** The complete nucleotide and deduced amino acid sequence of AHSV8vir M6 gene. The conserved 5' and 3' hexanucleotides are underlined and the termination codon is marked with a \*.

ttgttaatttttccagaagccATGGGAAAGTTCACATCCTTCTTGAAGCGTGGGGTAGCGCAACCAAGAAAGCACTA ACTTCAGATGCG 23 90  
 A K R M Y K M A G K A L Q K V V E S E V G S A A I D G V M Q 53  
 GCTAAAAGGATGTATAAGATGGCTGGTAAAGCGTTACAGAAAGTCGTAGAAAGT GAGGTGGGAAGCGCGGCGATTGATGGAGTAATGCAA 180  
 G T F Q S I I Q G E N L G D S I K Q A V I L N V A G T L E S 83  
 GGAACATTTTCAGAGCATAATACAGGGT GAAAATTTGGGGGACTCAATCAAACAAGCAGTAATTTTGAACGTAGCTGGCACGTTAGAGTCG 270  
 A P D P L S P G E Q L L Y N K V S E I E R A E K E D R V I E 113  
 GCTCCAGACCCATTAAGCCCAGGTGAACAACTATTATATAATAAAGTATCTGAAATCGAAAGAGCGGAGAAGGAAGATCGTGTGATTGAG 360  
 T H N K K I V E K Y G E D L L K I R K I M K G E A E A E Q L 143  
 ACACATAATAAAAAGATTGTCGAAAAGTATGGGGAAGATTTATTGAAGATCCGAAAATAATGAAGGGAGAGGCTGAGGCAGAGCAGCTC 450  
 E G K E M E Y V E K A L R G M L K I G K D Q S E R I T R L Y 173  
 GAAGGAAAAGAAATGGAATACGTCGAAAAGCGCTAAGGGGCATGCTGAAAATCGGGAAAGATCAATCTGAGCGTATTACACGGTTGTAC 540  
 R A L Q T E E D L R T S D E T R I I S E Y R E K F D A L K Q 203  
 CGCGTCTCCAAACGGAGGAGGATTTAAGA AACTTCGGATGAGACGAGGATCATCAGCGAGTATAGAGAAAATTTGATGCATTGAAACAG 630  
 A I E L E Q Q A T H E E A V Q E M L D L S A E V I E T A A E 233  
 GCGATTGAACTTGAACAGCAGGCAACGCATGAAGAAGCTGTGCAGGAAATGTTGGATTTAAGTGCCGAGGTCATCGAAACGGCGGCTGAG 720  
 E V P V F G A G A A N V V A T T R A I Q G G L K L K E I I D 263  
 GAGGTGCCAGTCTTTGGCGCAGGCGCAGCAAATGTTGTTGCGACGACACGCGCAATCCAAGGAGGCTAAAGCTGAAGGAGATAATAGAT 810  
 K L T G I D L S H L K V A D I H P H I I E K A M L K D K I P 293  
 AAACCTCACAGGGATCGATCTCTCCATTTGAAAGTAGCAGATATTCATCCTCACATAATTGAGAAAAGCAATGTTAAAGGATAAAAATCC 900  
 D N E L A M A I K S K V E V V D E M N T E M E H V I E S I M 323  
 GACAACGAGTTAGCGATGGCGATAAAGTCGAAGGTTGAGGTTGTCGATGAGATGAATACGGAGATGGAACACGTTATAGAGTCCATCATG 990  
 P L V K K E Y E K H D N K Y H V N I P S A L K I H S E H T P 353  
 CCTTTAGTGAAGAAAGAATACGAAAAGCATGATAACAAATACCATGTAATATACCAAGTGCCTTGAAAATACATTTCAGAGCATAACGCCA 1080  
 K V H I Y T T P W D S D K V F I C R C I A P H H Q Q R S F M 383  
 AAGGTACACATATACTACGCCGTGGGACTCTGATAAAGTTTTTATATGCAGATGCATTGCGCCACATCACCAGCAGAGGAGTTTTATG 1170  
 I G F D L G I E F V F Y E D T S V E G H I M H G G A V S I E 413  
 ATTGGATTTGATTTAGGGATCGAATTTGTCTTCTATGAAGATACCTCGGTTGAGGGTCACATTATGCATGGGGGAGCGGTGTCGATTGAG 1260  
 G R G F R Q A Y S E F M N A A W S M P S T P E L H K R R L Q 443  
 GGACGAGGATTTAGACAGGCTTATAGT GAGTTCATGAACGCGGCTTGGTCTATGCCTTCGACTCCAGAGCTACATAAGAGAAGGTTACAA 1350  
 R S L G S H P I Y M G S M D Y T I S Y E Q L V S N A M K L V 473  
 CGTAGTTTGGGCTCACATCCGATTTATATGGGATCGATGGATTATACCATAAGTTATGAACAGCTCGTTTCGAACGCGATGAAGTTAGTC 1440  
 Y D T D L Q M H C L R G P L K L Q R R T L M N A L L F G V K 503  
 TATGACACGGACCTACAGATGCACTGTTTACGTGGACCACTGAAACTCCAAAGGCGCACCCCTGATGAACGCGCTTCTCTTTGGTGTGAAA 1530  
 V A \* 505  
 GTAGCTtgaagcctcacggcgcggaacacatac 1568

**Figure 2.3.10** The complete nucleotide and deduced amino acid sequence of AHSV9vir M6 gene. The conserved 5' and 3' hexanucleotides are underlined and the termination codon is marked with a \*.

**Table 2.3.1** The nucleotide base composition of the M6 gene segments of the various AHSV serotypes sequenced. Values in the first four rows correspond to the actual number of nucleotides found.

	AHSV3vir1	AHSV3vir2	AHSV6vir1	AHSV6vir2	AHSV8vir	AHSV9vir
<b>G</b>	405	404	404	402	401	409
<b>T</b>	343	341	338	342	352	345
<b>C</b>	263	267	267	264	246	262
<b>A</b>	505	503	506	508	507	499
<b>G+C (%)</b>	42	42	42	43	41	42
<b>A+T (%)</b>	58	58	58	57	59	58

The M6 nucleotide sequences of the various serotypes were aligned and the results compared using the distance matrix program of ClustalX, as tabulated in Table 2.3.2.

**Table 2.3.2** Conservation of the nucleotide sequences of all the AHSV VP5 sequenced in this study.

	AHSV9vir	AHSV8vir	AHSV3vir2	AHSV3vir1	AHSV6vir1	AHSV6vir2
<b>AHSV9vir</b>		80%	98.90%	99%	99%	98.70%
<b>AHSV8vir</b>			79.70%	80%	79.70%	79.80%
<b>AHSV3vir2</b>				99.50%	99.50%	99.2%
<b>AHSV3vir1</b>					99.70%	99.40%
<b>AHSV6vir1</b>						99.20%
<b>AHSV6vir2</b>						

The percentage of conservation between all the serotypes sequenced range from 79% to 99%, indicating that the VP5 genes are relatively conserved. The AHSV3, 6 and 9 genes of these field isolates are especially highly conserved, showing approximately 99 % homology across these serotypes. The AHSV8 gene showed the least amount of conservation, differing from the mentioned serotypes by approximately 80 %. Du Plessis and Nel, (1997) and Filter, (2000) compared AHSV VP5 genes from serotypes 9 and 3 (respectively) with other published VP5 sequences and found the percentage of conservation to range from 74-93%.

#### 2.3.4 Amino acid sequence analysis

The amino acid (aa) sequences of the VP5 genes were deduced from the nucleotide sequences and are indicated above the nucleotide sequence in Figures 2.3.5. - 2.3.10. The deduced protein sequences of all the serotypes were 505 amino acids in length, with an expected molecular weight of approximately 56 kDa. The amino acid composition of all the proteins was determined with the computer program DNAssist (version 2.0) and compared to already published AHSV VP5 protein sequences (see Table 2.3.3).

The results clearly show that AHSV VP5 proteins have an overall similar amino acid composition, being abundant in alanine and glutamate whilst being relatively deficient in cysteine and tryptophan. Overall, most of the amino acids (33%) are hydrophobic in nature, whilst the minority is aromatic (see Table 2.3.4).

**Table 2.3.3 Amino acid composition of the VP5 proteins analysed in this study, compared to published data (see key for references). The number of residues as well as molar % (in brackets) is shown.**

Amino acid	AHSV3vir2	AHSV3vir1	AHSV3♣	AHSV6vir2	AHSV6vir1	AHSV6♠
Alanine (A)	41 (8%)	41 (8%)	40 (7%)	40 (7%)	41 (8%)	37 (7%)
Arginine R	22 (4%)	23 (4%)	22 (4%)	22 (4%)	23 (4%)	24 (4%)
Asparagine (N)	12 (2%)	12 (2%)	12 (2%)	12 (2%)	12 (2%)	13 (2%)
Aspartate (D)	25 (4%)	25 (4%)	27 (5%)	24 (4%)	25 (4%)	24 (4%)
Cysteine (C.)	3 (0%)	3 (0%)	3 (0%)	3 (0%)	3 (0%)	3 (0%)
Glutamate (E)	51 (10%)	53 (10%)	51 (10%)	53 (10%)	53 (10%)	54 (10%)
Glutamine (Q)	22 (4%)	21 (4%)	21 (4%)	22 (4%)	21 (4%)	22 (4%)
Glycine (G)	31 (6%)	30 (5%)	30 (5%)	30 (5%)	30 (5%)	30 (5%)
Histidine (H)	18 (3%)	18 (3%)	18 (3%)	17 (3%)	18 (3%)	18 (3%)
Isoleucine (I)	39 (7%)	39 (7%)	40 (7%)	40 (7%)	39 (7%)	41 (8%)
Leucine (L)	43 (8%)	42 (8%)	43 (8%)	43 (8%)	42 (8%)	43 (8%)
Lycine (K)	43 (8%)	43 (8%)	44 (8%)	44 (8%)	43 (8%)	40 (7%)
Methionine (M)	20 (3%)	21 (4%)	22 (4%)	21 (4%)	21 (4%)	21 (4%)
Phenylalanine (F)	13 (2%)	13 (2%)	13 (2%)	13 (2%)	13 (2%)	13 (2%)
Proline (P)	15 (2%)	15 (2%)	16 (3%)	15 (2%)	15 (2%)	15 (2%)
Serine (S)	31 (6%)	31 (6%)	31 (6%)	30 (5%)	31 (6%)	32 (6%)
Threonine (T)	26 (5%)	26 (5%)	26 (5%)	26 (5%)	26 (5%)	26 (5%)
Tryptophan (W)	2 (0%)	2 (0%)	2 (0%)	2 (0%)	2 (0%)	1 (0%)
Tyrosine (Y)	15 (2%)	15 (2%)	15 (2%)	15 (2%)	15 (2%)	15 (2%)
Valine (V)	33 (6%)	32 (6%)	29 (5%)	33 (6%)	32 (6%)	32 (6%)
No of amino acids	505	505	505	505	505	504
Molecular weight (kDa)	57	57	57	57	57	57
Iso-electric point	5.9	5.8	5.8	5.9	5.8	5.7

AHSV3 (♣) Filter, (2000)  
AHSV6 (♠) Williams *et al.*, (1998)

**Table 2.3.4** Different residue types of amino acids of the VP5 protein analysed in this study, compared to published data (see key for references). The number of residues as well as molar % (in brackets) is shown.

AHSV Serotype	Acidic (D+E)	Basic (R+K)	Aromatic (F + W + Y)	Hydrophobic (Aromatic + I + L + M + V)
AHSV3vir2	76 (15%)	65 (13%)	30 (0.1%)	165 (33%)
AHSV3vir1	78 (15%)	66 (13%)	30 (0.1%)	164 (33%)
AHSV3 ♣	78 (15%)	66 (13%)	30 (0.1%)	164 (33%)
AHSV6vir2	77 (15%)	66 (13%)	30 (0.1%)	167 (33%)
AHSV6vir1	78 (15%)	66 (13%)	30 (0.1%)	164 (33%)
AHSV6 ♠	78 (15%)	64 (13%)	29 (0.1%)	166 (33%)
AHSV9vir	77 (15%)	66 (13%)	30 (0.1%)	165 (33%)
AHSV9 ♦	74 (15%)	65 (13%)	29 (0.1%)	171 (34%)
AHSV8vir	76 (15%)	65 (13%)	30 (0.1%)	166 (33%)
AHSV4 ♥	78 (15%)	64 (13%)	30 (0.1%)	165 (33%)

AHSV3 (♣) Filter, (2000)  
AHSV9 (♦) du Plessis and Nel, (1997)  
AHSV4 (♥) Iwata et al., (1992b)  
AHSV6 (♠) Williams *et al.*, (1998)

The amino acid sequences of all VP5 proteins determined in this study, as well as VP5 sequences published previously, were aligned using the software program ClustalX. These included individual alignments within and between serotypes. A combined alignment showing all analyzed AHSV VP5 sequences is presented in Fig 2.3.11. Alignments that include the VP5 proteins from BTV10 and EHDV1 are shown in Fig 2.3.12. A distance matrix (using the PAUP\* version 4.0b10 phylogenetic software program for Macintosh) was also compiled in order to calculate the percentage difference between all the aligned serotypes (Figure 2.3.13).



Alignment comparisons between the three AHSV3 amino acid sequences (included in Figure 2.3.11) reveal that these proteins were highly conserved. The field strains from this study, AHSV3vir1 and AHSV3vir2 were 99.2% identical, with the laboratory strain sequenced by Filter, (2000) differing from AHSV3vir1 and AHSV3vir2 by 2.4% and 3% respectively (see distance matrix Table 2.3.13, page 80). This represents 4 aa changes between AHSV3vir1 and AHSV3vir2, 12 aa changes between AHSV3vir1 and the VP5 of the laboratory strain and 15 aa changes between AHSV3vir2 and the laboratory strain. AHSV3 isolates therefore shared at least 97% identical amino acids. When similar amino acids were considered, the percentage rose to 99.6%. Markedly, only two of the 505 amino acids were different in both amino acid type and character and occurred in amino acid positions 156 and 401 respectively. Of the two AHSV3 field serotypes sequenced, the only two amino acid differences found occurred at these two positions.

Alignment comparisons between the three AHSV6 serotypes (included in Figure 2.3.11) reveal that these proteins were slightly less conserved than those between serotype 3. The field strains from this study, AHSV6vir1 and AHSV6vir2 were 99% identical. The isolate sequenced by Williams *et al.*, (1998), assumedly from an attenuated laboratory strain, differed from AHSV6vir1 and AHSV6vir2 by 4% and 5% respectively (see distance matrix Table 2.3.13). The AHSV6 isolates therefore shared at least 95% identical amino acids, representing at most 21 intraserotype amino acid changes between AHSV6vir2 and the published sequence. When similar amino acids were considered, the percentage of conservation rose to 98%. Ten of the 505 amino acids were different in both aa type and character. The AHSV6 VP5 sequence presented by Williams *et al.*, (1998) had one less amino acid, being 504 aa in length instead of 505 aa. The two AHSV6 field VP5 proteins were more similar to each other than to the published sequence differing only at 6 aa positions. Four of these six amino acid changes were similar in type and character. Of all the differences, no similar aa changes were observed between AHSV6vir2 and the published sequence, assumed to have been obtained from an attenuated laboratory strain.



Alignment comparisons between AHSV9vir and the published sequence by Du Plessis and Nel (1997) (included in Figure 2.3.11) reveal that these VP5 proteins were the least conserved as compared to the VP5 proteins between serotypes 3 and 6. The AHSV9 VP5 proteins contained 90.5% identical amino acids, representing a total of 48 aa changes across the length of the protein (see distance matrix Table 2.3.13, page 80). The percentage of conservation rose to 94.9% when similar amino acids were considered. The N-terminal regions were found to be the most conserved and the changes noted were spread across the whole protein without a distinctive pattern.

No intraserotype comparisons for AHSV8vir could be done, since there is no published sequence for this VP5 sequence. Comparisons between AHSV8vir and the sequenced field isolates of serotype 3, 6 and 9 show a relatively high degree of variation. The percentage of amino acid differences ranged from 5.2- 7%, representing 26-35 actual amino acid changes (see distance matrix Table 2.3.13, page 80).

Comparisons show that no correlation between specific amino acid differences or changes in particular regions can be attributed to the virulent phenotype. Also, no preferential amino acid changes were found to occur within the N-terminal region, which contains the amphipatic helix regions.

Figure 2.3.12 shows the amino acid comparison between all the AHSV serotypes sequenced and those published to two other orbiviral VP5 protein sequences (BTV10 and EHDV1). Conserved cysteine are highlighted and are shown to reside in amino acid positions 370, 372 and 482 for all AHSV VP5 proteins (except for AHSV4 in position 372) and position 372 for BTV and EHDV. A conserved glycine residue in position 2, directly after the methionine start codon is also shown. In summary, a genetic relationship of 80 % or more is observed between AHSV serotypes with a lesser similarity (40-50%) observed between serogroups.

In order to reveal some insights to the phylogenetic relationship between all the compared sequences with other orbiviruses, clustal aligned comparisons were used to construct neighbor-joining phylograms using the PAUP\* version 4.0b10 phylogenetic software program for Macintosh (Figures 2. 3. 14 and –15 for nucleotide and amino acid sequence comparisons respectively). Bootstrap values of a 1000 were used and those groups having a value of greater than 60% are considered to be relatively confident. Both phylograms grouped the VP5 sequences of the AHSV3, 6 and 9 field serotypes together, whilst grouping their laboratory-adapted counterparts together. This indicates that the VP5 sequences from the field strains are more closely related to each other than to their own serotype counterpart. The nucleotide phylogram grouped AHSV8 field VP5 separately in contrast to its grouping together with the laboratory adapted AHSV serotypes in the amino acid phylogram. This shows that although the primary sequences are quite diverse, synonymous amino acid substitutions in the protein sequence aid to increase the homology between AHSV8 and other serotypes. Both phylograms show AHSV4 VP5 as being the least homologous to all the other AHSV strains, by grouping apart in a distinctive branch. As expected, the BTV and EHDV cluster together as out-groups relative to the AHSV serogroup.



AHSV3vir1 MGKFTSFLKRAGSATKKALTS DAAKRMKYMAGKTLQKVVESEVGSAAIDGVMQGTIQSII 60  
 AHSV6vir1 MGKFTSFLKRAGSATKKALTS DAAKRMKYMAGKTLQKVVESEVGSAAIDGVMQGTIQSII  
 AHSV9vir MGKFTSFLKRAGSATKKALTS DAAKRMKYMAGKTLQKVVESEVGSAAIDGVMQGTIQSII  
 AHSV6vir1 MGKFTSFLKRAGSATKKALTS DAAKRMKYMAGKTLQKVVESEVGSAAIDGVMQGTIQSII  
 AHSV3vir2 MGKFTSFLKRAGSATKKALTS DAAKRMKYMAGKTLQKVVESEVGSAAIDGVMQGTIQSII  
 AHSV3 ♣ MGKFTSFLKRAGSATKKALTS DAAKRMKYMAGKTLQKVVDSEVGSAAIDGVMQGTIQSII  
 AHSV6 ♠ MGKFTSFLKRAGSATKNALTS DAAKRMKYMAGKTLQKVVESEVGSAAIDGVMQGTIQSII  
 AHSV8vir MGKFTSFLKRAGSATKKALTS DTAARMKYMAGKTLQKVVESEVGSAAIDGVMQGTIQSII  
 AHSV9 ♠ MGKFTSFLKRAGSATKKALTS DAAKRMKYMAGKTLQKVVESEVGSAAIDGVMQGTIQSII  
 AHSV4 ♥ MGKFTSFLKRAGNATKRALTS DSAKMYKLAGKTLQKVVESEVGSAAIDGVMQGTIQSII  
 AHSV4 JK MGKFTSFLKRAGNATKRALTS DSAKMYKLAGKTLQKVVESEVGSAAIDGVMQGTIQSII  
 \*\*\*\*\*:\*.\*\*\*.\*\*\*\*\*:\*\*\*:\*\*\*:\*\*\*:\*\*\*:\*\*\*:\*\*\*:\*\*\*\*\*:\*\*\*\*\*:\*\*\*\*\*:\*\*\*\*\*

AHSV3vir1 QGENLGDSIKQAVILNVAGTLESAPDPLSPGEQLLYNKVSEIERAEKEDRVIETHNKKIV 120  
 AHSV6vir1 QGENLGDSIKQAVILNVAGTLESAPDPLSPGEQLLYNKVSEIERAEKEDRVIETHNKKIV  
 AHSV9vir QGENLGDSIKQAVILNVAGTLESAPDPLSPGEQLLYNKVSEIERAEKEDRVIETHNKKIV  
 AHSV6vir1 QGENLGDSIKQAVILNVAGTLESAPDPLSPGEQLLYNKVSEIERAEKEDRVIETHNKKIV  
 AHSV3vir2 QGENLGDSIKQAVILNVAGTLESAPDPLSPGEQLLYNKVSEIERAEKEDRVIETHNKKIV  
 AHSV3 ♣ QGENLGDSIKQAVILNVAGTLESPPDPLSPGEQLLYNKVSKIERAEKEDRVIETHNEKII  
 AHSV6 ♠ QGENLGDSIRQAVILNVAGTLESAPDPLSPGEQLLYNKVSEIERAEKEDRVIETHNKKII  
 AHSV8vir QGENLGDSIRQAVILNVAGTLESAPDPLSPGEQLLYNKVAELERAERAEKEDRVIETHNEKII  
 AHSV9 ♠ QGENLGAQFKQAVILNVAGTLESAPDPLNPGEQHII INVSEIERAEKEDRVIETHNKKII  
 AHSV4 ♥ QGENLGDSIKQAVILNVAGTLESAPDPLSPGEQLLYNKVSEIEKMEKEDRVIETHNAKIE  
 AHSV4 JK QGENLGDSIKQAVILNVAGTLESAPDPLSPGEQLLYNKVSEIEKMEKEDRVIETHNAKIE  
 \*\*\*\*\* :\*:\*\*\*\*\*:\*\*\*\*\*.\*\*\*.\*\*\* : :\*:\*\*\*: \*\*\*\*\* \*\* \*\*

AHSV3vir1 EKYGEDLLKIRKIMKGEAEAEQLEGKEMEYVEKALRGMLKIGKDQSERITRLYRALQTEE 180  
 AHSV6vir1 EKYGEDLLKIRKIMKGEAEAEQLEGKEMEYVEKALRGMLKIGKDQSERITRLYRALQTEE  
 AHSV9vir EKYGEDLLKIRKIMKGEAEAEQLEGKEMEYVEKALRGMLKIGKDQSERITRLYRALQTEE  
 AHSV6vir1 EKYGEDLLKIRKIMKGEAEAEQLEGKEMEYVEKALRGMLKIGKDQSERITRLYRALQTEE  
 AHSV3vir2 EKYGEDLLKIRKIMKGEAEAEQLEGKEMEYVEKALGGLLKIGKDQSERITRLYRALQTEE  
 AHSV3 ♣ EKYGEDLLKIRKIMKGEAEAEQLEGKEMEYVEKALGMLKIGKDQSERITRLYRALQTEE  
 AHSV6 ♠ EKYGEDLLEIRKIMKGEAEAEQLEGKEMEYVEKALGMLKIGKDQSERITRLYRALQTEE  
 AHSV8vir QEYGDLLKIRKIMKGEAKAEQLEGKEIEYVEMALKGMLKIGKDQSERITQLYRALQTEE  
 AHSV9 ♠ ERFGGHLLKIRKIMKGEAEAEQLEGKEMMQVEKALGMLRIGKDQSERITRLYRALQTEE  
 AHSV4 ♥ EKFGKDLLAIRKIVKGEVDAEKLEGNEIKYVEKALSGLLEIGKDQSERITKLYRALQTEE  
 AHSV4 JK EKFGKDLLAIRKIVKGEVDAEKLEGNEIKYVEKALSGLLEIGKDQSERITKLYRALQTEE  
 :\*: \* \*\* \*\*\*\*\*:\*\*\*.\*\*\*:\*\*\*:\*\*\*: \* \* \* \* \* \*\*\*\*\*:\*\*\*\*\*

AHSV3vir1 DLRTSDETRIISEYREKFDALKQAIIELEQQATHEEAVQEMLDLSAEVIETAAEEVPVFGA 240  
 AHSV6vir1 DLRTSDETRIISEYREKFDALKQAIIELEQQATHEEAVQEMLDLSAEVIETAAEEVPVFGA  
 AHSV9vir DLRTSDETRIISEYREKFDALKQAIIELEQQATHEEAVQEMLDLSAEVIETAAEEVPVFGA  
 AHSV6vir2 DLRTSDETRIISEYREKFDALKQAIIELEQQATHEEAVQEMLDLSAEVIETAAEEVPVFGA  
 AHSV3vir2 DLRTSDETRIISEYREKFDALKQAIIELEQQATHEEAVQEMLDLSAEVIETAAEEVPVFGA  
 AHSV3 ♣ DLRTSDETRMISEYREKFDALKQAIIELEQQATHEEAVQEMLDLSAEVIETAAEDLPIFGA  
 AHSV6 ♠ DLRTSDETRMISEYREKFDALKQAIIELEQQATHEEAMQEMLDLSAEVIETAAEEVPIFGA  
 AHSV8vir DLRTSDETRMINEYREKFDALKQAIIELEQQATHEEAVQEMLDLSAEVIETAAEEVPIFGA  
 AHSV9 ♠ DLRTSDETRMISEYREKFEALKQAIIELEQQATHGEAVQEMLDLSAEVIETAAEEVPVFGA  
 AHSV4 ♥ DLRTSDETRMINEYREKFDALKEAIEIEQQATHDEAIEQEMLDLSAEVIETASEEVPIFGA  
 AHSV4 JK DLRTSDETRMINEYREKFDALKEAIEIEQQATHDEAIEQEMLDLSAEVIETASEEVPIFGA  
 \*\*\*\* \*\*\*\*\*:\*.\*\*\*\*\*:\*\*\*:\*\*\*:\*\*\*\*\* \*\* \*\*\*\*\*:\*\*\*\*\*:\*\*\*\*\*:\*\*\*\*\*









```

AHSV3vir1  HCLRGPLKFQRRITLMNALLFGVKVA  505
AHSV6vir1  HCLRGPLKFQRRITLMNALLFGVKVA
AHSV9vir   HCLRGPLKLRRTLMNALLFGVKVA
AHSV6vir2  HCLRGPLKFQRRITLMNALLFGVKVA
AHSV3vir2  HCLRGPLKFQRRITLMNALLFGVKVA
AHSV3 ♣    HCLRGPLKFQRRITLMNALLFGVKVA
AHSV6 ♠    HCLRGPLKFQRRITLMNALLFGVKVA
AHSV8vir   HCLRGPLKFQRRITLMNALLFGVKIA
AHSV9 ♦    HCLRGPLKIPKGTLMNALLFAVKVA
AHSV4 ♥    HCLRGPLKFQRRITLMNALLYGVKIA
AHSV4 JK   HCLRGPLKFQRRITLMNALLYGVKIA
*****: : *****:.*:*

```

AHSV3 (♣) Filter, (2000)  
AHSV9 (♦) du Plessis and Nel, (1997)  
AHSV4 (♥) Iwata et al., (1992b)  
AHSV6 (♠) Williams *et al.*, (1998)  
AHSV4 (JK) Jeanne Korsmann  
(University of Pretoria, 2003)

**Figure 2.3.11:** Amino acid comparison of all the AHSV sequences obtained with that of published AHSV VP5 sequences. Identical amino acids are indicated by a (\*), whilst similar amino acids by a (:). The conserved cysteine residues found in AHSV are highlighted in green and the conserved glycine residue at the N-terminal is highlighted in yellow. Differences in amino acids are highlighted in teal. Grey shaded areas depict the various N terminal (1-123aa), central (192-273aa) and C terminal (460-505aa) regions respectively.





AHSV3vir1 MGKFTSFLKRAGSATKKALTS DAAKRM YKMAGKTLQKVVESEVGSAAIDGVMQGTIQSII  
 AHSV6vir1 MGKFTSFLKRAGSATKKALTS DAAKRM YKMAGKTLQKVVESEVGSAAIDGVMQGTIQSII  
 AHSV9vir MGKFTSFLKRAGSATKKALTS DAAKRM YKMAGKTLQKVVESEVGSAAIDGVMQGTIQSII  
 AHSV6vir2 MGKFTSFLKRAGSATKKALTS DAAKRM YKMAGKTLQKVVESEVGSAAIDGVMQGTIQSII  
 AHSV3vir2 MGKFTSFLKRAGSATKKALTS DAAKRM YKMAGKTLQKVVESEVGSAAIDGVMQGTIQSII  
 AHSV3 ♣ MGKFTSFLKRAGSATKKALTS DAAKRM YKMAGKTLQKVVESEVGSAAIDGVMQGTIQSII  
 AHSV6 ♠ MGKFTSFLKRAGSATKALTS DAAKRM YKMAGKTLQKVVESEVGSAAIDGVMQGTIQSII  
 AHSV8vir MGKFTSFLKRAGSATKKALTS DAAKRM YKMAGKTLQKVVESEVGSAAIDGVMQGTIQSII  
 AHSV9 ♦ MGKFTSFLKRAGSATKKALTS DAAKRM YKMAGKTLQKVVESEVGSAAIDGVMQGTIQSII  
 AHSV4 ♥ MGKFTSFLKRAGSATKKALTS DAAKRM YKMAGKTLQKVVESEVGSAAIDGVMQGTIQSII  
 AHSV4 JK MGKFTSFLKRAGSATKKALTS DAAKRM YKMAGKTLQKVVESEVGSAAIDGVMQGTIQSII  
 BTV10 ∞ MGKFTSFLKRAGSATKKALTS DAAKRM YKMAGKTLQKVVESEVGSAAIDGVMQGTIQSII  
 EHDV1 □ MGKFTSFLKRAGSATKKALTS DAAKRM YKMAGKTLQKVVESEVGSAAIDGVMQGTIQSII  
 \*\* : . \* . : \* . . \*\*\*\*\* : : : : : \* . : . . . . \* : : : : : : : : : : : : : : : \*

AHSV3vir1 QGENLGDSIKQAVILNVAGTLESAPDPLSPGEQLLYNKVSEIERAEKEDRVIETHNKKIV  
 AHSV6vir1 QGENLGDSIKQAVILNVAGTLESAPDPLSPGEQLLYNKVSEIERAEKEDRVIETHNKKIV  
 AHSV9vir QGENLGDSIKQAVILNVAGTLESAPDPLSPGEQLLYNKVSEIERAEKEDRVIETHNKKIV  
 AHSV6vir2 QGENLGDSIKQAVILNVAGTLESAPDPLSPGEQLLYNKVSEIERAEKEDRVIETHNKKIV  
 AHSV3vir2 QGENLGDSIKQAVILNVAGTLESAPDPLSPGEQLLYNKVSEIERAEKEDRVIETHNKKIV  
 AHSV3 ♣ QGENLGDSIKQAVILNVAGTLESAPDPLSPGEQLLYNKVSEIERAEKEDRVIETHNKKIV  
 AHSV6 ♠ QGENLGDSIKQAVILNVAGTLESAPDPLSPGEQLLYNKVSEIERAEKEDRVIETHNKKIV  
 AHSV8vir QGENLGDSIKQAVILNVAGTLESAPDPLSPGEQLLYNKVSEIERAEKEDRVIETHNKKIV  
 AHSV9 ♦ QGENLGDSIKQAVILNVAGTLESAPDPLSPGEQLLYNKVSEIERAEKEDRVIETHNKKIV  
 AHSV4 ♥ QGENLGDSIKQAVILNVAGTLESAPDPLSPGEQLLYNKVSEIERAEKEDRVIETHNKKIV  
 AHSV4 JK QGENLGDSIKQAVILNVAGTLESAPDPLSPGEQLLYNKVSEIERAEKEDRVIETHNKKIV  
 BTV10 ∞ QGENLGDSIKQAVILNVAGTLESAPDPLSPGEQLLYNKVSEIERAEKEDRVIETHNKKIV  
 EHDV1 □ QGENLGDSIKQAVILNVAGTLESAPDPLSPGEQLLYNKVSEIERAEKEDRVIETHNKKIV  
 \*\* . \* . : : : : : \* : : . \*\*\*\*\* : : : : : \* : : : : : \* : : \* : : \*

AHSV3vir1 EKYGEDLLKIRKIMKGEAEAEQLEGKEMEYVEKALRGMLKIGKDQSERITRLYRALQTEE  
 AHSV6vir1 EKYGEDLLKIRKIMKGEAEAEQLEGKEMEYVEKALRGMLKIGKDQSERITRLYRALQTEE  
 AHSV9vir EKYGEDLLKIRKIMKGEAEAEQLEGKEMEYVEKALRGMLKIGKDQSERITRLYRALQTEE  
 AHSV6vir2 EKYGEDLLKIRKIMKGEAEAEQLEGKEMEYVEKALRGMLKIGKDQSERITRLYRALQTEE  
 AHSV3vir2 EKYGEDLLKIRKIMKGEAEAEQLEGKEMEYVEKALRGMLKIGKDQSERITRLYRALQTEE  
 AHSV3 ♣ EKYGEDLLKIRKIMKGEAEAEQLEGKEMEYVEKALRGMLKIGKDQSERITRLYRALQTEE  
 AHSV6 ♠ EKYGEDLLKIRKIMKGEAEAEQLEGKEMEYVEKALRGMLKIGKDQSERITRLYRALQTEE  
 AHSV8vir QEYGDLLKIRKIMKGEAEAEQLEGKEMEYVEKALRGMLKIGKDQSERITRLYRALQTEE  
 AHSV9 ♦ ERFGGHLLKIRKIMKGEAEAEQLEGKEMEYVEKALRGMLKIGKDQSERITRLYRALQTEE  
 AHSV4 ♥ EKFGKDLLAIRKIVKGEVDAEKLEGNEIKYVEKALSGLLEIGKDQSERITRLYRALQTEE  
 AHSV4 JK EKFGKDLLAIRKIVKGEVDAEKLEGNEIKYVEKALSGLLEIGKDQSERITRLYRALQTEE  
 BTV10 ∞ EKFGKELGEVYDFMNGEAEVEAVEEQYTMLCKAVDSYEKILKEEDSKMAILARALQREA  
 EHDV1 □ RRFGADLDEVYKFAVSEYKEGVEEKDQFEILKKALTSYGELTKAEFGELKRLEKALQKES  
 ..\* . \* : . : . \* . . . : : : \* : . . : : \* : . : : \* : : : \* : : : \*

AHSV3vir1 DLRTSDETRIISEYREKFDALKQAIIELEQQATHEEAVQEMLDLSAEVIETAAEEVPVFGA  
 AHSV6vir1 DLRTSDETRIISEYREKFDALKQAIIELEQQATHEEAVQEMLDLSAEVIETAAEEVPVFGA  
 AHSV9vir DLRTSDETRIISEYREKFDALKQAIIELEQQATHEEAVQEMLDLSAEVIETAAEEVPVFGA  
 AHSV6vir2 DLRTSDETRIISEYREKFDALKQAIIELEQQATHEEAVQEMLDLSAEVIETAAEEVPVFGA  
 AHSV3vir2 DLRTSDETRIISEYREKFDALKQAIIELEQQATHEEAVQEMLDLSAEVIETAAEEVPVFGA  
 AHSV3 ♣ DLRTSDETRMISEYREKFDALKQAIIELEQQATHEEAVQEMLDLSAEVIETAAEDLPIFGA  
 AHSV6 ♠ DLRTSDETRMISEYREKFDALKQAIIELEQQATHEEAMQEMLDLSAEVIETAAEEVPIFGA  
 AHSV8vir DLRTSDETRMINEYREKFDALKQAIIELEQQATHEEAVQEMLDLSAEVIETAAEEVPIFGA  
 AHSV9 ♦ DLRTSDETRMISEYREKFEALKQAIIELEQQATHGEAVQEMLDLSAEVIETAAEEVPVFGA  
 AHSV4 ♥ DLRTSDETRMINEYREKFDALKEAIEIEQQATHDEAIQEMLDLSAEVIETASEEVPIFGA  
 AHSV4 JK DLRTSDETRMINEYREKFDALKEAIEIEQQATHDEAIQEMLDLSAEVIETASEEVPIFGA  
 BTV10 ∞ AERSEDEIKMVKEYRQKIDALKSAIEIERDGMQEEAIQEIAGMTADVLEAAASEEVPLIGA  
 EHDV1 □ SERSKDESMVKEYRQKIEALKDAIEVESTGIQEEAIQEIAGMSADILESAEEVPLFGG  
 \* : \*\* : : .\*\*\*:\*. : : \*\*\*.\*\*\*:\* . : \*\*:\* : : : \* : : : : \* : \*

AHSV3vir1 GAANVVATTRAIQGGLKLKEIIDKLTGIDLShLKVADIHPHIEKAMLKD---KIPDNEL  
 AHSV6vir1 GAANVVATTRAIQGGLKLKEIIDKLTGIDLShLKVADIHPHIEKAMLKD---KIPDNEL  
 AHSV9vir GAANVVATTRAIQGGLKLKEIIDKLTGIDLShLKVADIHPHIEKAMLKD---KIPDNEL  
 AHSV6vir2 GAANVVATTRAIQGGLKLKEIIDKLTGIDLShLKVADIHPHIEKAMLKV---KIPDNEL  
 AHSV3vir2 GAANVVATTRAIQGGLKLKEIIDKLTGIDLShLKVADIHPHIEKAMLKD---KIPDNEL  
 AHSV3 ♣ GAANVVATTRAIQGGLKLKEIIDKLTGIDLShLKVADIHPHIEKAMLKD---KIPDNEL  
 AHSV6 ♠ GQANVVATTRAIQGGLKLKEIIDKLTGIDLShLKVADIHPHIEKAMLKD---RIPDNEL  
 AHSV8vir GAANVVATTRAIVQGGLKLKEIIDKLTGIDLShLKVADIHPHIEKAILKD---KIPDSEL  
 AHSV9 ♦ GRANVVATTRAIQGGLKLKEIIDKLTGIDLShLKVADIHPHIEKAMQSD---KIPDNEL  
 AHSV4 ♥ GAANVIATTRAIQGGLKLKEIVDKLTGIDLShLKVADIHPHIEKAMLRD---TVTDKDL  
 AHSV4 JK GAANVIATTRAIQGGLKLKEIVDKLTGIDLShLKVADIHPHIEKAMLRD---TVTDKDL  
 BTV10 ∞ GMATAVATGRAIEGAYKLLKVINALSIGIDLShMRSPKIEPTIATTLLEHR-FKDIPEQL  
 EHDV1 □ GVATSIATARAIEGGYKLLKVINALSIGIDLShLRTPKIQPKTLEAILEAPTKEEIKDLSL  
 \* \* . : \*\* \*\* : : \* . \*\*\* : : : \* : \*\*\*\*\* : : ..\*.\* : : : \* \*

AHSV3vir1 AMAIKSKVEVVDEMNTETEHVIESIMPLVKKEYEKH-----DNKYHVNI PSALKIHS  
 AHSV6vir1 AMAIKSKVEVVDEMNTETEHVIESIMPLVKKEYEKH-----DNKYHVNI PSALKIHS  
 AHSV9vir AMAIKSKVEVVDEMNTETEHVIESIMPLVKKEYEKH-----DNKYHVNI PSALKIHS  
 AHSV6vir2 AMAIKSKVEVVDEMNTETEHVIESIMPLVKKEYEKH-----DNKYHVNI PSALKIHS  
 AHSV3vir2 AMAIKSKVEVVDEMNTETEHVIESIMPLVKKEYEKH-----DNKYHVNI PSALKIHS  
 AHSV3 ♣ AMAIKSKVEVIDEMNTETEHVIESIMPLVKKEYEKH-----DNKYHVNI PSALKIHS  
 AHSV6 ♠ AMAIKSKVEVIDEMNTETEHVIESIIPLVKKEYEKH-----DNKYHVNI PSALKIHS  
 AHSV8vir AMAIKSKVEVIDEMNTETEHVIESIMPLVKKEYEKH-----DNKYHVNI PSALKIHS  
 AHSV9 ♦ AMAIKSKVEVIDEMNTETEHVYDPSCLIVKKEYEKH-----DNKYHVNI PSALKIHS  
 AHSV4 ♥ AMAIKSKVDVIDEMNVETQHVIDAVLPVIVKQEYERH-----DNKYHVRI PGALKIHS  
 AHSV4 JK AMAIKSKVDVIDEMNVETQHVIDAVLPVIVKQEYERH-----DNKYHVRI PGALKIHS  
 BTV10 ∞ AISVLNKKTAVADNCNEIAHIKQEILPKFKQIMNEE-KEIEGIEDKVIHPRVMMRFKIPR  
 EHDV1 □ VEGIOMKQLQNLEENRNEVLHIQEEILPKLREAMIEDHKEIGDERDKRILPKTAMRFKVP  
 . . : \* : : \* \* : . . : . . \* : . : \* :



```

AHSV3vir1 EHTPKVHIYTTTPWSDSKVFICRCIAPHHQQRSFMIGFDLEIEFVFYEDTSVEGHIMHGGA
AHSV6vir1 EHTPKVHIYTTTPWSDSKVFICRCIAPHHQQRSFMIGFDLEIEFVFYEDTSVEGHIMHGGA
AHSV9vir EHTPKVHIYTTTPWSDSKVFICRCIAPHHQQRSFMIGFDLGIEFVFYEDTSVEGHIMHGGA
AHSV6vir2 EQTPKVHIYTTTPWSDSKVFICRCIAPHHQQKSFMIGFDLEIEFVFYEDTSVEGHIMHGGA
AHSV3vir2 EHTPKVHIYTTTPWSDSKVFICRCIAPHHQQRSFMIGFDLEIEFVFYEDTSVVGHIMHGGA
AHSV3 ♣ EHTPKVHIYTTTPWSDSKVFICRCIAPHHQQRSFMIGFDLEIEFVFYEDTSVEGHIMHGGA
AHSV6 ♠ EHTPKVHIYTTTPWSDSKVFICRCIAPHHQQRSFMIGFDLEVEFVFYEDTSVEGHIMHGGA
AHSV8vir EHTPKVHIYTTTPWSDSKVFICRCIAPHHQQKSFMIGFDLEIEFVFYEDTSVEGHIMHGGA
AHSV9 ♦ EHTPKVHIYTTTPWSDSKVFICRCIAPHHQQRSFMIGFDLEIEFVFYEDTSVEGHIMHGGA
AHSV4 ♥ EHTPKIHIYTTTPWSDSDVFMCRAIAPHHQRSFFIGFDLEIEYVHFEDTSVEGHILHGGA
AHSV4 JK EHTPKIHIYTTTPWSDSDVFMCRAIAPHHQRSFFIGFDLEIEYVHFEDTSVEGHILHGGA
BTV10 ∞ TQQPQIHIYAAPWSDDDVFFHCVSYHHRNESFFLGFDLGDVVFHFDLTSWHALG-MA
EHDV1 □ TQQPVIQIYSAPWSDDDVFMFHCISHHHLNESSFFLGFDLELEYVHYEDLTRHWHALG-AA
: * :*:*:*:*:*:*:*:*:*:*:*:*:*:*:*:*:*:*:*:*:*:*:*:*:*:*:*:*:*:*:*:*:*:*:

```

```

AHSV3vir1 VSIEGRGFRQAYSEFMNAAWSMPSTPELHKRRLQRSSLGSHPIYMGSMDTISYEQLVSNA
AHSV6vir1 VSIEGRGFRQAYSEFMNAAWSMPSTPELHKRRLQRSSLGSHPIYMGSMDTISYEQLVSNA
AHSV9vir VSIEGRGFRQAYSEFMNAAWSMPSTPELHKRRLQRSSLGSHPIYMGSMDTISYEQLVSNA
AHSV6vir2 VSIEGRGFRQAYSEFMNAAWSMPSTPELHKRRLQRSSLGSHPIYMGSMDTISYEQLVSNA
AHSV3vir2 VSIEGRGFRQAYSEFMNAAWSMPSTPELHKRRLQRSSLGSHPIYMGSMDTISYEQLVSNA
AHSV3 ♣ VSIEGRGFRQAYSEFMNAAWSMPSTPELHKRRLQRSSLGSHPIYMGSMDTISYEQLVSNA
AHSV6 ♠ VSIEGRGFRQAYSEFMN-SLVYPSTPELHKRRLQRSSLGSHPIYMGSMVITVSYEQLVSNA
AHSV8vir VSIEGRGFRQAYSEFMNAAWSMPSTPELHKRRLQRSSLGSHPIYMGSMDTISYEQLVSNA
AHSV9 ♦ VSIEGRGFRQAYSEFMNAAWSMPSTPELHKEKMQRSSLGSHPIYMGSMDTISYEQLVSNE
AHSV4 ♥ ITVEGRGFRQAYTEFMNAAWGMPTPELHKRKLQRSMGTHPIYMGSMDISYEQLVSNA
AHSV4 JK ITVEGRGFRQAYTEFMNAAWGMPTPELHKRKLQRSMGTHPIYMGSMDISYEQLVSNA
BTV10 ∞ QEASGRTLTEAYREFLNLSISSTFSSAIHARRMIRSRAVHPIFLGSMHYDITYEALKNNA
EHDV1 □ QEVTGRSLKEAYSEFFQLAAQIDGAGAIHQKRLIRSKSYHPIYLGAMHYDIAYRELKNNA
* * :*:*:*:*:*:*:*:*:*:*:*:*:*:*:*:*:*:*:*:*:*:*:*:*:*:*:*:*:*:*:*:*:*:*:

```

<pre> AHSV3vir1 MKLVYD<del>TDLQMHCLRGPLK</del>FQ<del>RRTLMNALL</del>FGV<del>KVA</del>---- AHSV6vir1 MKLVYD<del>TDLQMHCLRGPLK</del>FQ<del>RRTLMNALL</del>FGV<del>KVA</del>---- AHSV9vir MKLVYD<del>TDLQMHCLRGPLK</del>LQ<del>RRTLMNALL</del>FGV<del>KVA</del>---- AHSV6vir2 MKLVYD<del>TDLQMHCLRGPLK</del>FQ<del>RRTLMNALL</del>FGV<del>KVA</del>---- AHSV3vir2 MKLVYD<del>TDLQMHCLRGPLK</del>FQ<del>RRTLMNALL</del>FGV<del>KVA</del>---- AHSV3 ♣ MKLVYD<del>TDLQMHCLRGPLK</del>FQ<del>RRTLMNALL</del>FGV<del>KVA</del>---- AHSV6 ♠ MKLVYD<del>TDLQMHCLRGPLK</del>FQ<del>RRTLMNALL</del>FGV<del>KVA</del>---- AHSV8vir MKLVYD<del>TELQMHCLRGPLK</del>FQ<del>RRTLMNALL</del>FGV<del>KIA</del>---- AHSV9 ♦ MKLVYD<del>TDLQMHCLRGPLK</del>IP<del>KGTLMNALL</del>F<del>AVKVA</del>---- AHSV4 ♥ MRLVYD<del>SELQMHCLRGPLK</del>FQ<del>RRTLMNALLY</del>G<del>VKIA</del>---- AHSV4 JK MRLVYD<del>SELQMHCLRGPLK</del>FQ<del>RRTLMNALLY</del>G<del>VKIA</del>---- BTV10 ∞ QRIVYD<del>DELQMHILRGPLH</del>FQ<del>RRAILGALK</del>FG<del>VKILGDKIDVPL</del>FL<del>RNA</del> EHDV1 □ LKIVN<del>DSEVQKHL</del>LRG<del>PKHFQRR</del>AILS<del>ALKDGVKLLGG</del>-V<del>DLAE</del>FM<del>RYA</del> </pre>	<p>AHSV3 (♣) Filter, (2000)</p> <p>AHSV9 (♦) du Plessis and Nel, (1997)</p> <p>AHSV4 (♥) Iwata <i>et al.</i>, (1992b)</p> <p>AHSV6 (♠) Williams <i>et al.</i>, (1998)</p> <p>AHSV4 (JK) Jeanne Korsmann (University of Pretoria, 2003)</p> <p>BTV10 (∞) Purdy <i>et al.</i>, (1996)</p> <p>EHDV1 (□) Iwata <i>et al.</i>, (1991)</p>
--	--

: : \* \* : \* \* \* \* \* : : : : : \* \* . \* \* :

**Figure 2.3.12** Amino acid comparison of all the AHSV VP5 sequences obtained with that of selected published BTV and EHDV VP5 sequences (see key for references). Identical amino acids are indicated by a (\*), whilst similar amino acids by a (:). The conserved cysteine residue found in both AHSV and BTV and EDHV are highlighted in green and the conserved glycine residue at the N-terminal is highlighted in yellow. Differences in amino acids are highlighted in teal (only within the N-Terminal regions). Grey shaded areas depict the various N terminal (1-123aa), central (192-273aa) and C terminal (460-505aa) regions respectively.



	AHSV3vir1	AHSV6vir1	AHSV9vir	AHSV6vir2	AHSV3vir2	AHSV3 ♣	AHSV6 ♠	AHSV8vir	AHSV9♦	AHSV4 ♥	AHSV4 JK	BTV10 ∞	EHDV1 □
AHSV3vir1		0	5	6	4	12	21	28	44	78	79	284	295
AHSV6vir1	0		5	6	4	12	21	28	44	78	79	284	295
AHSV9vir	0.10%	0.10%		11	9	17	26	33	48	83	84	283	298
AHSV6vir2	1.00%	1.00%	2.00%		10	18	27	32	50	83	84	283	294
AHSV3vir2	0.80%	0.80%	1.80%	2%		15	24	30	47	78	79	284	295
AHSV3 ♣	2.40%	2.40%	3.40%	4%	3%		21	26	46	81	82	290	297
AHSV6 ♠	4.00%	4.00%	5.20%	5%	4.80%	4.20%		35	53	85	86	286	296
AHSV8vir	5.50%	5.50%	6.50%	6%	6%	5.20%	7%		59	82	83	286	294
AHSV9 ♦	8.70%	8.70%	9.50%	10%	9.30%	9.10%	10.50%	12%		98	99	300	306
AHSV4 ♥	15.50%	15.50%	16.40%	16.40%	15.50%	16%	17%	16.20%	19.40%		1	280	291
AHSV4 JK	15.60%	15.60%	16.60%	16.60%	15.60%	16.20%	17%	16.40%	19.60%	0.20%		280	291
BTV10 ∞	56.40%	56.40%	56.20%	56.20%	56.40%	57.50%	57%	56.80%	59.50%	56.50%	56%		200
EHDV1 □	58.50%	58.50%	59.10%	58.30%	58.50%	59%	59%	58.30%	61%	58%	58%	38%	

AHSV3 (♣) Filter, (2000)

AHSV4 (♥) Iwata et al., (1992b)

AHSV4 (JK) Jeanne Korsmann (University of Pretoria, 2003)

AHSV9 (♦) du Plessis and Nel, (1997)

AHSV6 (♠) Williams et al., (1998)

BTV10 (∞) Purdy et al., (1996)

EHDV1 (□) Iwata et al., (1991)

**Figure 2.3.13** Distance matrix showing the percentage amino acid difference between sequences compared (lower triangle) and the actual amino acid changes between the sequences compared (upper triangle) between the VP5 sequences of various AHSV serotypes (both sequenced and published, see key for references) and two out-group sequences of BTV and EHDV (PAUP, version 4.0b10).

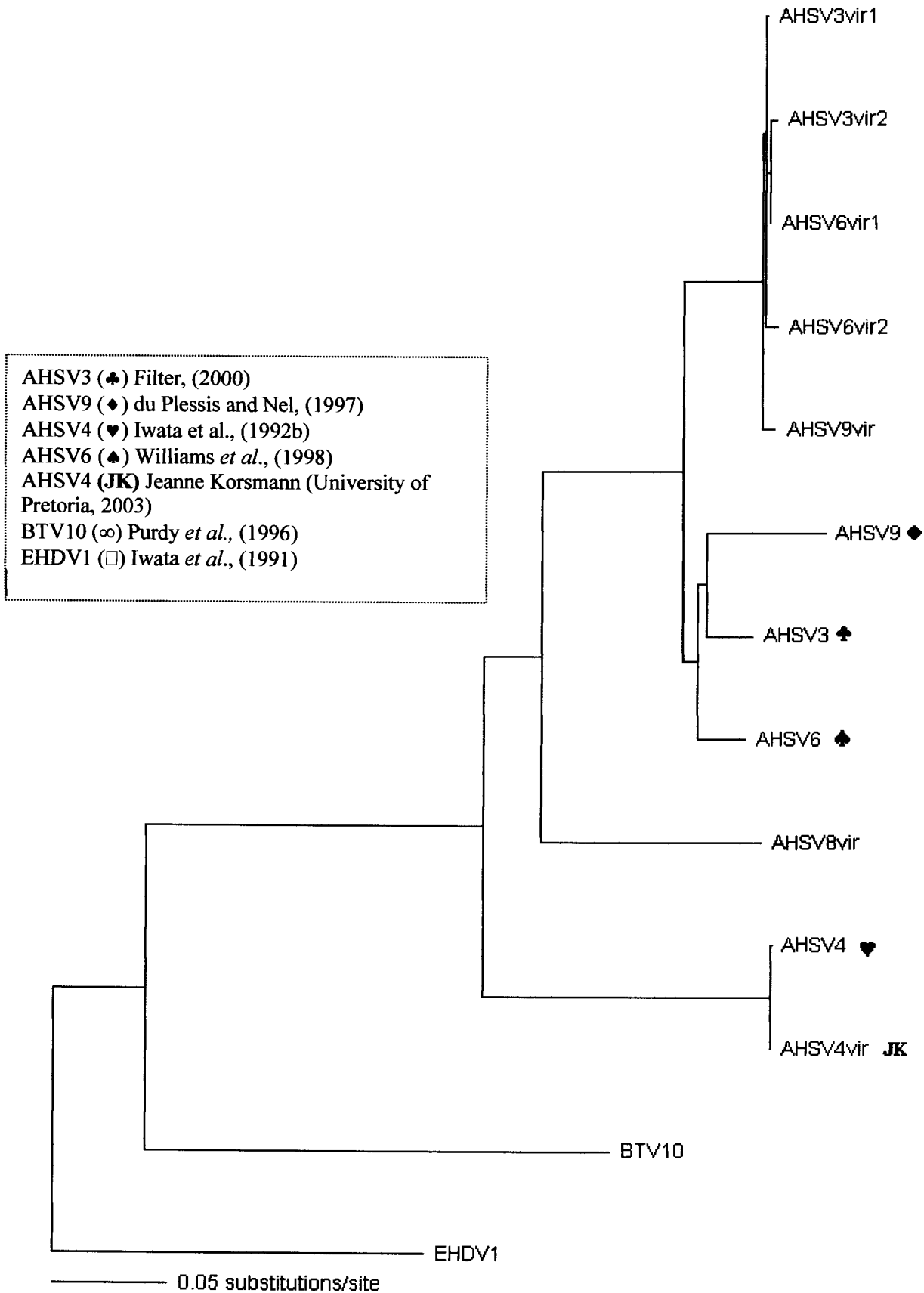


**Figure 2.3.14** Neighbor-joining phylogram of compared VP5 nucleotide sequences between AHSV serotypes using related *Orbivirus* BTV and EHDV VP5 sequences as outgroups.

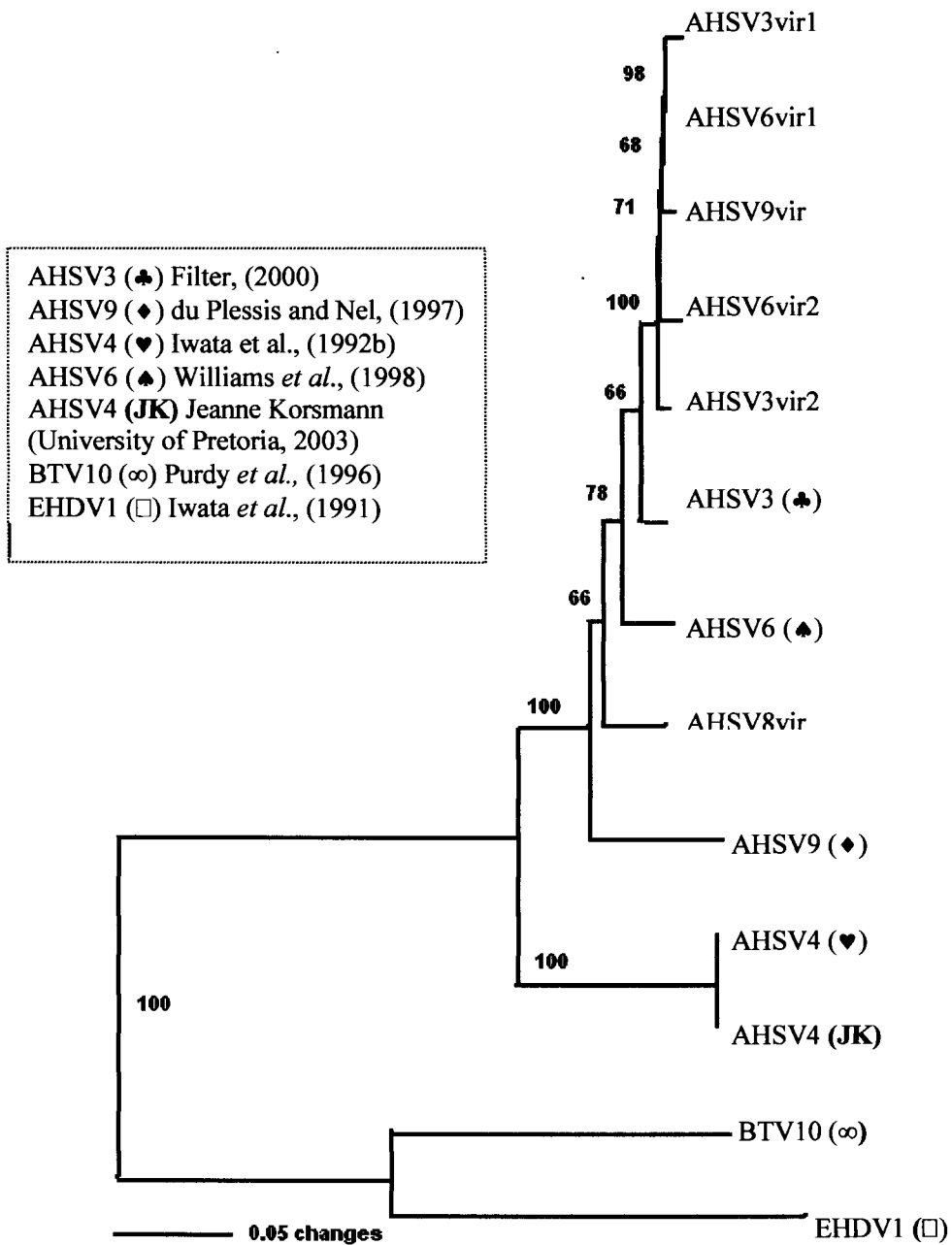


**Figure 2.3.15** Neighbour-joining phylogram of compared VP5 protein sequences between AHSV serotypes using related *Orbivirus* BTV and EHDV VP5 sequences as outgroups.

Structural analysis was performed and is shown for AHSV3vir2 VP5, as all the profiles generated for all sequenced strains showed high similarity and thus only one example would suffice. Firstly, hydrophilicity profiles using the ANTHEPROT program were generated using algorithms based on the findings by Kyte and Doolittle, (1982). Profiles generated for AHSV3vir2 VP5, AHSV4 VP5 (Iwata *et al.*, 1992b) and that of BTV10 VP5 proteins (Purdy *et al.*, 1986) show great resemblance (see Figure 2.3.16).

In general, comparisons between these profiles show a very comparable trend between hydrophilic and hydrophobic regions along the VP5 protein. It is noted that a predominantly hydrophilic region stretches from about amino acid 80 to 220 and also corresponds to the findings by du Plessis and Nel, (1997) regarding that of AHSV9 VP5. Other hydrophilic regions, albeit smaller are seen in regions 260 to 390 and 410 to 490 in all the observed proteins. Predominantly hydrophobic regions are seen in the N terminal region (40-80) and in the center region (220 to 260). Figure 2.3.17 shows a diagram representing all these hydrophilic and hydrophobic regions within the VP5 protein.

Comparing the hydrophilic profiles of AHSV3vir2 and AHSV4 VP5 reveal two regions of dissimilarity. In the 300-320 aa region, AHSV3 is more hydrophilic than AHSV4. Between amino acids 385-410, AHSV3 on the other hand is more hydrophobic than AHSV4 in this position. Comparing these specific positions to the profile of BTV10, shows that AHSV3 and BTV 10 share similar hydrophobic profiles. In the region of amino acids 430-450, AHSV3vir2 and AHSV4 are predominantly hydrophilic compared to BTV10, which is predominantly hydrophobic.

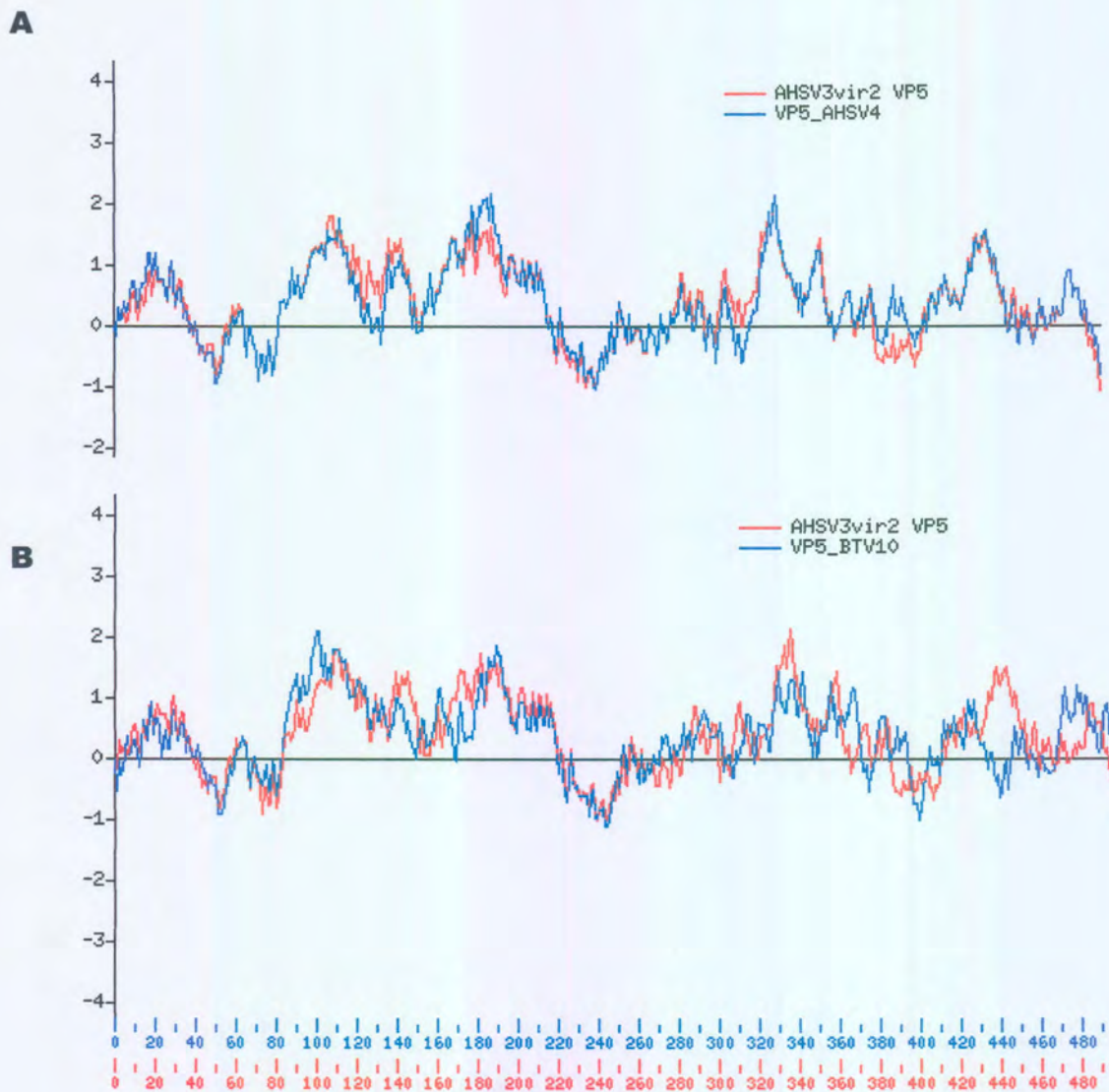


**Figure 2.3.16** Results of comparing the hydrophilic profiles of AHSV3vir2 VP5 to both  
 a) AHSV4 VP5 and  
 b) BT10 VP5.

The method of Kyte and Dolittle was used and generated (over a window length of 17) by the Bioinformatics and Biological Computing Unit, Weizmann Institute of Science, Israel. Areas above the centerline have a net hydrophilic value; whilst negative values (below the center line) indicate a net hydrophobic value.



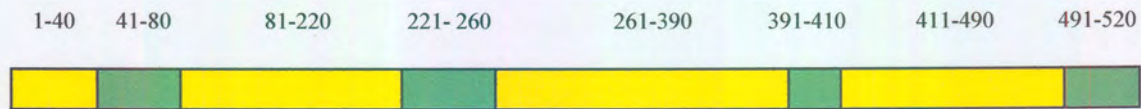
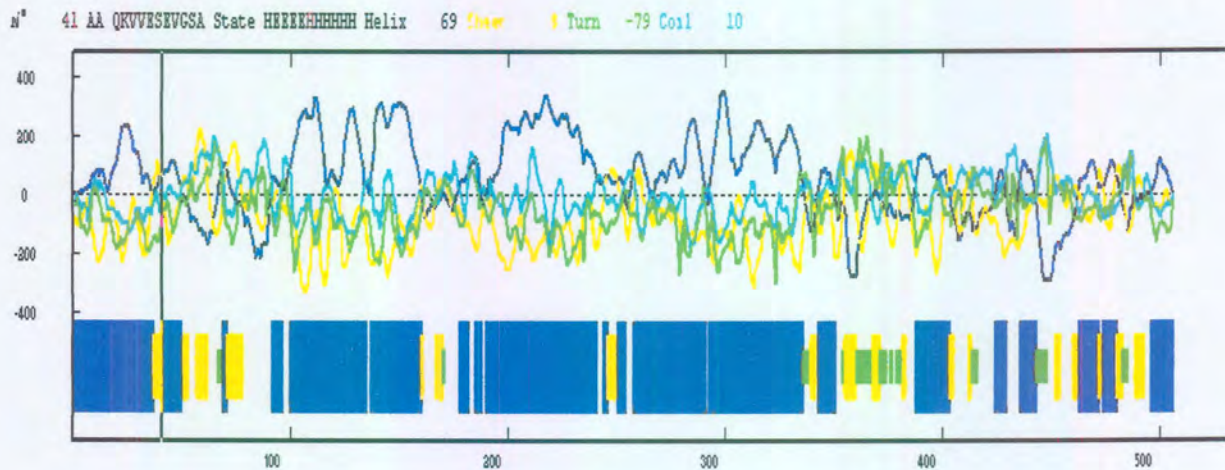


**Figure 2.3.17** Schematic diagram showing proposed regions of exposed hydrophilic (yellow) and buried (hydrophobic) residues (green) within the VP5 protein in general.

Predictions of the secondary structure from the amino acid sequence of AHSV3vir2 VP5 was done and compared to that of BTV10, using the GOR I method first described by Garnier *et al.*, (1978) by using the ANTHEPROT software analysis program (Figure 2.3.18). Significantly, the N-terminal regions of these two compared proteins differ to some degree, whilst the C-terminal regions are more similar. The  $\alpha$ -helix domains in BTV seem to be predominantly stretched over one large area (amino acids 95-260) whilst the N-terminal  $\alpha$ -helix domains of AHSV3 are divided into blocks. Less  $\beta$ -sheets are noted in the N-terminal region of AHSV3vir2 VP5 than in BTV10 VP5. Also, cognitive turn regions (shown in green) within the N-terminal are found in two different positions (approximately amino acid position 60 and amino acid position 13) in AHSV3vir2 and BTV10 respectively.

**A**



**B**

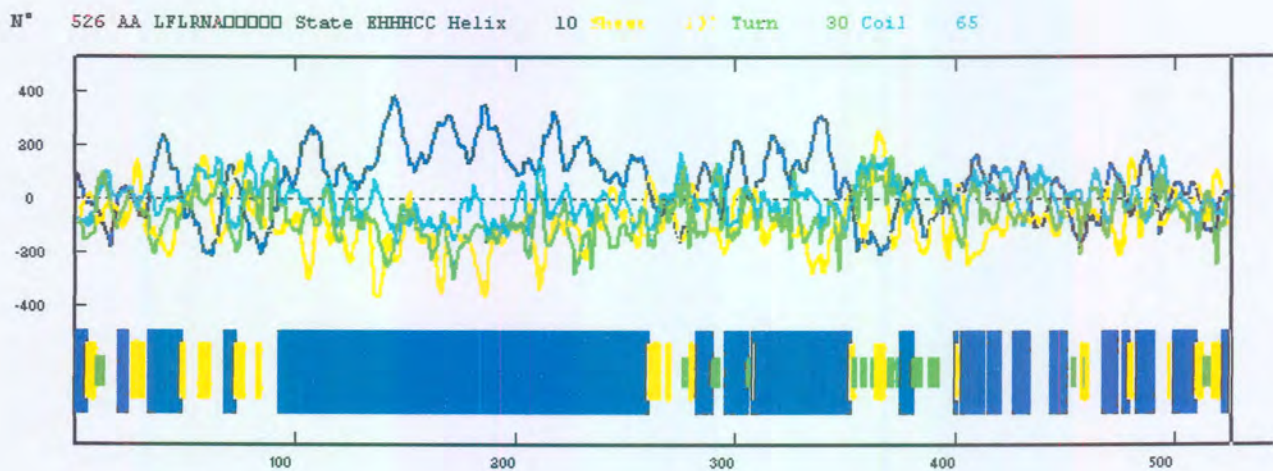


**Figure 2.3.18** Secondary structure prediction of a) AHSV3vir2 VP5 and b) BTV10 using GOR I analysis (originally described by Garnier et al., 1978) by the ANTHEPROT v4.9 protein analysis software program. The dark blue bars represent the  $\alpha$ -helix domains and yellow bars represent the  $\beta$ -sheet domains. Green bars indicate turns whilst light blue bars indicate coils.



In BTV, it was observed that two amphipatic helices occur in the N-terminal region of VP5 (Hassan *et al.*, 2001), between amino acids 1-19 and 20-39 respectively. In order to elucidate whether these helices are likely to occur in AHSV, helical wheels of the first 40 amino acids of both AHSV3vir2 VP5 and the more diverse AHSV4 were drawn and compared to BTV10 using two different programs. The helical wheel projection is used to calculate the hydrophobic moment (as originally described by Eisenberg *et al.*, 1982) in order to distinguish between surface helices (having a high hydrophobic moment), membranous helices (having a combination of both low and high hydrophobicity and soluble helices (with low hydrophobic moment and hydrophobicity).

The wheels projected by ANTHEPROT (results not shown), show that the overall pattern for the two N-terminal regions looks similar, with minor differences at various points. In the wheels generated by HelixDraw v1.00 ([www.eXpasy.org](http://www.eXpasy.org)), a more realistic representation of the amino acid positions are given, as well as the differentiation of hydrophilic amino acids into polar and charged amino acids (charged being more hydrophilic in nature than polar) (Figures 2.3.19 and 2.3.20).

In both AHSV and BTV, the second wheel projections (amino acids 20-39) have all their hydrophobic amino acids occurring on one side. This arrangement would support the formation of an amphipatic helix. For the first wheel projection (amino acids 1-19), two amino acids (amino acid K) occur on the hydrophobic side in AHSV, which is different to the arrangement found in the first 19 amino acids in BTV, where all the hydrophobic amino acids occur on one side. Although these three groups show significant differences in their amino acid sequences in general, both types of helical projections show that both BTV and AHSV VP5 N-terminal helices have their hydrophilic and hydrophobic surfaces facing opposite sides. These results strongly indicates that AHSV3vir2, as well as AHSV4 have the ability to form the two amphipatic helices in its N-terminal region.

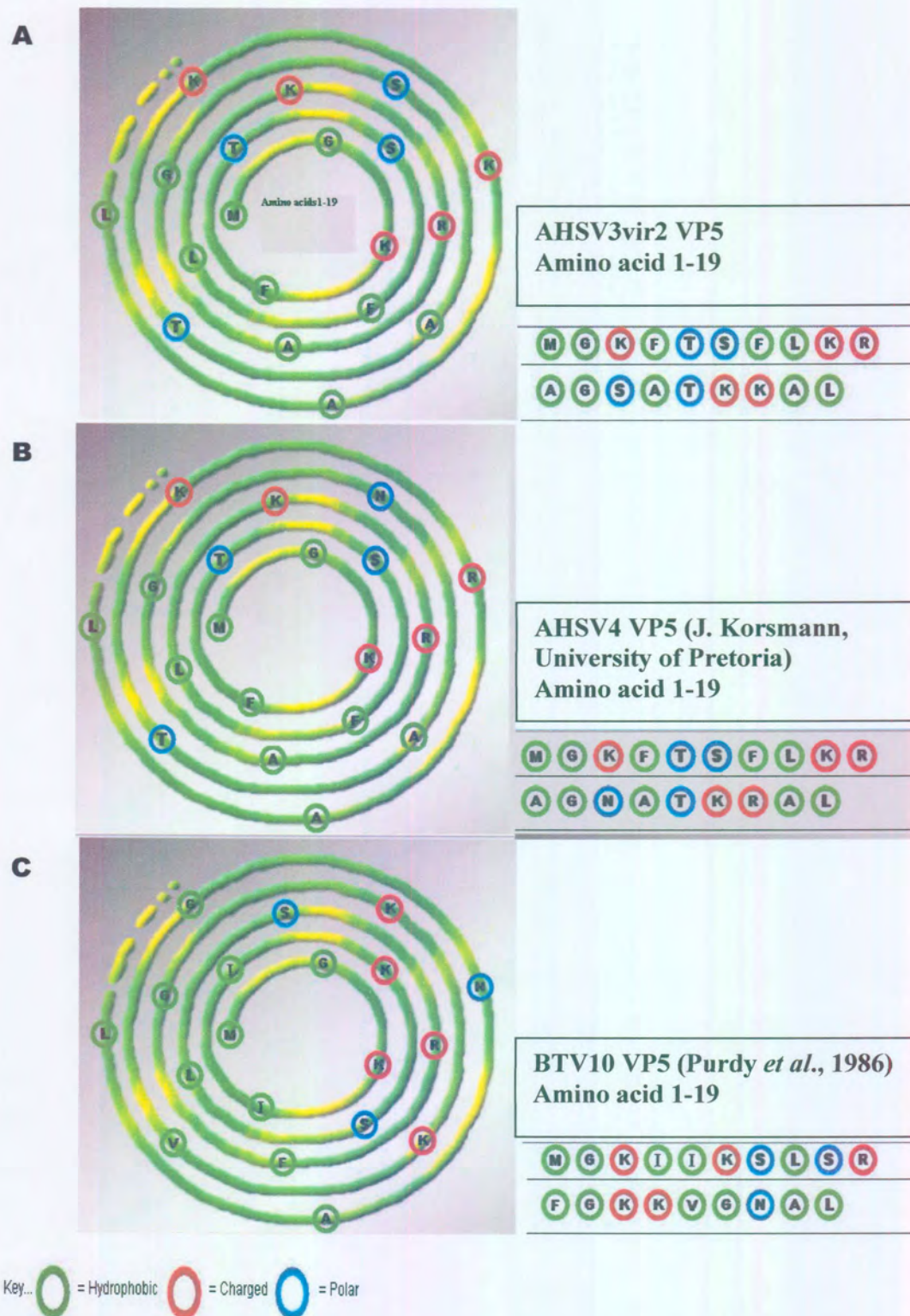
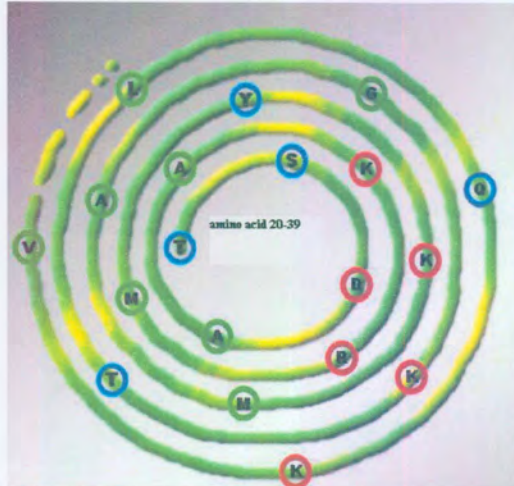


**Figure 2.3.19** Helical wheels generated by HelixDraw v1.0 software. Figures A-C represents the first amphipatic helix (amino acids 1-19) of AHSV3vir2, AHSV4 and BTV10 respectively, found at the N-terminal of VP5.



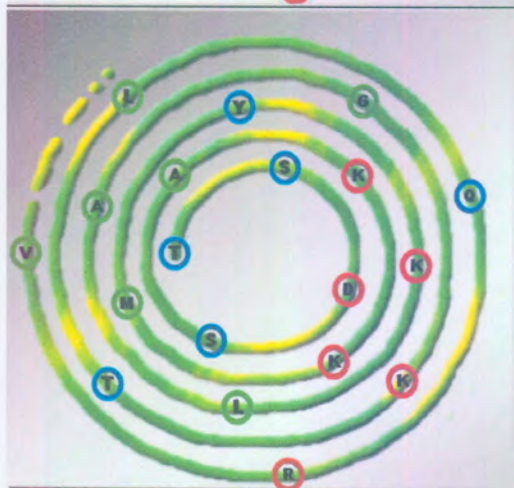
**A**



AHSV3vir2 VP5  
Amino acid 20-39

T S D A A K R M Y K  
M A G K T L Q K V

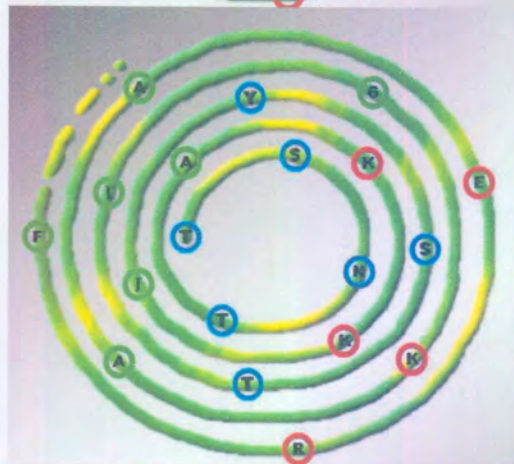
**B**



AHSV4 VP5 (J. Korsmann,  
University of Pretoria)  
Amino acid 20-39

T S D S A K K M Y K  
L A G K T L Q R V

**C**



BTV10 VP5 (Purdy *et al.*, 1986)  
Amino acid 20-39

T S N T A K K I Y S  
T I G K A A E R F

Key... = Hydrophobic = Charged = Polar

**Figure 2.3.20** Helical wheels generated by HelixDraw v1.0 software. Figures A-C represents the second amphipatic helix (amino acids 20-39) of AHSV3vir2, AHSV4 and BTV10 respectively, found at the N-terminal of VP5.

Lastly, a complete physico-chemical profile using the ANTHEPROT v4.9 protein analysis software program was generated for both AHSV3vir2 and BTV10 VP5 proteins (Figure 2.3.21), for comparative purposes. The methods employed by the program to infer the profile was a combined antigenicity profile (Parker *et al.*, 1986), a hydrophobicity profile (Kyte and Doolittle, 1982), an antigenicity profile (Welling *et al.*, 1985), a prediction of transmembrane regions (Von Heijne, 1992) and a solvent accessibility profile (Boger *et al.*, 1986). The antigenicity method (Welling *et al.*, 1985) is a useful tool to predict the location of antigenic regions within the protein.

The most noteworthy observation from the analyses are that the two profiles generated for AHSV3vir2 and BTV10 VP5 are remarkably similar, despite the fact that these serogroups share only 55% amino acid identity in their VP5 proteins. Notable differences are encircled in Figure 2.3.21 to aid comparison. In observing the antigenicity profiles generated for the two VP5 proteins, there are no distinct antigenic regions predicted, but rather the profiles indicate that predicted epitopes seem to be dispersed evenly across the protein. No transmembrane regions are predicted in either the AHSV3 or BTV10 proteins. Interestingly, the most probable helical regions of both VP5 proteins are likely to occur at the outer extremes of both termini.



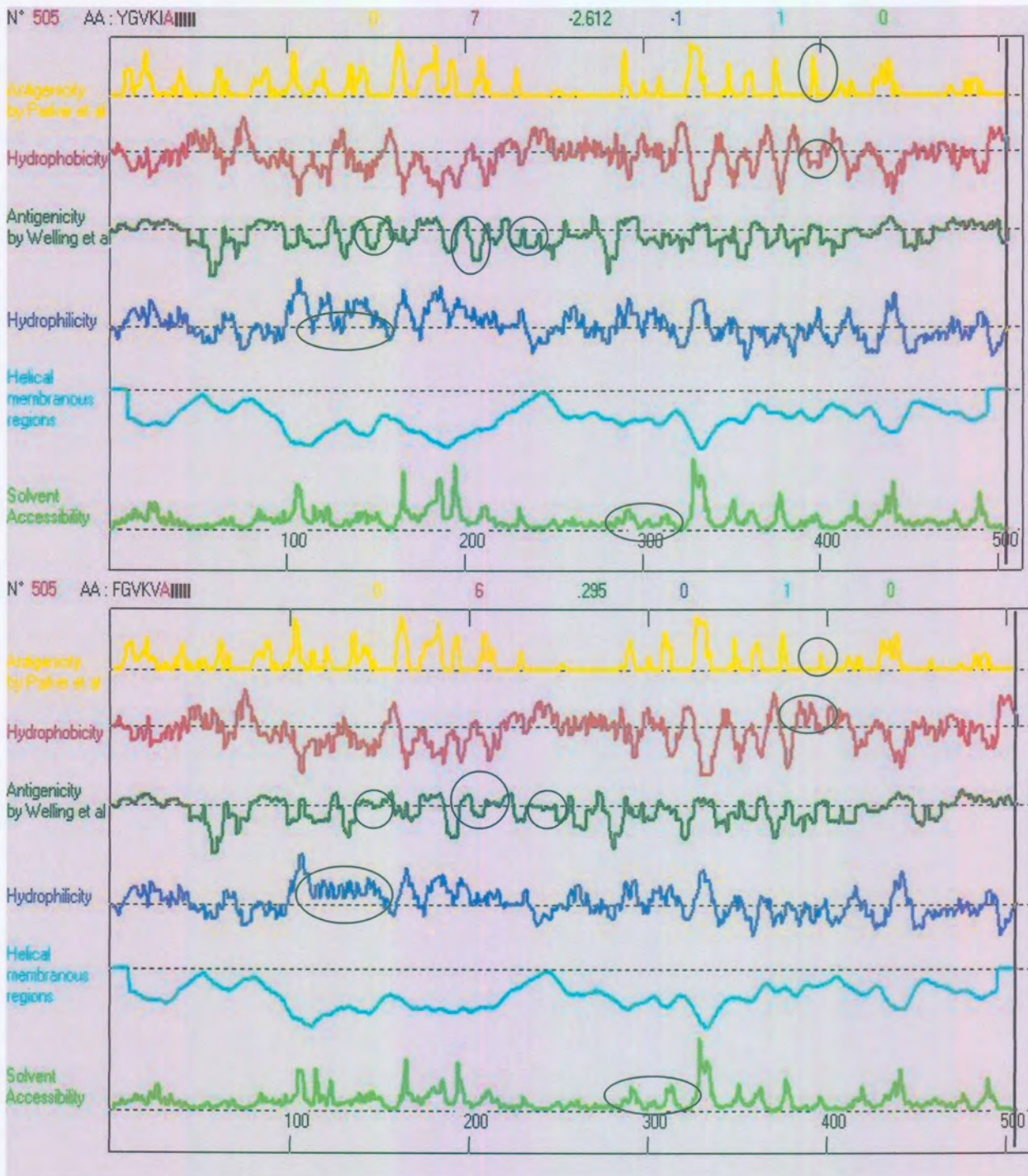


Figure 2.3.21

All profiles (antigenicity, hydrophobicity, hydrophilicity, helical membranous regions and solvent accessibility) generated for both  
 a) AHSV3vir2 VP5 and  
 b) BTV10 VP5 (Purdy *et al.*, 1986)  
 Using the ANTHEPROT v4.9 protein analysis software program. Notable differences are encircled in black.

### 2.3.5 Cloning of AHSV4 VP5 into the pET expression vector

As mentioned in the introduction to the chapter, the cytotoxic nature of AHSV VP5 could be evaluated by using an inducible bacterial system, such as the pET System designed by Novagen. By cloning the VP5 gene into the pET expression vector, expression can be selectively induced with the addition of IPTG and so enable quantification of any cytotoxic effects on bacterial cells.

The initial step in the pET cloning strategy was to prepare both the pET-41b vector DNA and the VP5 insert DNA for subsequent ligation. The VP5 gene of AHSV4 was already cloned into a TOPO® vector (Invitrogen™) and supplied by Dr Wilma Fick, (University of Pretoria). The pET-41b plasmid DNA was transformed into *XL1 Blue* cells and purified for subsequent digestion (see *Methods 2.2.2, 2.2.3 and 2.2.6 respectively*). Figure 2.3.22a below shows the purified TOPO-XL-AHSV4 VP5 (lane 2) and pET-41b (+) plasmid preparations (lane 3), relative to a size marker.

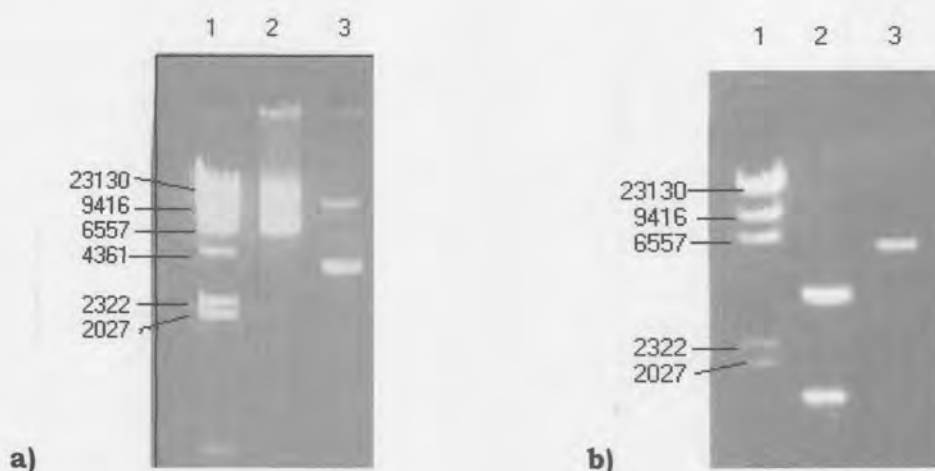


**Figure 2.3.22** 1% agarose gel analysis of a) undigested and b) *Eco* RI digested plasmid DNA. Lane 1: Molecular weight size marker. Lane 2: TOPO-XL-AHSV4 VP5. Lane 3: pET-41b (+) plasmid.

To confirm the correct plasmid sizes and to excise the VP5 band from the TOPO-XL-AHSV4 VP5 plasmid, endonuclease digestion with *Eco* RI was performed (Figure 2.3.22b). The expected linearised bands of sizes 5933 bp for the pET41b vector and 3500bp for the TOPO-XL-AHSV4 VP5 vectors were observed, as well as the excised VP5 gene fragment of 1566bp.



The VP5 gene from TOPO-XL-VP5 was amplified by PCR with the primers HS4M6FowNde and HS4M6EcoRev described in Table 2.2.1. As mentioned in the primer description, the incorporated primers within newly synthesized PCR products provided the respective *Eco* RI and *Nde* I enzyme sites for cloning purposes. The amplified VP5 gene (Figure 2.3.23 lanes 3 and 4) as well as the pET41b (+) vector (Figure 2.3.23, lane 2) was digested with *Eco* RI and *Nde* I to facilitate directional cloning. By choosing these respective enzymes, the GST tag within the pET41b (+) plasmid was excised (see faint 700bp band in lane 2 of Figure 2.3.23) to facilitate cloning of authentic VP5 without the tag, in the event that the tag might interfere with inherent VP5 cytotoxicity.



**Figure 2.3.23** A 1% agarose gel analysis of prepared vector and insert DNA. Lane 1: 100bp ladder marker. Lane 2: pET-41b (+) plasmid digested with *Eco* RI and *Nde* I. Lanes 3 and 4: PCR reactions in which the VP5 gene was amplified from TOPO-XL-AHSV-4 VP5.

The digested and column purified VP5 insert was ligated to the linearised, dephosphorylated pET41b (+) plasmid and transformed into X1Blue competent cells (according to methods 2.2.2, -3 and -7). Numerous attempts of this procedure did not yield any recombinant pET41b (+)/VP5 clones and it was concluded that these failed cloning attempts might be attributed to inefficient digestion of the PCR products. The undigested VP5 PCR fragment was then cloned into the pCR-XL-TOPO vector (Invitrogen™) as an intermediate step to generate the recombinant plasmid Topo-XL-VP5 *Eco/Nde* (Figure 2.3.24). Double digestion of Topo-XL-VP5 *Eco/Nde* with the restriction enzymes *Eco* RI and *Nde* I (Figure 2.3.24 lane 2) allowed for the



VP5 gene to be excised and gel purified for subsequent cloning into the pET41b (+) vector .



**Figure 2.3.24** 1% agarose gel analysis of recombinant TOPO-XL-VP5 *Eco/Nde* plasmid. Lane 1: Molecular weight size marker. Lane 2: undigested plasmid. Lane 3: Plasmid digested with *Eco* RI and *Nde* I to excise the VP5 band.

Ligation of the digested and dephosphorylated pET41b (+) vector DNA with this newly excised and digested insert allowed for successful cloning of the VP5 gene into this vector. A recombinant clone selected from kanamycin plates was named pET/VP5 (Fig 2.3.25). Various attempts to excise the VP5 gene from the new construct to confirm its presence, however, proved difficult. A reason for this was probably due to inefficient digestion with the *Nde* I enzyme, albeit extended incubation time (Figure 2.3.25, lane 3). Due to this partial digestion, only a faint VP5 band of the correct 1566bp size was observed upon *Nde* I and *Eco* RI double digestion. Incompletely digested vector DNA as well as completely digested vector DNA is therefore present (Figure 2.3.25, lane 3) as bands of approximately 6800 and 5200bp respectively.



**Figure 2.3.25** 1% agarose gel analysis of digested pET/VP5 plasmid DNA. Lane 1: Molecular weight size marker. Lane 2: *Eco* RI digestion. Lane 3; *Nde* I and lane 4: Double digestion with *Eco* RI and *Nde* I.

To further confirm that the VP5 gene was present in this construct, a PCR reaction using the primers used for original amplification of the gene was performed (Figure 2.3.26). An intense band (lane 5) corresponding to the size of the VP5 band, as amplified from two positive controls (lanes 3 and 4) was observed. This confirmed the presence of the VP5 gene in pET41b (+). The pET/VP5 construct was also sequenced to confirm that no aberrant mutations occurred during the amplification process and that the gene was cloned in the correct orientation (data not shown).

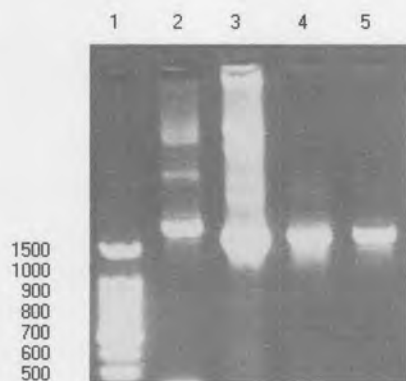


**Figure 2.3.26** 1% agarose gel analysis of PCR amplified DNA using VP5 specific primers. Lane 1: 100bp ladder, lane 2: amplified VP5 control, lane 3: Amplification from TOPO-XL-VP5, lane 4: Amplification from TOPO-XL-VP5 *Eco/Nde* (intermediate construct) and lane 5: Amplification from pET/VP5.

### 2.3.6. Transforming of the pET/VP5 clone into an expression host

The recombinant plasmid being established in its non-expression host could then be transferred into its expression host to induce expression of the target gene. Consequently, 250ng of pET/VP5 recombinant DNA was used to transform competent BL21 (DE3) expression host cells. Glycerol stocks of BL21 (DE3) cells containing wild type pET41a (+) was also streaked out on kan+ agar plates and used as a control. Resulting colonies were picked and grown in L.B. broth for subsequent procedures.

### 2.3.7. Induction of VP5 expression

Expression of the VP5 gene from the recombinant pET/VP5 construct is induced when IPTG is added to the expression host cell line, which allows for the expression of the T7 RNA polymerase under lacUV5 control. IPTG induction was done according to Method 2.2.9.1 and repeated in at least four separate experiments. Recombinant colonies within expression host cells were grown in culture until growth was indicative of a log phase. IPTG was added to both recombinant and wild type cultures to induce protein expression of target genes. Optical density measurements of both cultures were taken every half an hour for 120 minutes to determine the change in growth of the bacterial cells (Table 2.3.4 and Figure 2.3.27). As observed from the OD measurements, the expression of VP5 within bacterial cells negatively influenced cell growth. As time passed, the density of the cell culture containing the pET-VP5 construct decreased. In contrast, the cell culture containing the control plasmid (pET41b (+) vector with no insert) continued to increase in optical density as time progressed. The results indicated that expression of AHSV VP5 has a cytotoxic effect in bacterial cells.



**Table 2.3.4** Average OD measurements taken at various time intervals post induction to indicate cytotoxicity related to the expression of AHSV4 VP5 on bacterial cell growth.

Construct present within the expression host	Time interval post induction (minutes)	Average OD reading taken at 550nm
pET 41b (+) vector (control)	0	0.614
	30	0.83
	60	1.04
	120	1.204
pET/VP5	0	0.698
	30	0.746
	60	0.742
	120	0.556

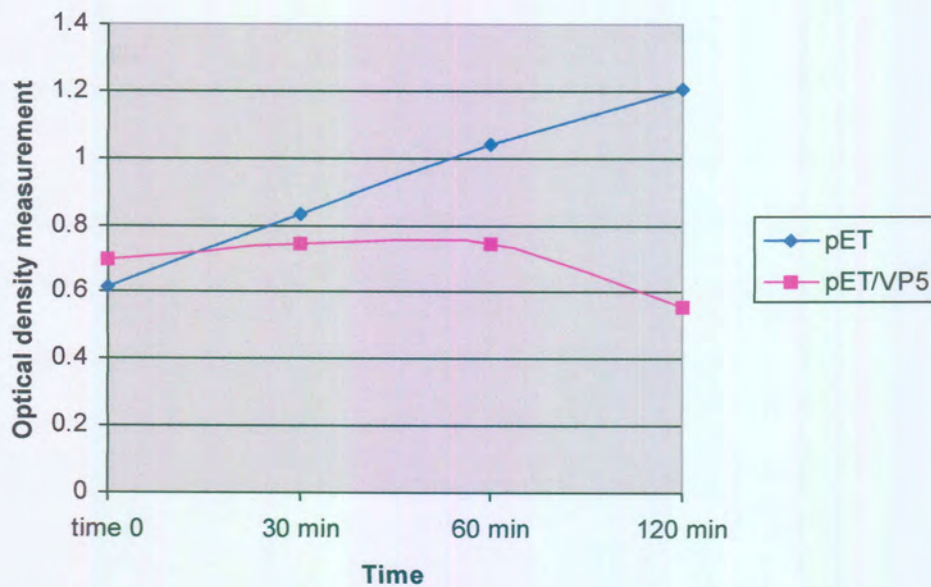


**Figure 2.3.27** A graphic representation of the results shown in Table 2.3.1. Optical density measurements are represented on the Y-axis, whereas the different time intervals are represented on the X-axis.

To confirm expression of the VP5 protein in the induced cell culture containing the pET/VP5 construct, the cellular proteins were analysed by SDS-PAGE at different times post induction. However, no unique band correlating to the 56kDa size expected for VP5 could be identified (results not shown). This could possibly be attributed to either low levels of expression or the fact that the protein band was obscured within all the bacterial protein bands. Consequently, *in vitro* labelling of the proteins expressed within the bacterial cell culture was performed. The proteins were pulse-labelled by <sup>35</sup>S-methionine labelling (see 2.2.12) and should theoretically allow for visualization of small amounts of expressed VP5. In order to eliminate background bacterial host expression, the potent transcription inhibitor rifampicin (Blackburn and Gait, 1996) was also added to the induced culture.

Despite numerous attempts and following the procedure closely, the expressed VP5 protein could not be identified with certainty. On the other hand, the GST tag of approximately 32 KDa from the unaltered pET41b (+) vector was well expressed upon induction (Figure 2.3.28, lanes 2 and 3). The presence of rifampicin proved to eliminate the background bacterial host expression when compared to their presence in the un-inhibited culture. This confirmed that the induction procedure was successful, i.e. expression from pET41b (+) was occurring in the bacterial hosts. By implication therefore, experimental conditions sufficed for VP5 protein expression. Very few cellular proteins were observed for the culture containing the pET/VP5 construct after induction (Figure 2.3.28, lane 5) and almost no proteins observed with the addition of rifampicin (Figure 2.3.28, lane 6). This is in agreement with OD reading results, indicating that the bacterial culture is not growing logarithmically, but rather decreasing at a rapid rate.

Certain alterations to the procedure were attempted, such as shortening the time from induction to completed labelling by reducing the time (from 30 minutes to 5 minutes) taken just before and after adding rifampicin. This was done by assuming that the expressed VP5 was rapidly killing the cells and by shortening all incubation times, cell death would be reduced and allows for VP5 visualisation.

In addition, the cultures were also labelled with  $^{35}\text{S}$  met for two different time intervals (15 and 25 minutes respectively) instead of one long 30-minute interval to compare the results and find the optimum time period before most of the cells has died. Figure 2.3.28A shows the results analysed by SDS-PAGE of the experiment performed during the labelling period of 25 minutes. The contrast of the gel was modified using computer software (Figure 2.3.28B) in order to intensify the proteins bands in the pET/VP5 induced experiment lanes. Protein bands of the approximate correct size of 56Kda were identified (Figure 2.3.28B, lanes 5, 6) and could be that of the expressed VP5 protein.

The supernatant of the cell culture was also retained, along with microcentrifuged pellet when preparing the samples for SDS-PAGE analysis. The supernatant was then subjected to TCA precipitation (according to Method 2.2.12) in order to visualize if any VP5 protein that might have been released into the supernatant. The results from the TCA precipitation (Figure 2.3.28, lanes 7 and 8) also showed no visible VP5 band. Upon altering the contrast of the acrylamide gels, faint bands that could be indicative of VP5 were observed.

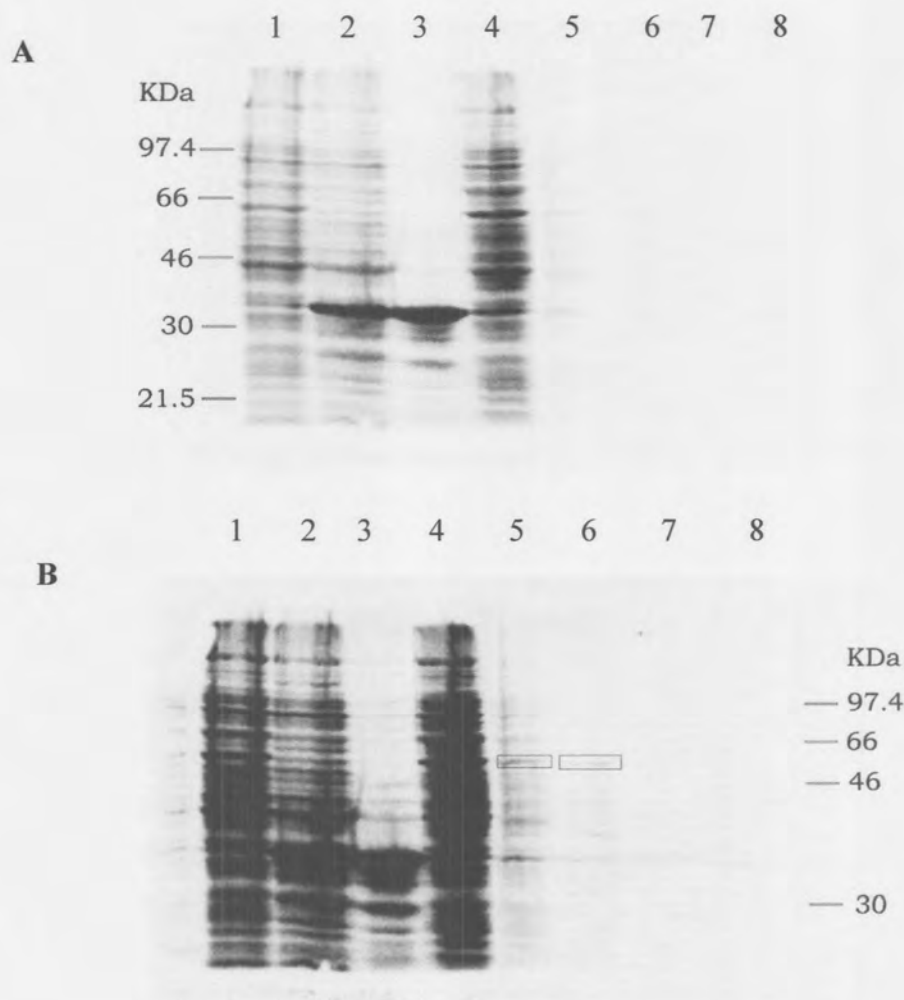


**Figure 2.3.28** A 10% polyacrylamide gel of  $^{35}\text{S}$ -met radiolabelled samples used in the pET cytotoxic expression studies with labelling for 25 minutes. Gel B is the more over-exposed version of gel A.

**Lane 1: uninduced pET 41b(+) vector**

**Lane 2: IPTG induced pET 41b (+) vector**

**Lane 3: IPTG induced pET 41b (+) vector in the presence of rifampicin**

**Lane 4: uninduced pET/VP5 recombinant expression vector**

**Lane 5: IPTG induced pET /VP5**

**Lane 6: IPTG induced pET /VP5 in the presence of rifampicin**

**Lane 7: TCA precipitated proteins in the uninduced pET/VP5 culture supernatant**

**Lane 8 TCA precipitated proteins in the IPTG induced pET/VP5 culture supernatant**

**Possible VP5 protein bands are shown in blocks.**



## **2.4. Discussion**

In order to gain a clearer understanding of the primary structure and level of variation of the VP5 outer capsid protein of AHSV, various field serotypes were characterised and compared to VP5 proteins of published AHSV, likely to be avirulent as well as other *Orbivirus* strains available in our laboratories. In total, 6 VP5 gene sequences from AHSV field serotypes 3, 6, 8 and 9 were sequenced and the subsequent protein sequences derived. This study represents new sequence data for AHSV field strains 3, 6 and 9 not previously published and previously unpublished AHSV8. The VP5 nucleotide sequences of all six isolates were 1566bp in length, which corresponds to the length of most AHSV VP5 genes sequenced to date. The G+C content of these genes averaged at 42%, whereas the A+T content averaged 58%, also in agreement with the base composition of other published sequences. The 5' and 3' terminal hexanucleotides were determined to be GTTAAT and ACATAC respectively, which are in agreement with the conserved AHSV terminal sequences described previously by Mizukoshi *et al.*, (1993).

The 505 amino acid long protein sequences of these VP5 genes were deduced from the longest ORF. This size is in agreement to those already published and represents VP5 proteins of approximately 56kDa in size. The amino acid composition of the VP5 proteins were compared and showed great overall similarity. The most abundant amino acids were alanine and glutamate whilst the relatively deficient amino acids were cysteine and tryptophan. More hydrophobic residues than hydrophilic occur, indicating that many of the VP5 protein residues are indeed unexposed. The cysteine residues are suggested to play an important role in the secondary and tertiary structure of a protein, because of their inherent ability to form disulphide bonds. These residues are conserved in amino acid positions 370, 372 and 482 in all AHSV VP5 genes except for AHSV4 VP5 in position 372. Interestingly, this 372-cysteine position is also conserved in BTV and EHDV and may play an important structural role between serogroups.

The VP5 sequences were aligned using the Clustal X software program and the intra- and inter- serotype/group conservation was deduced. The intraserotype variation between all the field and laboratory adapted VP5 amino acid sequences showed AHSV3 being the most conserved; with 99.2% between AHSV3vir1 and AHSV3vir 2, 97.6% between AHSV3vir1 and laboratory adapted AHSV3 (Filter, 2000) and 97% conservation between AHSV3vir 2 and laboratory adapted AHSV3 (Filter, 2000). Serotype 6 was also highly conserved, with 99% identity between AHSV6vir1 and AHSV6vir2, 96% between AHSV6vir1 and laboratory adapted AHSV6 (Williams *et al.*, 1998), and 95% conservation between AHSV6vir2 and laboratory adapted AHSV6 (Williams *et al.*, 1998). Of all the

serotypes compared, AHSV 9 showed the least amount of conservation between the field and laboratory adapted strains, being 90.5% conserved between AHSV9vir and laboratory adapted AHSV9 (du Plessis and Nel, 1997).

The interserotype variation showed AHSV3 and AHSV6 being the most conserved (95.2%-100%) in their VP5 sequences. Further comparisons between AHSV3 and other AHSV serotypes show 90.7%-99.9% (compared to AHSV9), ~94.5% (compared to AHSV8) and ~84% conservation when compared to AHSV4. Comparisons between AHSV6 and other serotypes reveal 89.5%-97.8% conservation with AHSV9, 93-94% with AHSV8 and the least amount with AHSV4 (83-84.5%). When compared to other serotypes, AHSV9 shows lesser homology with AHSV8 (88-93.5%) and AHSV4 (80.6-83.6%). AHSV4 and AHSV8 are only 83.8% conserved within their VP5 sequence. Interserogroup variation showed that AHSV VP5 was more conserved to BTV (40.5-43.8%) as to EDHV (39-41.7%). These results confirm other published results, showing that the AHSV VP5 genes are relatively conserved (at least in certain regions). Considering that VP5 interacts with both VP2 in the outer core and VP7 of the inner within the virion, the relatively high level of nucleotide conservation may be mostly due to structural constraints imposed on the encoded protein. The especially high percentage of conservation between the sequenced field strains in this study may also be a reflection of the fact that they are recent field isolates. The higher percentage of variation found between AHSV VP5 genes from the published data refer to vaccine strains that have been passaged extensively.

When considering each serotype independently, the comparisons between the field and laboratory adapted strains of AHSV3 are reviewed. Considering that alignments between all the AHSV3 amino acid sequences reveal amino acid identities of 97% and similarities of 99.6%, only 2 of the 14 amino acid differences were non-synonymous. The AHSV3 field strains (AHSV3vir1 and AHSV3vir2) were more closely related compared to either of them to the laboratory-adapted strain sequenced by Renate Filter, (2000). This was also confirmed in the compiled distance matrix and the resulting phylogram. Interestingly, more than 75% of the amino acid changes occurred within the first 240 amino acids, which is also shown to be hydrophilic in the hydropathic plot created for the AHSV3vir2 strain. No amino acid changes occurred within the first 40 amino acids where the two-amphipathic helices of the VP5 protein are suggested to reside (Hassan *et al.*, 2001). This result indicates that the virulence of AHSV3 may not be associated with specific changes within the N-terminal region, known to cause cytotoxicity in the related BTV. Considering that only two field strains were sequenced, there is not sufficient evidence to deduce any associated cause of virulence with certainty.

Alignment comparisons between the VP5 proteins of AHSV6 isolates reveal that the proteins were less conserved than those between serotype 3 with identities of 94.5% and similarities of 98%. Interestingly, the published strain had one less amino acid in position 427, followed by six changes when compared to those sequenced. Eleven of the 29 amino acid changes were non-synonymous; this is not surprising considering the 1 amino acid length difference between the field and laboratory adapted strains. All the changes were distributed evenly throughout the gene, except for the end region that contained the missing amino acid in laboratory adapted AHSV6 (Williams *et al.*, 1998). As with the AHSV3 field strains sequenced, the two AHSV6 field VP5 proteins were much more similar to each other than to the published AHSV6 vaccine strain (Williams *et al.*, 1998). Only two amino acid changes were noted in the two-amphipatic helices and both were synonymous, also showing that the virulence of AHSV6 may not be attributed to specific changes within the probable cytotoxic regions. Of the three field serotypes sequenced and compared to their laboratory adapted counterparts, AHSV9vir and AHSV9avir (du Plessis and Nel, 1997) were the least conserved, with amino acid identities of 90.5% and similarities of 94.9%. Synonymous amino acid changes comprised 65% of the total changes and all the changes noted were spread across the whole protein without a distinctive pattern. Only one synonymous change occurred within the first 40 amino acids, also suggesting that the virulence of this serotype cannot be related to any changes in the regions possibly responsible for cytotoxicity.

Overall, when comparing the VP5 protein of laboratory versus field strains of AHSV, no obvious single amino acid change(s) in particular regions through-out the protein were found that could be used to distinguish between the strains, i.e. no common single amino acid change correlated with the virulence phenotype. Any amino acid changes in the amphipatic helices regions may also be speculated to be involved in cytotoxicity and VP5 functioning by penetrating the endocytic membrane upon adsorption of virus. Since no obvious changes appear to occur in these particular, three amino acid regions between the serotypes analysed and the fact that this region is highly conserved (at least ~80% between all serotypes), indicates a high degree of function conservation, despite this region being relatively exposed.

The method of Kyte and Doolittle, (1982) used by the ANTHEPROT analysis program in the hydrophobicity method was used to predict the buried and exposed regions of VP5. Profiles generated for comparing AHSV3vir2 VP5 with both AHSV4 VP5 (Iwata *et al.*, 1992b) and BTV10 VP5 (Purdy *et al.*, 1986) showed a great degree of overall similarity. In particular 3 aa regions were found to be dissimilar in either serotype/group. In the 300-

320 amino acid region, AHSV3 compares to that of BTV10 VP5 aa residues by being more exposed in comparison to AHSV4. Similarly, AHSV3 and BTV10 aa residues are more buried in the 380-410aa region than AHSV4. Amino acid residues of AHSV3 and 4 are similarly exposed, where BTV10 are buried in the 430-450aa region. Hydrophobic regions within the protein compared to other profiles generated in published data for AHSV9 (du Plessis and Nel, 1997).

In general, the VP5 proteins between AHSV serotypes and BTV and EHDV are between 40-50% conserved and cluster distinctively apart from the AHSV clade within the compiled phylograms (Figures 2.3.14 + 15). Despite having this low percentage of amino acid identity, all the profiles and physico-chemical predictions were near identical. It can be concluded that the VP5 proteins of the various serogroups are structurally comparable, which is indicative of similar function.

The secondary structure prediction was generated by the ANTHPROT software using the GOR I method (originally described by Garnier *et al.*, 1978). The data suggests that the N-terminal of VP5 consists mostly of  $\alpha$ -helix domains interspersed by a few  $\beta$ -sheet domains and a small coil region. The C-terminal is dispersed with many more coils and  $\beta$ -sheet domains with less  $\alpha$ -helices. The  $\alpha$ -helix domain, at the extreme N-terminal (indicative of the two amphipathic helices) is observed when comparing the sequences of AHSV and BTV and is also confirmed with the helical membrane region analysis done with ANTHEPROT (Figure 3.2.26). Helical wheels drawn for the first 40 amino acids of the AHSV3 field VP5 correspond to the BTV wheels, indicating that the net-positive charge found on the hydrophilic face of the VP5 protein is able to interact with the negatively charged phospholipids within cell membranes.

In conclusion, the AHSV VP5 protein sequences analysed between the various serotypes were relatively well conserved, but became more variable when comparing between serogroups. The high degree of structural similarity between VP5s is expected, considering its position and core interactions. All the data obtained corresponds to those already published (Iwata *et al.*, 1991; Iwata *et al.*, 1992b; Purdy *et al.*, 1996; du Plessis and Nel, 1997; Williams *et al.*, 1998 and Filter, 2000). Furthermore, we could not identify a single amino acid change common to all assumedly virulent field strains, when compared to the laboratory adapted strains likely to be avirulent. It stands to reason that many factors within virion structures/proteins may be implicated in the degree of virulence of a particular strain. The suspected role of AHSV VP5, having membrane-destabilizing activity (Hassan *et al.*, 2001) such as to allow for core access into the cytoplasm is supported with the data obtained and compares well with the comparative

analysis with BTV. In the future, the next step would be to obtain and compare all the unknown VP5 sequences of the remaining AHSV serotypes and to correlate the data obtained.

In order to evaluate whether the AHSV VP5 protein displayed cytotoxicity activity, as was observed for the BTV VP5 (Hassan *et al.*, 2001) it was important to find a biological system to test this activity. The pET expression system was chosen to easily monitor the expression the VP5 protein within bacterial cells and to quantify the effects. Many studies have made use of various pET expression system to implicate a target protein's role in membrane permeability. Ciccaglione *et al.*, (2001) showed that the expression of the E1 glycoprotein of hepatitis C virus induced a change in membrane permeability that is toxic to *E.coli* cells. By cloning different fragments of E1 into the pET-3a expression vector and transforming them into BL21 (DE3) pLysS cells, the C-terminal hydrophobic region was shown to be responsible for membrane association and induced changes in membrane permeability. Similarly, the gp41 transmembrane glycoprotein of HIV-1 has been cloned and expressed in *E.coli* using the pET-3a vector (Arroyo *et al.*, 1995). Their studies showed two regions in gp41 that enhances membrane permeability, which supported theories that implicated gp41 in the cytopathology observed during HIV infection. Considering that VP5 is inherently known to be cytotoxic (Hassan and Roy, 2001), it was of great importance to be able to regulate the expression of this protein within host cells in order to control and circumvent the killing of cells. The pET system designed by Novagen, is an inducible system and could be used to only express the VP5 protein when desired.

The actual cloning of the VP5 gene into the pET transfer plasmid proved cumbersome and was later long-routed to obtain the desired recombinants. The reason for the initial unsuccessful attempts could partly be attributed to the fact that the PCR products were digested inefficiently with endonucleases, due to the lack of supporting nucleotides on the alternate side of the restriction site. Eventually, by first cloning the gene (together with its undigested restriction sites) into the PCR-XL-TOPO cloning vector later enabled the effective digestion of these restriction sites. The transformation of the recombinant pET vector into its expression host was very efficient but known to be short-lived, due to the maintenance of the cytotoxic gene. For that reason, most of the cultures or colonies were freshly grown from glycerol stocks prior to every experiment.

In assessing the effects of the expressed VP5 protein on bacterial cells, the OD readings obtained were highly reproducible across the four different experimental times, making



this form of evaluation uncomplicated and robust. As was seen in the results, the VP5 protein is very cytotoxic and hampers cell growth dramatically already after 30 minutes after expression. Considering that the growth curve obtained increased very slightly after induction and tapered off until eventually a negative increase of growth was observed, it indicated that the expression of VP5 severely retards cell growth and progressively caused cell death.

Visualisation of the expressed VP5 protein proved very difficult. Various changes to the protocol did nothing to increase the chance of confirming expression, because as soon as the cells were induced with IPTG, a distinct decrease in the production of cellular proteins occurred. A possible explanation could be that if VP5 was cell membrane associated (via amphipatic helices), only a small amount of membrane destabilizing VP5 would be needed to attach and cause rapid destabilization and cell death. This cessation of cellular processes will in turn stop the expression of cellular proteins, including that of VP5 and could explain the lack of VP5 protein observed. The remaining molar concentrations of VP5 may thus be too low to distinguish on a protein gel. Even when TCA precipitation was used, most of the VP5 expressed would be cell membrane associated and such fragments could have been lost upon the isolation procedure. In order to visualize this protein in future, it may be feasible to raise antibodies against this protein and analyse expression by Western blotting. These results confirm the findings by Hassan *et al.*, (2001) on BTV expressed VP5 that also found that VP5 expressed alone was highly cytotoxic and were easily degraded following expression.

Future experiments could entail the design and construction of various N-terminal deletion mutants of the VP5 protein in order to map the actual sequences responsible for cytotoxicity, such as already done by Hassan *et al.*, (2001), with BTV VP5. A possible approach was investigated for rapidly producing N-terminal deletant mutants by using unique restriction enzyme sites that would facilitate the removal of the N-terminal by digestion and subsequent re-ligation. Subsequent evaluation by the same experimental procedures could indicate a change in cytotoxicity and could be used to speculate more precisely which regions were responsible for this activity. Although unique restriction enzyme sites were identified in this region, it would have changed the reading frame of the VP5 gene upon digestion and re-ligation, making this strategy futile. Due to time restraints, the re-cloning of new PCR products to create deletion mutants, such as those made by Hassan *et al.*, (2001) for BTV, was not done and could serve as the aim for a new project.



## Chapter 3

# The construction and expression of AHSV VP5 epitopes in a VP7 expression vector.

## **3.1 Introduction**

As reviewed in Chapter 1, certain antigenic regions were discovered on the AHSV4 VP5 protein (Martinez-Torrecuadrada *et al.*, 1999). These antigenic regions were mapped to VP5 by using monoclonal antibodies (MAbs) that recognize two different epitopes. The epitopes were able to elicit a significant neutralizing response, albeit the titres were lower than observed with those induced by the VP2 capsid protein alone.

Martinez-Torrecuadrada *et al.*, (1999) found that the most immunodominant region was located in the N-terminal 330 residues of VP5. Two antigenic regions, I (residues 151–200) and II (residues 83–120) were defined. Epitopes were further defined by PEPSCAN analysis using 12mer peptides, which determined eight antigenic sites in the N-terminal half of VP5. At position 85–92, the neutralizing epitope (PDPLSPGE) recognized by MAb 10AE12 was defined. Similarly, at position 179–185 the neutralizing epitope (EEDLRTR), which was recognized by MAb 10AC6 was defined. Epitope 10AE12 is highly conserved between the different orbiviruses, by being able to recognize BTV VP5 and EHDV by several techniques, implying that mAb 10AE12 can be used as a group specific reagent suitable in the detection of an orbiviral infection.

The antigenic region recognized by MAb 10AC6 defines a hot immunogenic spot in the VP5 protein of orbiviruses. In particular, this region is hydrophilic, indicating exposure and accessibility to the immune system. Considering that the AHSV VP5 is able to induce neutralizing antibodies, these defined antigenic regions may be potentially useful in new generations of AHSV vaccines.

In order to investigate the antigenicity of these epitope regions defined by Martinez-Torrecuadrada *et al.*, (1999), one has to present them to the immune system. It is well known that small peptides need to be conjugated to larger structures (acting as carriers) in order to induce an immune response within a host. Alternatively, the use of sub-unit vaccines (as discussed in Chapter 1) can

allow for epitope regions to be expressed within appropriate vectors and presented to the immune system.

A novel approach in presenting these VP5 epitope regions will be investigated in this study, where it will be displayed on the surface of small particulate protein structures. This particulate presentation system is based on the VP7 protein of AHSV9 that has been modified to serve as a vector for the delivery of antigens to the immune system. The VP7 protein of AHSV is extremely hydrophobic and trimers of the protein spontaneously assemble to flat crystalline particles when expressed by baculoviruses in insect cells (Chuma *et al.*, 1992; Burroughs *et al.*, 1994; Maree *et al.*, 1998). Wade-Evans *et al.*, (1998) showed that unmodified VP7 crystals elicited a protective immune response to a lethal, heterologous serotype challenge in mice. The use of VP7 as a vaccine delivery system is based on the assumption that the surface of these flat particles presents an opportunity to display foreign peptides to the immune system.

A number of hydrophilic regions within the VP7 top domain that are exposed as loops on the VP7 surface have been identified to serve as potential insertion sites for foreign antigens. By inserting multiple cloning sites at codon positions 144, 177 and 200 of the VP7 genes (Maree, 2000; Riley, 2003 and van Rensburg, 2004) various modified forms of VP7 were previously created. These modified VP7 vectors have since been used to express a wide range of peptides, both short (9 to 50 amino acids) and longer (up to 250 amino acids) so as to evaluate all aspects related to the display potential of the system. These include variables such as the size limitations of inserts, best sites for insertion, particle formation, solubility and ultimately the ability to elicit antigen-specific neutralizing antibodies when used for immunization.

The chimeric VP7 proteins are produced in large quantities using a recombinant baculovirus system. Certain features of the baculovirus expression vector make it a desirable system to utilize; such as high levels of target gene expression, safety in working with and easy growth in the fall armyworm *Spodoptera frugiperda* (Sf) cell line. Luckow *et al.*, (1993) developed the novel baculovirus

expression system called BAC-TO-BAC™ that is commercially available. This system permits rapid and efficient generation of recombinant baculoviruses by the transposition of a DNA expression cassette into a bacmid<sup>1</sup>, which is propagated within *E.coli*.

The bacmid contains a mini-F replicon, a kanamycin resistance marker and a Lac *Zα* gene. Thus, the bacmid is able to replicate as a plasmid in *E.coli* DH10BAC cells by conferring kanamycin resistance and also complements the LacZ deletion present in the bacterial genome. This complementation (Lac+) allows for the formation of blue colonies in the presence of the chromogenic substrate X-gal and the IPTG inducer. The target gene is first cloned into the MCS of a pFASTBAC donor plasmid within a non-expression host cell line. Transposition of the mini-Tn7 found within this donor plasmid to the mini-Tn7 attachment site found on the bacmid generates recombinant bacmids in the presence of a helper plasmid. This transposition event disrupts Lac *Zα* protein expression allowing recombinants to be discerned on the basis of its white coloring in comparison to the wild type bacmid (see Figure 3.1.2). Recombinant bacmid DNA is isolated and transfected into insect cells, which allows expression of the target gene. In addition to its ability to increase the recombination frequency, this system also eliminates the need for repeated rounds of plaque purification in order to purify the recombinant from the wild type baculoviruses.

In this study, the display vector pFastbac VP7mt177 (having three enzyme restriction sites to facilitate cloning in amino acid site 177, see Figure 3.1.1), will be investigated for displaying AHSV4 VP5 epitopes. Regions encoding two individual VP5 epitopes of AHSV4, together with their flanking regions are to be inserted individually into site 177 of the pFB-VP7mt177 vector and recombinant baculoviruses generated. Consequently, the expression of the two different chimeric VP7 proteins from constructed recombinant baculoviruses should display each VP5 epitope on the surface of the resulting particles. In addition,

---

<sup>1</sup> Bacmid: baculovirus shuttle vector, derived from the *Autographa californica nuclear polyhedrosis virus* (AcNPV) genome

the region encoding both VP5 epitopes (with flanking regions) are also to be inserted into site 177 for the simultaneous presentation on a single VP7 protein. This may result in higher antibody titres than the presentation of each epitope independently. Also, the additional amino acids that flank the epitopes may facilitate a more immunologically favored conformation. The main aim of this study involved the initial characterization of these chimeric proteins' properties by isopycnic gradient fractionation and electron microscopy.

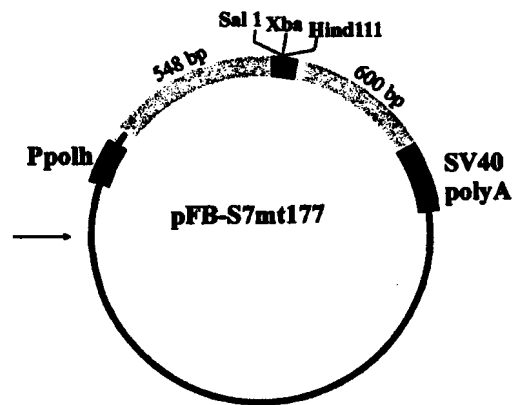


**Figure 3.1.1:** Diagram depicting the modified AHSV-9 VP7 protein cloned into the pFASTBAC donor plasmid (pFB-mt 177) for use in the BAC-TO-BAC™ expression system (taken from Maree, 2000).



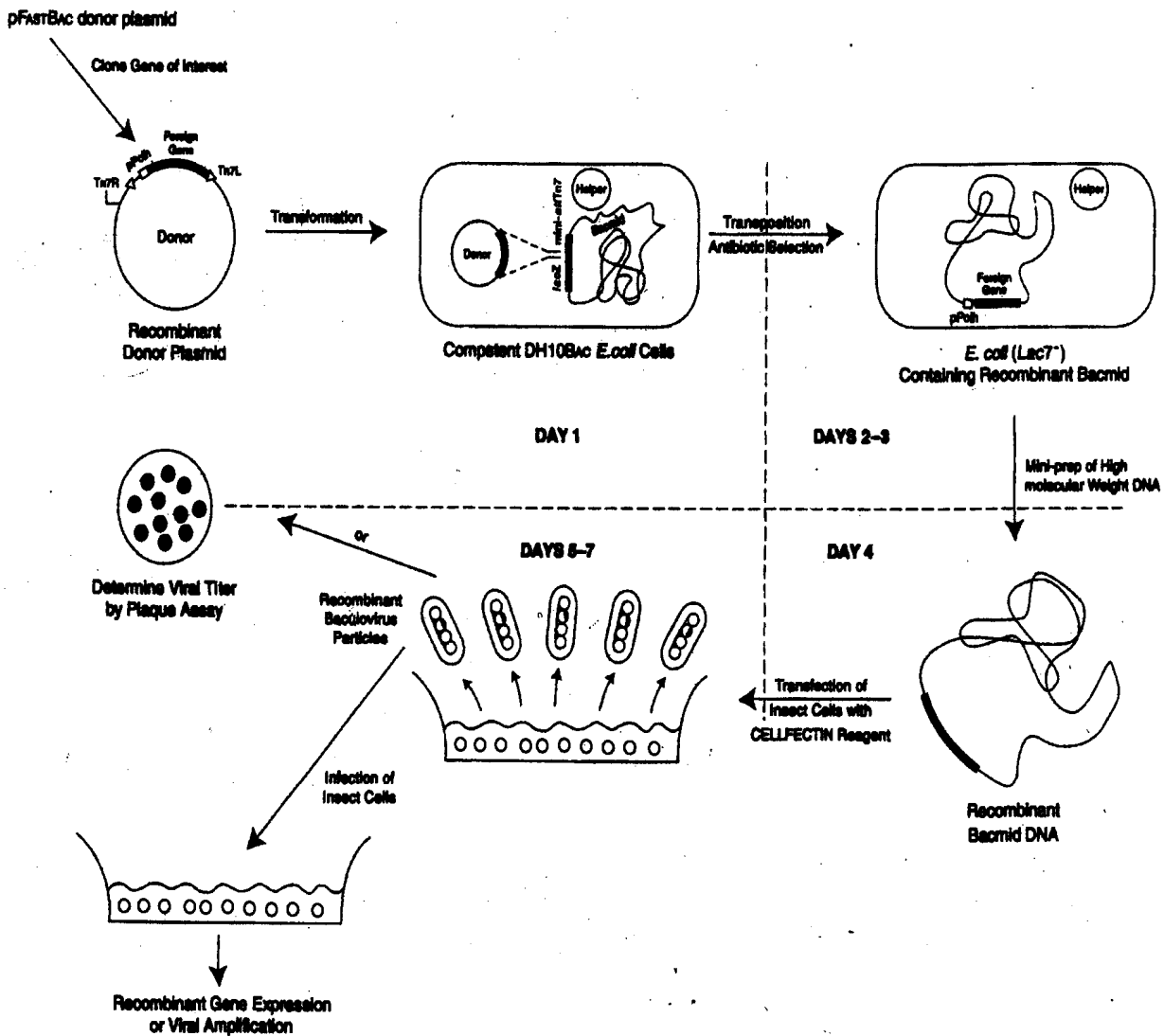


**Figure 3.1.2** Diagram showing the generation of recombinant baculovirus as well as subsequent gene expression with the BAC-TO-BAC™ Expression system. The target gene is first cloned into a pFastbac donor plasmid. The recombinant donor plasmid is then transformed into DH10BAC competent cells, which contains the bacmid DNA with mini-attTn7 target site as well as a helper plasmid. The mini-attTn7 target site on the donor plasmid can transpose to the mini-attTn7 target site on the bacmid in the presence of transposition proteins provided by the helper plasmid. Recombinant bacmid colonies are identified through the disruption of the lacZ $\alpha$  gene. Mini-preparations of recombinant bacmid DNA is prepared and used to transfect insect cells.

## 3.2 Materials and Methods

### 3.2.1. Amplification of gene regions encoding the AHSV VP5 epitopes

The primers used to amplify the VP5 epitope regions via PCR (as described previously in section 2.2.5) are tabulated in Table 3.2.1 below.

**Table 3.2.1 Custom primers designed to amplify the AHSV-4 VP5 epitope regions (Inquaba Biotech)**

Primer name	Sequence	T <sub>m</sub>	Target site on gene	PCR conditions
<b>1. HS4epi1HindF</b> Forward primer amplifying epitope 1. The <i>Hind</i> III restriction enzyme site is underlined.	5' CCC <u>AAG CTT</u> GTT GCG GGG ACA TTG GAA 3'	56°C	Nucleotide position 246-264.	95°C, 5 min x1, (95°C, 45 s), (58°C, 45 s) (72°C, 2 min) x30, 72°C, 10 min
<b>2. HS4epi1SalR</b> Reverse primer amplifying epitope 1. The <i>Sal</i> I restriction enzyme site is underlined	5' CCC <u>GTC GAC</u> TTC AAT CAC TCG ATC CTC 3'	54°C	Nucleotide position 342-360.	
<b>3. HS4epi2HindF</b> Forward primer amplifying epitope 2. The <i>Hind</i> III restriction enzyme site is underlined.	5' CCC <u>AAG CTT</u> AGC GGT TTG CTG GAG 3'	56°C	Nucleotide position 483-498.	
<b>4. HS4epi2SalR</b> Reverse primer amplifying epitope 2. The <i>Sal</i> I restriction enzyme site is underlined.	5' CCC <u>GTC GAC</u> CGC TTC TTT CAA CGC GTC 3'	56°C	Nucleotide position 618-630.	

### 3.2.2 Sequencing of recombinant pFastbac vector

Recombinant pFastbac vectors containing the two VP5 epitopes (either separately or simultaneously) were confirmed using DNA sequencing as described previously in section 2.2.15. The table below describes the primers used to amplify the full-length nucleotide sequence of VP7mt177 together with its accompanying insert.

**Table 3.2.2 Custom primers designed to amplify the AHSV9 VP7 gene within pFastbac VP7 mt177 vector (Inquaba Biotech).**

Primer	Sequence	T <sub>m</sub> 4(G+C) n + 2(A+T) n	Target
Forward primer VP7 FWD1	5'd(TTACGTACCGCAAGGTCG)	56°C	Native AHSV-9 VP7 (440-457bp)
Reverse primer VP7 RVH1	5'd(GAACCGTGTCTAGCGATC)	56°C	Native AHSV-9 VP7 (781-798 bp)

### 3.2.3 Bacmid transposition

Competent *E.coli* DH10Bac cells were prepared according to the CaCl<sub>2</sub> method (as described in 2.2.1). The competent cells were kept on ice until transformed with 50µg recombinant pFastbac vector containing the desired target gene region (see 2.2.2). Instead of shaking the 1ml transformation mixture for 1 hour (as described in 2.2.2), the glass tubes were left shaking for 4 hours at 37°C. The transposition mixture (50-100µl) was plated out onto 1.2% (m/v) agar plates containing 50µg/ml kanamycin, 7µg/ml gentamicin, 10µg/ml X-gal<sup>2</sup> (Biosolve) and 40µg/ml IPTG (Boehringer Mannheim). Plates were incubated for at least 24 hours at 37°C to facilitate differentiation between resulting white (recombinant) and blue (non-recombinant) colonies. Candidate white colonies were replica-plated in order to verify their phenotypes.

### 3.2.4 Isolation of Bacmid DNA

Isolating recombinant bacmid DNA was accomplished by using an adaptation of the alkaline lysis method (described in 2.2.3). This protocol as described in the BAC-TO BAC™ Baculovirus Expression system manual was used and proceeds as follows: verified white colonies are picked with sterile toothpicks and used to inoculate 2ml LB broth supplemented with 50µg/ml kanamycin, 7µg/ml gentamicin, 10µg/ml tetracycline. These cultures were grown O/N at 37°C with shaking. Cells were pelleted by centrifugation at 5000r.p.m for 10 minutes and the supernatant discarded. The cell pellet was gently resuspended in 300µl

<sup>2</sup> X-gal: 5-Bromo-4-chloro-3-Indolyl-β-D-galactopyranoside

Solution 1 (25mM Tris-HCL at pH 8, 50mM glucose and 10mM EDTA<sup>3</sup>) and left on ice. Following the addition of an equal volume of solution II (0.2M NaOH-1% SDS, pH 7.4) the cells were kept on ice for a period not exceeding 5 minutes before adding 300µl of a KOAc (pH 5.5) solution slowly and gently mixing. The samples were incubated on ice for a further 10 minutes before being centrifuged at 13000r.p.m for 15 minutes. The clear supernatant was transferred to a new eppendorf containing 0.6 volumes of isopropanol at RT. The tubes were inverted to mix the contents and the bacmid DNA was consequently precipitated by incubating on ice for a further 10 minutes. At this stage, the samples could be stored at -20°C for a few weeks. Following centrifugation (at 13000r.p.m for 20 minutes), the bacmid DNA pellet was washed with 70% ethanol and centrifuged again. The supernatant was aspirated in sterile conditions and the pellet was allowed to dry in a laminar flow cabinet. The dried pellet was dissolved in 40µl Sabax water for a period of approximately 10 minutes before transfecting Sf9 insect cells.

### 3.2.5 Transfection of Sf9 cells

Spodoptera frugiperda cells (Sf9), originally obtained from the NERC institute of Virology (United Kingdom), were grown as suspension cultures in spinner flasks (Pyrex) at 27°C with rotational shaking at 114rp.m in a rotational shaker. The cell culture medium, Grace's Insect Medium, was supplemented with 10% Foetal Calf Serum (FCS) and 1.2x antibiotic-antibiotic solution (both supplied by Highveld Biological). Cell density of suspension cultures were determined by using a haemocytometer (Neubauer) with 0.4% trypan blue (Sigma) in 1XPBS, which serves to assess cell viability. Cell cultures were sub-cultured when a cell density of 2-2.4 X 10<sup>6</sup> cells/ml was reached.

A six-well plate (Nunc™) was seeded with Sf9 cells at a density of 1x10<sup>6</sup> cells/35mm well. Cells were allowed to attach at 27°C for at least an hour before transfection. Cells were transfected with recombinant bacmid DNA using the optimized cationic lipid reagent Cellfectin® (Invitrogen). Five microlitres of

---

<sup>3</sup> EDTA: ethylenediamine tetraacetate; functions to inactivate nucleases by binding mg<sup>2+</sup> co-factors and so promotes the destabilization of bacterial cell walls (Brown, 1986).

newly isolated bacmid DNA was added to 100µl Grace's medium, which did not contain any supplements. A second solution, containing 6µl of Cellfectin® reagent in 100µl Grace's medium, also without any supplements, was prepared as well. The two solutions were added together and gently mixed. The mixture was incubated at RT for 15-45 minutes to allow for the formation of lipid-DNA complexes. Grace's insect medium (800µl) was then added and gently mixed. The attached Sf9 cells were washed with Grace's medium (not containing any supplements). The wash medium was removed and the 1ml diluted DNA-lipid complex mixture was added to the cells of each well. The cells were incubated for a further 5 hours at 27°C to allow for complete transfection. The transfection mixture was removed and replaced with 2ml cell culture medium, which contained both FCS and antibiotics. The cells were incubated for a further 96 hours at 27°C before harvesting the supernatant containing baculoviruses.

### 3.2.6 Propagation of recombinant baculovirus

A six-well plate (Nunc™) was seeded with Sf9 cells at a density of  $1 \times 10^6$  cells/35mm well. Cells were allowed to attach at 27°C for at least an hour, before the insect cell medium was removed. Approximately 1/10<sup>th</sup> of the transfection supernatant (*from above in 3.2.4*) was used to infect these newly attached cells, together with fresh insect medium to make up a final volume of 1ml. Cells were incubated at 27°C for 1 hour before another 2ml of medium was added. The cells were left to incubate at 27°C for a further 72 hours before harvesting the supernatant for subsequent passaging and preparation of virus stocks.

Rinsing with PBS<sup>4</sup> and centrifuging in a microcentrifuge at 1500rpm for 5 minutes aided in the collection of the infected Sf9 cells. Further washing with PBS-A facilitated excess salt and serum removal. Subsequent resuspension of cells in 30µl of PBS allowed for the analysis of proteins by SDS-PAGE (see sections 2.2.10 and 3.2.7).

---

<sup>4</sup> PBS: 137mM NaCl, 2.7mM KCl, 4.3 Mm Na<sub>2</sub>HPO<sub>4</sub>, 2H<sub>2</sub>O, 11.4 MKHPO<sub>4</sub>, pH 7.



### 3.2.7 Sucrose gradient purification by ultracentrifugation.

The Sf9 cell lysate of a 1x 75cm<sup>2</sup> flask baculovirus infection was harvested after 96 hours. The cell pellet was collected by centrifugation at 3000 r.p.m for 5 minutes. In the meantime, 10ml of 1x PBS was added to the cell monolayer and resuspended to allow dissociation of the cells from the flask. The resuspended cells were added to the harvested cell pellet and centrifuged again. The resulting cell pellet was resuspended in 1ml cold lysis buffer (1X PBS, 0.5% Nonidet P-40) and incubated on ice for 30 minutes. Fifty to seventy percent sucrose in 1x PBS was packed into sterile 5mL Beckman polyallomer ultracentrifuge tubes by layering from the bottom using 800µl of the lowest percentage (50%) sucrose followed by the next highest (i.e. 800µl of 55% sucrose) to form a 50-70% (w/v) sucrose gradient. Eventually, the bottom layer in the tube contained the 70% sucrose with the lesser dense sucrose percentages above that. Five hundred microlitres of the lysis sample was loaded per sucrose gradient and centrifuged in a SW50.1 rotor at 12000r.p.m for 1 hour and 15 minutes at 4°C.

Approximately 10-12 fractions were collected with a fractionator and the resulting pellet resuspended in 250µl 1x PBS. Half of each fraction was used to determine the protein content by SDS-PAGE analysis, (i.e. 200µl of a 400µl fraction was taken and added to 1300µl 1x PBS for centrifugation at 5000 r.p.m for 45 minutes before loading the pellet) The resuspended pellets were pooled and placed onto a new sucrose gradient for subsequent fractionation under the same centrifugal conditions. After analysis of the fractions by SDS-PAGE, the fractions that contained the protein of interest can be retained and stored at -4°C until S.E.M. preparation.

### 3.2.8 SDS-PAGE analysis of expressed proteins

Samples resuspended in PBS were loaded onto a polyacrylamide gel and the proteins were separated by 12% SDS polyacrylamide gel electrophoresis (SDS-PAGE)). Subsequent Staining in Coomassie Brilliant Blue staining solution facilitated subsequent visualization of protein bands on the polyacrylamide gel as described in 2.2.10.

Protein content of sucrose gradient fractions was analyzed by SDS-PAGE. Each fraction (1/50<sup>th</sup> of each) was resuspended in 10 $\mu$ l 2XPSB and analyzed on a 12% denaturing polyacrylamide gel, as described in section 2.2.10. An equal quantity of the pellet, also 1/50 of total volume, was loaded on the gel. The specified protein content of the fractions was quantified the Quantity One-Discovery series™ version 4.4.1 by Bio-Rad, which measures the relative band intensities on an SDS-PAGE gel.

### 3.2.9 Scanning electron microscope (S.E.M.) sample preparation

The remaining fractions that contain the protein of interest were pooled and added to 1300 $\mu$ l sterile filtered 1x PBS and centrifuged at 5000r.p.m for 45 minutes. The pellet was resuspended in 500 $\mu$ l sterile filtered 1x PBS. One milliliter of a 2.5% gluteraldehyde solution (25% gluteraldehyde stock and 0.2M NaPO<sub>4</sub> buffer) was added to the sample. A syringe was used to remove the sample and inject into a filter stub containing a filter. The sample was left for a further 10 minutes before washing with a filtered 1:1 solution of 0.2 M NaPO<sub>4</sub> buffer and Sabax water in order to fix the sample onto the filter. The sample was then washed a further six times (with 10 minute intervals) with 2.5ml of filtered fixing solution. Subsequent washes in order to dehydrate the sample, was done with 50%, 70%, 90% and 96% filtered ethanol. Each wash with an increasing percentage of ethanol was done with two sequential 2.5ml solution washes separated by 10 minutes. The samples were then dried in a critical point drier for 3 hours. The dried samples were subsequently mounted onto aluminum stubs and sputter coated with gold before viewing under the scanning electron microscope. The samples were viewed in a JEOL 840 Scanning electron microscope at 5 kV.

## **3.3 Results**

### **3.3.1 Amplification of the VP5 epitope regions**

In order to amplify the two different regions that encode the VP5 epitopes and their flanking regions from the pCR®-XL-TOPO® vector containing the AHSV4 VP5 gene (kindly provided by Jeanne Korsman, University of Pretoria), a combination of the primer sets in Table 3.2.1 were utilized. Both epitope regions were amplified independently as well as simultaneously by PCR, for subsequent cloning into the pFastbac-VP7 mt177 transfer plasmid. The construction of these three different plasmids is schematically shown in Figure 3.3.1.

The eight amino acid region (PDPLSPGE) representing the first epitope recognized by MAb 10AE12, together with flanking regions (8 amino acids downstream of the epitope and 20 amino acids upstream) will be defined as epitope A from here on forward. Similarly, epitope B is collectively defined as the seven amino acid region recognized by MAb 10AC6 together with flanking regions (23 amino acids downstream and 19 amino acids upstream of the epitope) see Table 3.3.2.

Epitope A was amplified using the first two primers, HS4epiHindF and HS4epiSalR. An expected PCR product of approximately 108 nucleotides long, which corresponds to the 36 amino acid long region that containing the first epitope and its flanking regions was observed upon electrophoresis (lanes 3 of Figure 3.3.1) Similarly, epitope B was amplified using the other primer set HS4epi2HindF and HS4epi2SalR. The expected length of the second epitope and flanking regions is 49 amino acids, which correlates to the approximate band size of 147bp observed in Figure 3.3.1, lanes 2 and 4.

**Table 3.3.1** Schematic representation of the construction of three different recombinant transfer plasmids containing the two gene regions that encode the VP5 epitopes and their flanking regions for transposition into baculoviruses

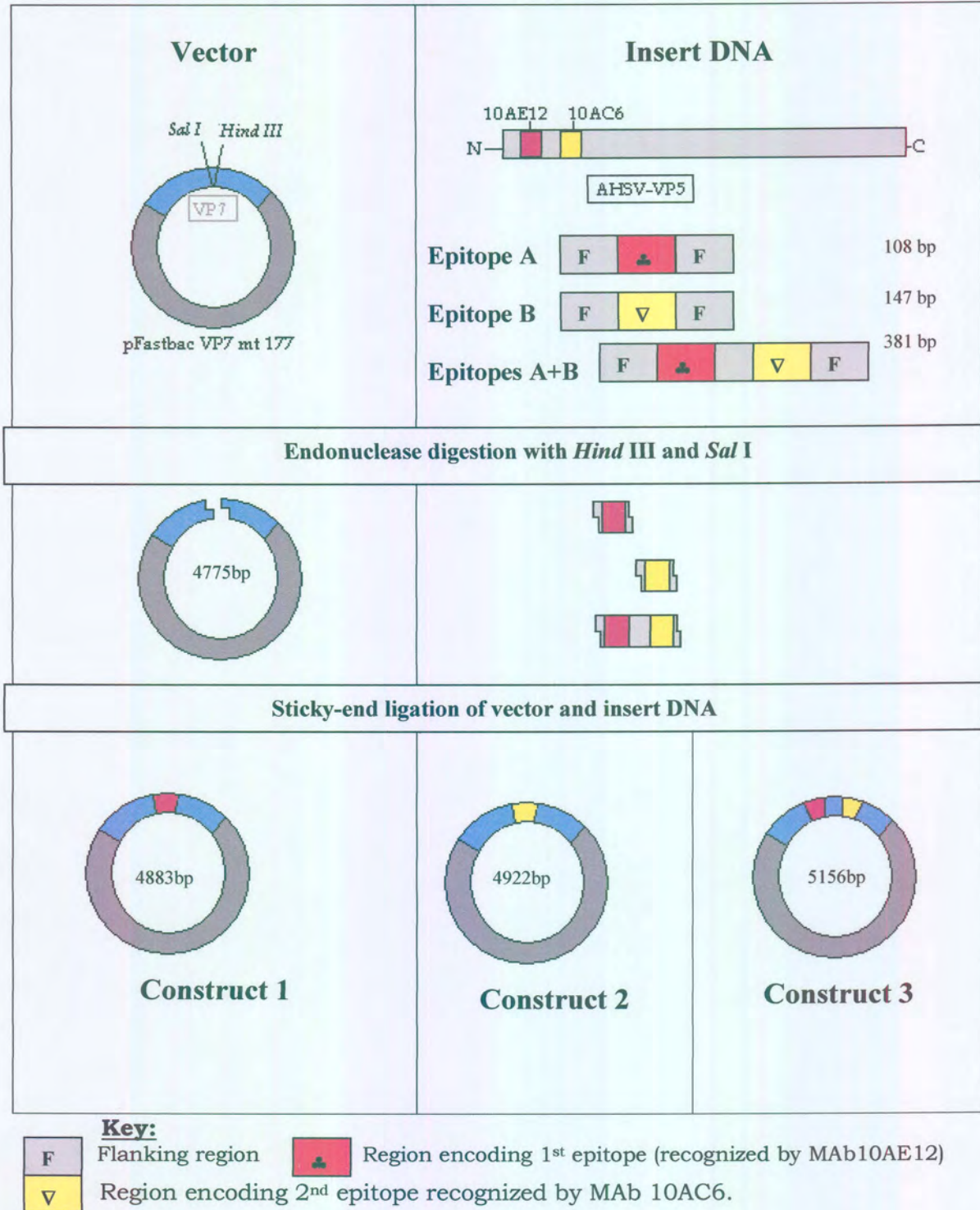


Table 3.3.2 Schematic representation of both the nucleotide and corresponding amino acid sequences representing the two VP5 epitope regions together with their flanking regions.

**Epitope A:**

Nucleotide region amplified using HS4epiHindF and HS4epiSalR:

5' **CCCAAGCTTGTTGCGGGGACATTGGAATCGGCGCCAGACCCGTTGAGCC**  
CAGGGGAGCAGCTCCTTTACAATAAGGTTTCTGAAATCGAGAAAATGGAAAA  
**AGAGGATCGAGTGATTGAA GTC GAC GGG** 3' (underlined regions represent  
the endonuclease restriction sites)

**Corresponding 36 amino acid region:**

N-VAGTLESAP**PDPLSPGE**QLLYNKVSEIEKMEKEDRVIE-C (underlined region  
represents the first 8 amino acid epitope)

**Epitope B:**

Nucleotide region amplified using HS4epi2HindF and HS4epi2SalR:

5' **CCCAAGCTTAGCGGTTTGCTGGAGATAGGGAAAGATCAGTCAGAACGCATTAC**  
AAAGCTATATCGCGCGTTACAAACAGAGGAAGATTTGCGGACACGAGATGAGACTAG  
AATGATAAACGAATATAGAGAGAAATTT**GACGCGTTGAAAGAAGCGGTCGACGG**  
3'(underlined regions represent the endonuclease restriction sites).

**Corresponding 49 amino acid region:**

N-SGLLEIGKDQSERITKLYRALQT**EEDLRTR**DETRMINEYREKFDALKEA-C  
(underlined region represents the second 7 amino acid epitope)

**Epitopes A + B:**

Nucleotide region amplified using HS4epiHindF and HS4epi2SalR:

5' **CCCAAGCTTGTTGCGGGGACATTGGAATCGGCGCCAGACCCGTTGAGCCCAG**  
GGGAGCAGCTCCTTTACAATAAGGTTTCTGAAATCGAGAAAATGGAAAAAGAGGATC  
GAGTGATTGAAACACACAATGCGAAAATAGAAGAAAAATTTGGTAAAGATTTATTAG  
CGATTGCAAAGATTGTGAAAGGCGAGGTTGATGCAGAAAAGCTGGAAGGTAACGAA  
ATTAAGTACGTAGAAAAAGCGCTTAGCGGTTTCTGGAGATAGGGAAAGATCAGTCA  
GAACGCATTACAAAGCTATATCGCGCGTTACAAACAGAGGAAGATTTGCGGACACGA  
GATGAGACTAGAATGATAAACGAATATAGAGAGAAATTT**GACGCGTTGAAAGAAG**  
**CG GTCGACGGG** 3' (underlined regions represent the endonuclease restriction sites).

**Corresponding 127 amino acid region:**

N-VAGTLESAP**PDPLSPGE**QLLYNKVSEIEKMEKEDRVIETHNAKIEEKFGKDLLAIRKI  
VKGEVDAEKLEGNEIKYVEKALSGLLEIGKDQSERITKLYRALQT**EEDLRTR**DETRMINE  
YREKFDALKEA-C (underlined regions represents both the 8 and 7 amino acid epitopes  
of VP5)



The simultaneously amplification of both epitopes and flanking regions from the VP5 gene is collectively referred to as Epitopes A + B from here on forward. Epitopes A + B were amplified using a combination of the first and fourth primers, HS4epiHindF and HS4epi2SalR. An amplified region of approximately 381 bp was observed (lane 5, Figure 3.3.1), which corresponds to the expected length of 127 amino acids encoded by this region.

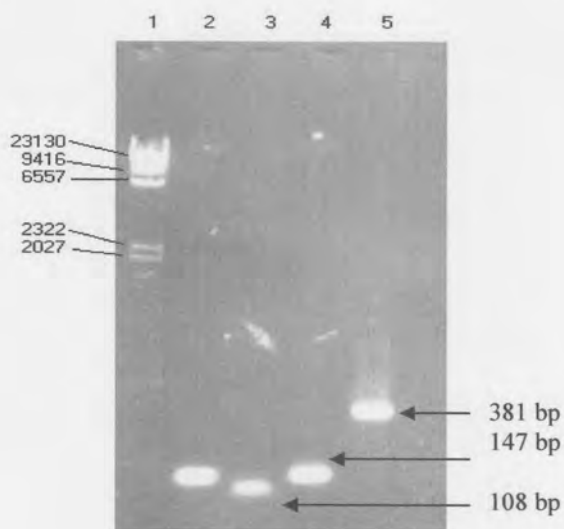


**Figure 3.3.1:** 1% Agarose gel of electrophoresed PCR products using VP5 specific primers that are used to amplify gene regions that encode the different epitopes and their flanking regions. Lane 1: Molecular weight marker II (MWII), lanes 2 and 4: The amplification of epitope B. Lane 3: The amplification of epitope A and lane 5: The amplification of the epitopes A+ B.

### 3.3.2. Cloning of the VP5 epitopes into the transfer vector

As described in the Chapter's introduction, cloning of the target DNA (in this case, the VP5 gene fragments encoding the epitope regions) into the transfer plasmid vector pFB VP7mt177, can allow for transposition into bacmid DNA and subsequent expression of the recombinant VP7 protein in insect cells. The VP7 mt177 transfer vector was kindly provided by Ms Daria Rutkowska, University of Pretoria. The primers used to amplify regions A, B and AB were custom designed to allow for the incorporation of unique *Hind* III and *Sal* I restriction enzyme sites, which would facilitate directional cloning into the transfer vector. After amplification, the fragments were digested, ligated to the vector and transformed into competent XL1 Blue cells. Resulting colonies that grew on 100µg/ml ampicillin (amp<sup>+</sup>) and 12.5µg/ml tetracycline (tet<sup>+</sup>) plates were selected.

Small-scale plasmid preparations from these colonies were analyzed by agarose electrophoresis (results not shown) and subsequently digested with the same enzymes to confirm the presence of the inserts. Figure 3.3.2 shows the three different pFastbac VP7 mt177 plasmids containing regions AB, A and B respectively after double digestions with the *Hind* III and *Sal* I enzymes. The correct sized inserts were observed for all three constructs, namely a 381bp insert representing region AB (Fig 3.3.2A lane 3), a 108bp insert representing region A (Fig 3.3.2B lane 2) and a 147bp insert representing region B (Fig 3.3.2C lane 3). The excised bands are rather faint due to the size of the inserts. These confirmed recombinant vectors were then purified on a large scale for subsequent procedures.

Large-scale preparations of recombinant transfer plasmids were used to transform DH10BAC cells. Several white colonies (as well as one control blue colony) for each transposition event were picked and isolated. Isolated bacmid DNA was conjugated to cationic lipids to allow for efficient transfection into Sf9 insect cells and generation of recombinant baculoviruses.

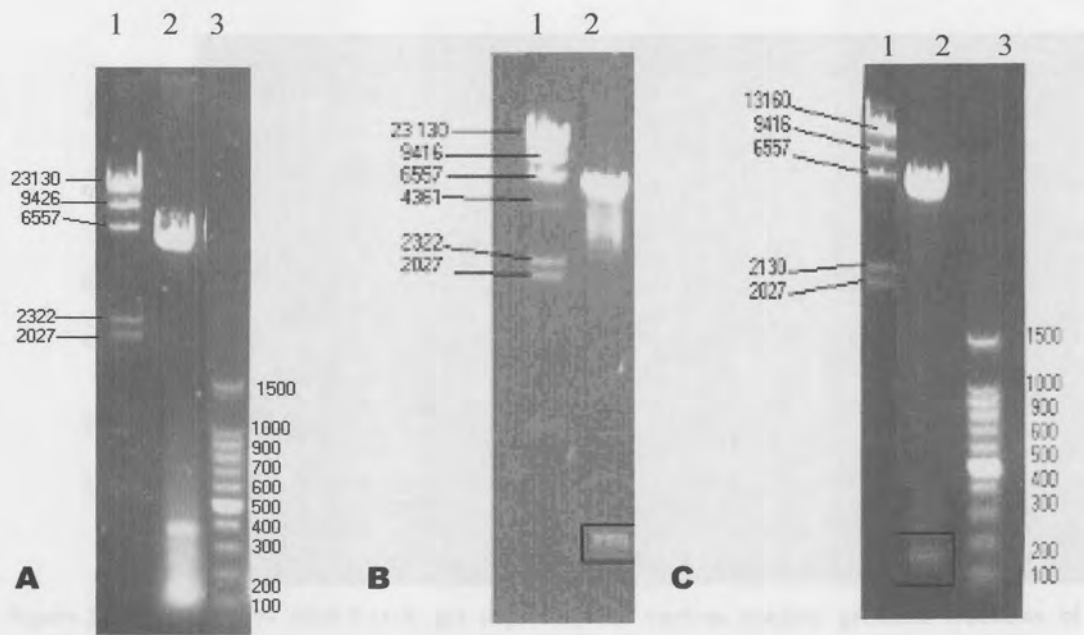


**Figure 3.3.2** 1% Agarose gel of electrophoresed minipreparations of recombinant pFastbac VP7 mt 177 plasmid colonies digested with *Hind* III and *Sal* I.

- A.** Lanes 1 and 3: MWII and 100bp ladder respectively, lane 2 pFastbac and excised epitope A + B.
- B.** Lane 1: MWII. Lane 2: pFastbac and excised epitope A (blocked).
- C.** Lane 1 and 3: MWII and 100bp ladder respectively Lane 2: pFastbac and excised epitope B (blocked).

### 3.3.3 Sequencing of the recombinant transfer plasmids

The nucleotide sequences of these three recombinant pFastbac VP7mt177 plasmids were confirmed with automated sequencing before attempting their transposition with bacmid DNA. These sequences, together with their corresponding amino acid sequences are shown in Figures 3.3.3-5.





1	atg gac gcg ata cga gca aga gcc ttg tcc gtt gta cgg gca tgt	45
1	M D A I R A R A L S V V R A C	15
46	gtc aca gtg aca gat gcg aga gtt agt ttg gat cca gga gtg atg	90
16	V T V T D A R V S L D P G V M	30
91	gag acg tta ggg att gca atc aat agg tat aat ggt tta aca aat	135
31	E T L G I A I N R Y N G L T N	45
136	cat tcg gta tcg atg agg cca caa acc caa gca gaa cga aat gaa	180
46	H S V S M R P Q T Q A E R N E	60
181	atg ttt ttt atg tgt act gat atg gtt tta gcg gcg ctg aac gtc	225
61	M F F M C T D M V L A A L N V	75
226	caa att ggg aat att tca cca gat tat gat caa gcg ttg gca act	270
76	Q I G N I S P D Y D Q A L A T	90
271	gtg gga gct ctc gca acg act gaa att cca tat aat gtt cag gcc	315
91	V G A L A T T E I P Y N V Q A	105
316	atg aat gac atc gtt aga ata acg ggt cag atg caa aca ttc gga	360
106	M N D I V R I T G Q M Q T F G	120
361	cca agc aaa gtg caa acg ggg cct tat gca gga gcg gtt gag gtg	405
121	P S K V Q T G P Y A G A V E V	135
406	caa caa tct ggc aga tat tac gta ccg caa ggt cga acg cgt ggt	450
136	Q Q S G R Y Y V P Q G R T R G	150
451	ggg tac atc aat tca aat att gca gaa gtg tgt atg gat gca ggt	495
151	G Y I N S N I A E V C M D A G	165
496	gct gcg gga cag gtc aat gcg ctg cta gcc cca agg aag ctt <b>GTT</b>	540
166	A A G Q V N A L L A P R K L V	180
541	<b>GCG GGG ACA TTG GAA TCG GCG CCA GAC CCG TTG AGC CCA GGG GAG</b>	585
181	<b>A G T L E S A P D P L S P G E</b>	195
586	<b>CAG CTC CTT TAC AAT AAG GTT TCT GAA ATC GAG AAA ATG GAA AAA</b>	630
196	<b>Q L L Y N K V S E I E K M E K</b>	210
631	<b>GAG GAT CGA GTG ATT GAA</b> gtc gac agg ggg gac gca gtc atg atc	675
211	E D R V I E V D R G D A V M I	225
676	tat ttc gtt tgg aga ccg ttg cgt ata ttt tgt gat cct caa ggt	720
226	Y F V W R P L R I F C D P Q G	240
721	gcg tca ctt gag agc gct cca gga act ttt gtc acc gtt gat gga	765
241	A S L E S A P G T F V T V D G	255
766	gta aat gtt gca gct gga gat gtc gtc gca tgg aat act att gca	810
256	V N V A A G D V V A W N T I A	270
811	cca gtg aat gtt gga aat cct ggg gca cgc aga tca att tta cag	855
271	P V N V G N P G A R R S I L Q	285

```

856   ttt gaa gtg tta tgg tat acg tcc ttg gat aga tcg cta gac acg   900
286   F  E  V  L  W  Y  T  S  L  D  R  S  L  D  T   300

901   gtt ccg gaa ttg gct cca acg ctc aca aga tgt tat gcg tat gtc   945
301   V  P  E  L  A  P  T  L  T  R  C  Y  A  Y  V   315

946   tct ccc act tgg cac gca tta cgc gct gtc att ttt cag cag atg   990
316   S  P  T  W  H  A  L  R  A  V  I  F  Q  Q  M   330

991   aat atg cag cct att aat ccg ccg att ttt cca ccg act gaa agg   1035
331   N  M  Q  P  I  N  P  P  I  F  P  P  T  E  R   345

1036  aat gaa att gtt gcg tat cta tta gta gct tct tta gct gat gtg   1080
346   N  E  I  V  A  Y  L  L  V  A  S  L  A  D  V   360

1081  tat gcg gct ttg aga cca gat ttc aga atg aat ggt gtt gtc gcg   1125
361   Y  A  A  L  R  P  D  F  R  M  N  G  V  V  A   375

1126  cca gta ggc cag att aac aga gct ctt gtg cta gca gcc tac cac   1170
376   P  V  G  Q  I  N  R  A  L  V  L  A  A  Y  H

```

**Figure 3.3.3** Diagram showing the nucleotide and corresponding amino acid sequence of the VP7mt177-epitope A construct. Nucleotides/amino acids highlighted in grey represent the multiple cloning site of the VP7mt177 and sequences highlighted in yellow represent epitope A with the 8 amino acid region recognised by MAb 10AE12 underlined.





1	atg gac gcg ata cga gca aga gcc ttg tcc gtt gta cgg gca tgt	45
1	M D A I R A R A L S V V R A C	15
46	gtc aca gtg aca gat gcg aga gtt agt ttg gat cca gga gtg atg	90
16	V T V T D A R V S L D P G V M	30
91	gag acg tta ggg att gca atc aat agg tat aat ggt tta aca aat	135
31	E T L G I A I N R Y N G L T N	45
136	cat tcg gta tcg atg agg cca caa acc caa gca gaa cga aat gaa	180
46	H S V S M R P Q T Q A E R N E	60
181	atg ttt ttt atg tgt act gat atg gtt tta gcg gcg ctg aac gtc	225
61	M F F M C T D M V L A A L N V	75
226	caa att ggg aat att tca cca gat tat gat caa gcg ttg gca act	270
76	Q I G N I S P D Y D Q A L A T	90
271	gtg gga gct ctc gca acg act gaa att cca tat aat gtt cag gcc	315
91	V G A L A T T E I P Y N V Q A	105
316	atg aat gac atc gtt aga ata acg ggt cag atg caa aca ttc gga	360
106	M N D I V R I T G Q M Q T F G	120
361	cca agc aaa gtg caa acg ggg cct tat gca gga gcg gtt gag gtg	405
121	P S K V Q T G P Y A G A V E V	135
406	caa caa tct ggc aga tat tac gta ccg caa ggt cga acg cgt ggt	450
136	Q Q S G R Y Y V P Q G R T R G	150
451	ggg tac atc aat tca aat att gca gaa gtg tgt atg gat gca ggt	495
151	G Y I N S N I A E V C M D A G	165
496	gct gcg gga cag gtc aat gcg ctg cta gcc cca agg aag ctt AGC	540
166	A A G Q V N A L L A P R K L S	180
541	GGT TTG CTG GAG ATA GGG AAA GAT CAG TCA GAA CGC ATT ACA AAG	585
181	G L L E I G K D Q S E R I T K	195
586	CTA TAT CGC GCG TTA CAA ACA GAG GAA GAT TTG CGG ACA CGA GAT	630
196	L Y R A L Q T E E D L R T R D	210
631	GAG ACT AGA ATG ATA AAC GAA TAT AGA GAG AAA TTT GAC GCG TTG	675
211	E T R M I N E Y R E K F D A L	225
676	AAA GAA GCG gtc gac agg ggg gac gca gtc atg atc tat ttc gtt	720
226	K E A V D R G D A V M I Y F V	240
721	tgg aga ccg ttg cgt ata ttt tgt gat cct caa ggt gcg tca ctt	765
241	W R P L R I F C D P Q G A S L	255
766	gag agc gct cca gga act ttt gtc acc gtt gat gga gta aat gtt	810
256	E S A P G T F V T V D G V N V	270
811	gca gct gga gat gtc gtc gca tgg aat act att gca cca gtg aat	855
271	A A G D V V A W N T I A P V N	285

856	g	t	t	g	a	a	c	c	t	g	g	g	g	c	a	c	g	c	a	g	a	t	c	a	a	t	t	a	c	a	t	t	g	a	a	g	t	g	900				
286	V	G	N	P	G	A	R	R	S	I	L	Q	F	E	V																					300							
901	t	t	a	t	g	g	t	a	c	t	c	c	t	t	g	g	a	t	a	g	a	t	c	g	c	t	a	g	a	c	g	t	t	c	c	g	g	a	a	945			
301	L	W	Y	T	S	L	D	R	S	L	D	T	V	P	E																					315							
946	t	t	g	g	c	t	c	c	a	a	c	g	c	t	c	a	c	a	a	g	a	t	g	t	t	a	t	g	c	g	t	a	t	g	t	c	c	c	a	c	t	990	
316	L	A	P	T	L	T	R	C	Y	A	Y	V	S	P	T																					330							
991	t	g	g	c	a	c	g	a	t	t	a	c	g	t	t	a	c	g	c	a	g	a	t	g	a	a	t	a	a	t	a	t	g	c	a	g						1035	
331	W	H	A	L	R	A	V	I	F	Q	Q	M	N	M	Q																					345							
1036	c	c	t	a	t	a	a	t	c	c	g	c	c	g	a	t	t	t	c	c	a	c	c	g	a	c	t	g	a	a	a	g	a	a	a	t						1080	
346	P	I	N	P	P	I	F	P	P	T	E	R	N	E	I																					360							
1081	g	t	t	g	c	g	t	a	t	c	t	a	t	t	a	g	t	a	g	t	c	t	t	t	t	t	a	g	c	t	g	a	t	g	t	g	t	a	g	c	t	1125	
361	V	A	Y	L	L	V	A	S	L	A	D	V	Y	A	A																					375							
1126	t	t	g	a	g	a	c	c	a	g	a	t	t	t	c	a	g	a	a	t	g	a	t	g	g	t	t	g	t	c	g	c	g	c	c	a	g	t	a	g	g	c	1170
376	L	R	P	D	F	R	M	N	G	V	V	A	P	V	G																					390							
1171	c	a	g	a	t	t	a	a	c	a	g	a	g	c	t	t	g	t	g	c	t	a	g	c	a	g	c	c	t	a	c	c	a	c						1206			
391	Q	I	N	R	A	L	V	L	A	A	Y	H																															

**Figure 3.3.4** Diagram showing the nucleotide and corresponding amino acid sequence of the VP7mt177 epitope B construct. Nucleotides/amino acids highlighted in grey represent the multiple cloning site of the VP7mt177 and sequences highlighted in yellow represent epitope A with the 7 amino acid region recognised by MAb 10AC6 underlined.





1	atg gac gcg ata cga gca aga gcc ttg tcc gtt gta cgg gca tgt	45
1	M D A I R A R A L S V V R A C	15
46	gtc aca gtg aca gat gcg aga gtt agt ttg gat cca gga gtg atg	90
16	V T V T D A R V S L D P G V M	30
91	gag acg tta ggg att gca atc aat agg tat aat ggt tta aca aat	135
31	E T L G I A I N R Y N G L T N	45
136	cat tcg gta tcg atg agg cca caa acc caa gca gaa cga aat gaa	180
46	H S V S M R P Q T Q A E R N E	60
181	atg ttt ttt atg tgt act gat atg gtt tta gcg gcg ctg aac gtc	225
61	M F F M C T D M V L A A L N V	75
226	caa att ggg aat att tca cca gat tat gat caa gcg ttg gca act	270
76	Q I G N I S P D Y D Q A L A T	90
271	gtg gga gct ctc gca acg act gaa att cca tat aat gtt cag gcc	315
91	V G A L A T T E I P Y N V Q A	105
316	atg aat gac atc gtt aga ata acg ggt cag atg caa aca ttc gga	360
106	M N D I V R I T G Q M Q T F G	120
361	cca agc aaa gtg caa acg ggg cct tat gca gga gcg gtt gag gtg	405
121	P S K V Q T G P Y A G A V E V	135
406	caa caa tct ggc aga tat tac gta ccg caa ggt cga acg cgt ggt	450
136	Q Q S G R Y Y V P Q G R T R G	150
451	ggg tac atc aat tca aat att gca gaa gtg tgt atg gat gca ggt	495
151	G Y I N S N I A E V C M D A G	165
496	gct gcg gga cag gtc aat gcg ctg cta gcc cca agg aag ctt <b>GTT</b>	540
166	A A G Q V N A L L A P R K L V	180
541	<b>GCG GGG ACA TTG GAA TCG GCG CCA GAC CCG TTG AGC CCA GGG GAG</b>	585
181	A G T L E S A P D P L S P G E	195
586	<b>CAG CTC CTT TAC AAT AAG GTT TCT GAA ATC GAG AAA ATG GAA AAA</b>	630
196	Q L L Y N K V S E I E K M E K	210
631	<b>GAG GAT CGA GTG ATT GAA ACA CAC AAT GCG AAA ATA GAA GAA AAA</b>	675
211	E D R V I E T H N A K I E E K	225
676	<b>TTT GGT AAA GAT TTA TTA GCG ATT CGA AAG ATT GTG AAA GGC GAG</b>	720
226	F G K D L L A I R K I V K G E	240
721	<b>GTT GAT GCA GAA AAG CTG GAA GGT AAC GAA ATT AAG TAC GTA GAA</b>	765
241	V D A E K L E G N E I K Y V E	255
766	<b>AAA GCG CTT AGC GGT TTG CTG GAG ATA GGG AAA GAT CAG TCA GAA</b>	810
256	K A L S G L L E I G K D Q S E	270
811	<b>CGC ATT ACA AAG CTA TAT CGC GCG TTA CAA ACA GAG GAA GAT TTG</b>	855



271	R	I	T	K	L	Y	R	A	L	Q	T	E	E	D	L	285
856	<u>CGG</u>	<u>ACA</u>	<u>CGA</u>	GAT	GAG	ACT	AGA	ATG	ATA	AAC	GAA	TAT	AGA	GAG	AAA	900
286	R	T	R	D	E	T	R	M	I	N	E	Y	R	E	K	300
901	<u>TTT</u>	<u>GAC</u>	<u>GCG</u>	<u>TTG</u>	<u>AAA</u>	<u>GAA</u>	<u>GCG</u>	gtc	gac	agg	ggg	gac	gca	gtc	atg	945
301	F	D	A	L	K	E	A	V	D	R	G	D	A	V	M	315
946	atc	tat	ttc	gtt	tgg	aga	ccg	ttg	cgT	ata	ttt	tgt	gat	cct	caa	990
316	I	Y	F	V	W	R	P	L	R	I	F	C	D	P	Q	330
991	ggt	gcg	tca	ctt	gag	agc	gct	cca	gga	act	ttt	gtc	acc	gtt	gat	1035
331	G	A	S	L	E	S	A	P	G	T	F	V	T	V	D	345
1036	gga	gta	aat	gtt	gca	gct	gga	gat	gtc	gtc	gca	tgg	aat	act	att	1080
346	G	V	N	V	A	A	G	D	V	V	A	W	N	T	I	360
1081	gca	cca	gtg	aat	gtt	gga	aat	cct	ggg	gca	cgC	aga	tca	att	tta	1125
361	A	P	V	N	V	G	N	P	G	A	R	R	S	I	L	375
1126	cag	ttt	gaa	gtg	tta	tgg	tat	acg	tcc	ttg	gat	aga	tcg	cta	gac	1170
376	Q	F	E	V	L	W	Y	T	S	L	D	R	S	L	D	390
1171	acg	gtt	ccg	gaa	ttg	gct	cca	acg	ctc	aca	aga	tgt	tat	gcg	tat	1215
391	T	V	P	E	L	A	P	T	L	T	R	C	Y	A	Y	405
1216	gtc	tct	ccc	act	tgg	cac	gca	tta	cgC	gct	gtc	att	ttt	cag	cag	1260
406	V	S	P	T	W	H	A	L	R	A	V	I	F	Q	Q	420
1261	atg	aat	atg	cag	cct	att	aat	ccg	ccg	att	ttt	cca	ccg	act	gaa	1305
421	M	N	M	Q	P	I	N	P	P	I	F	P	P	T	E	435
1306	agg	aat	gaa	att	gtt	gcg	tat	cta	tta	gta	gct	tct	tta	gct	gat	1350
436	R	N	E	I	V	A	Y	L	L	V	A	S	L	A	D	450
1351	gtg	tat	gcg	gct	ttg	aga	cca	gat	ttc	aga	atg	aat	ggt	gtt	gtc	1395
451	V	Y	A	A	L	R	P	D	F	R	M	N	G	V	V	465
1396	gcg	cca	gta	ggc	cag	att	aac	aga	gct	ctt	gtg	cta	gca	gcc	tac	1440
466	A	P	V	G	Q	I	N	R	A	L	V	L	A	A	Y	480
1441	cac															1443
481	H															

**Figure 3.3.5** Diagram showing the nucleotide and corresponding amino acid sequence of the VP7mt177 epitopes A + B construct. Nucleotides/amino acids highlighted in grey represent the multiple cloning site of the VP7mt177 and sequences highlighted in yellow represent epitope A + B with the 8 and 7 amino acid regions recognised by MAb 10AE12 and MAb 10AC6 respectively underlined.

### 3.3.4. Transfections of sample and control baculoviruses

All initial transfections were done on six-well plates with the appropriate controls (wild-type baculovirus infected and uninfected Sf9 cells). The supernatant from these cells were used to infect another six well to aid the amplification of recombinant baculoviruses before infecting cells on 25- and 75-cm<sup>3</sup> flasks, which allowed for the large-scale amplification of viruses. Infected cells were harvested from flasks and prepared for SDS-PAGE analysis (Figure 3.3.6) to confirm expression of the chimeric proteins.

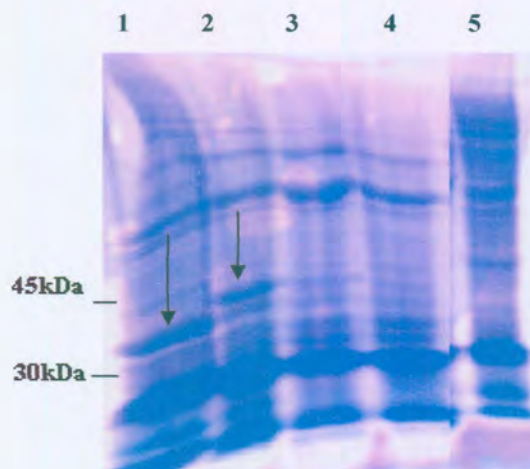


**Figure 3.3.6** An 10% SDS-polyacrylamide gel to analyse protein expression of baculovirus recombinants within Sf9 cells. Lane 1: VP7 positive control, (arrow indicating the VP7mt 177 protein) lane 2: Sf9 cells infected with VP7mt 177/epitope A baculoviruses lane 3: Sf9 cells infected with VP7mt 177/epitope B baculoviruses lane 4: Sf9 cells infected with VP7mt 177/epitope A + B baculoviruses and lane 5: Sf9 cells infected with wild type baculoviruses.

The PAGE gel results confirmed expression of a unique band in the cells infected with the baculovirus recombinant VP7mt177/epitope A (Fig 3.3.6 lane 2), but not in the other two infected cell cultures (Fig 3.3.6 lanes 3 and 4). It would appear as either no recombinant baculoviruses were generated in these infections, or that the chimeric proteins were not expressed for some reason. According to a general assumption that six amino acids have an approximate molecular weight of one kDa, the molecular weights of the chimeric proteins were estimated. Considering that the native VP7 protein is 39kDa in size,



chimeric protein VP7mt177/epitope A with the 36 amino acid insert should be approximately 45kDa in size, chimeric protein VP7mt177/epitope B with the 49 amino acid insert should be approximately 47kDa and chimeric protein VP7mt177/epitope A + B with the 127 amino acid insert should be approximately 60kDa in size.

### 3.3.5 Sucrose gradient purification of baculovirus expressed proteins

The recombinant VP7mt177/epitopeA baculoviruses were further propagated and analyzed by isopycnic centrifugation. In order to separate the proteins expressed during the baculovirus infection by sucrose gradient, the cell lysate was centrifuged for a short time (1hr) and fractions collected from the bottom of the tube. Under these conditions, proteins separated according to size and if large particulate structures are present, they should occur in the lower fractions of the gradient. Sucrose gradient purification revealed the chimeric VP7 protein to lay in the bottom two fractions of the gradient (Figure 3.3.7 lanes 2 and 3) as well as in the pellet (Figure 3.3.7 lane 14). The presence of the VP7mt177/epitope A protein in the bottom fractions indicated that these chimeras are large particulate structures. A size comparison with the vector VP7mt177 protein of approximately 39 KDa (Figure 3.3.7, lane 15) confirmed the expression of the correct chimeric protein, of approximately 45kDa was indeed analyzed.



**Figure 3.3.7** A 12% SDS-PAGE gel depicting the various sucrose gradient fractions of the chimeric VP7 mt 177 protein containing the first VP5 epitope. Lane 1: Rainbow protein marker, lane 2-13: sucrose gradient fractions 1-12, lane 14: sucrose gradient pellet and lane 15: VP7mt 177 positive control. Arrows are indicative of the chimeric VP7 protein containing the first epitope of AHSV VP5.

### 3.3.6 Scanning electron microscopy of chimeric VP7 particles

The crystalline particles observed are shown in Figures 3.3.8 and 3.3.9, in comparison to non-recombinant VP7 mt177 crystals previously photographed by Ms. Daria Rutkowska, University of Pretoria (Figure 3.3.10). The chimeric VP7 formed hexagonal crystals, similar to those formed by the VP7 mt177 vector containing no insert. The preparation of the chimeric crystals examined at low magnification (2500-3500X) revealed a large number of intact, flat and hexagonal structures that do not have the same surface morphology as the non-recombinant vector. By increasing the magnitude (>12000X), the surface became increasingly jagged and showed that no rosette type configuration occurred with the assembling of the chimeric VP7 proteins. The different surface views shown in Figure 3.3.8 may be indicative of the various phases in crystal development or be an artifact of the preparation procedure.

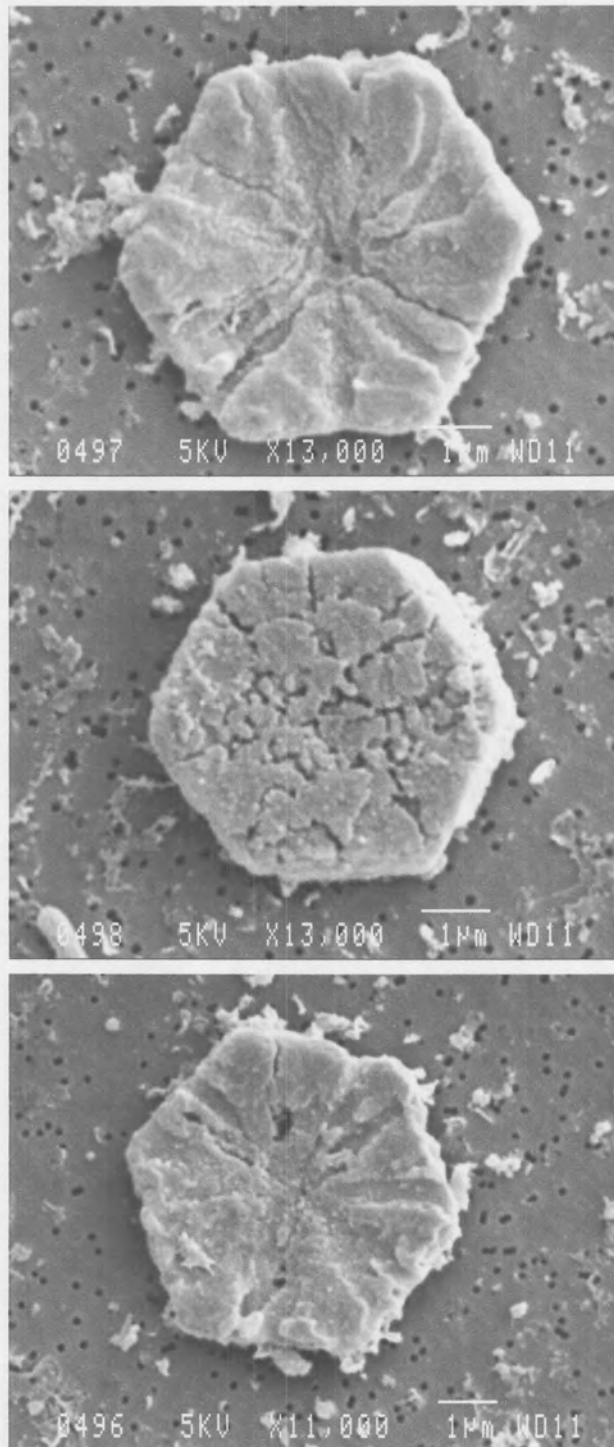


**Figure 3.3.8** Electron microscope pictures taken of individual chimeric VP7 crystals containing the VP5 epitope A recognized by MAb 10AE12, found in the viewing field at a magnification of between 12-13000X. The size bar indicates a size of 1µm.

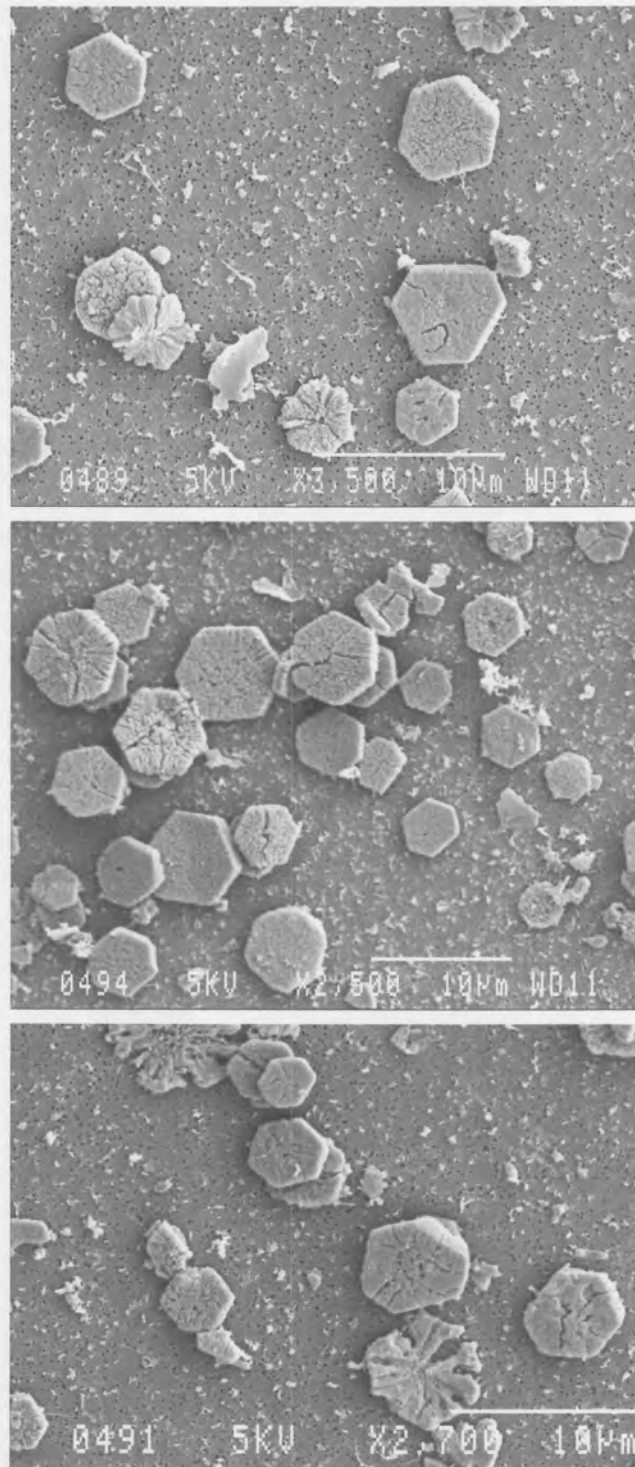


**Figure 3.3.9** Electron microscope pictures taken of various chimeric VP7 crystals containing the VP5 epitope A recognized by MAb 10AE12, found in the viewing field at a magnification of between 2500-3500X. The size bar indicates a size of 10µm.



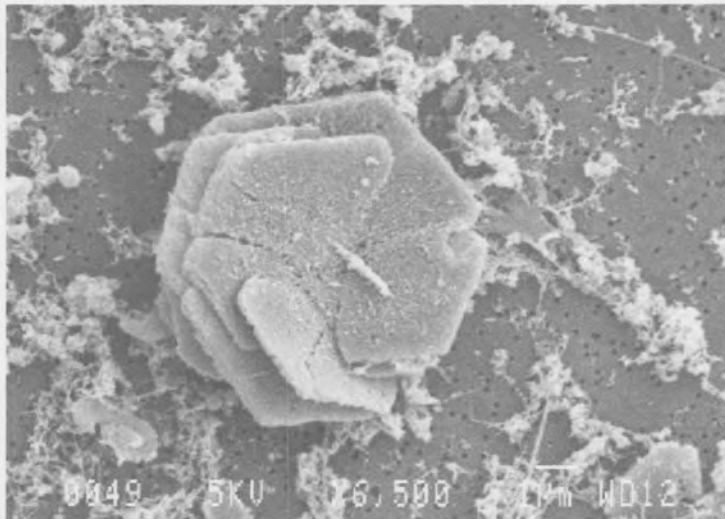
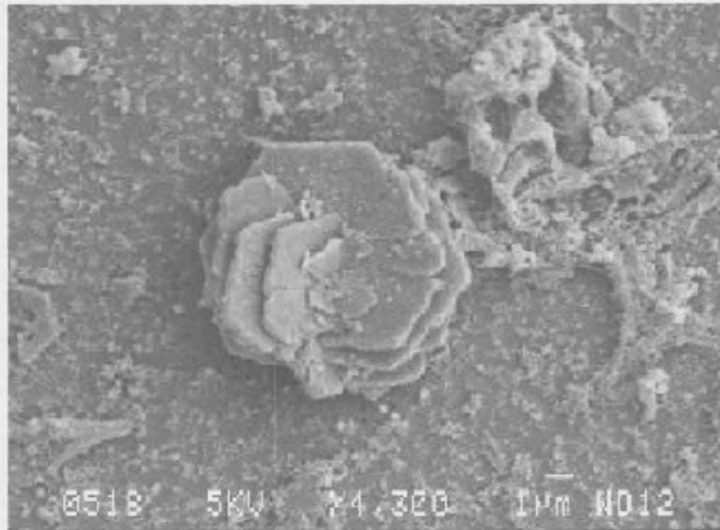


**Figure 3.3.10** Electron microscope pictures taken of VP7 mt 177 crystals containing no insert, found in the viewing field at a magnification of between 4300-6500X (kindly provided by Ms. Daria Rutkowska, University of Pretoria). The size bar indicates a size of 1µm.

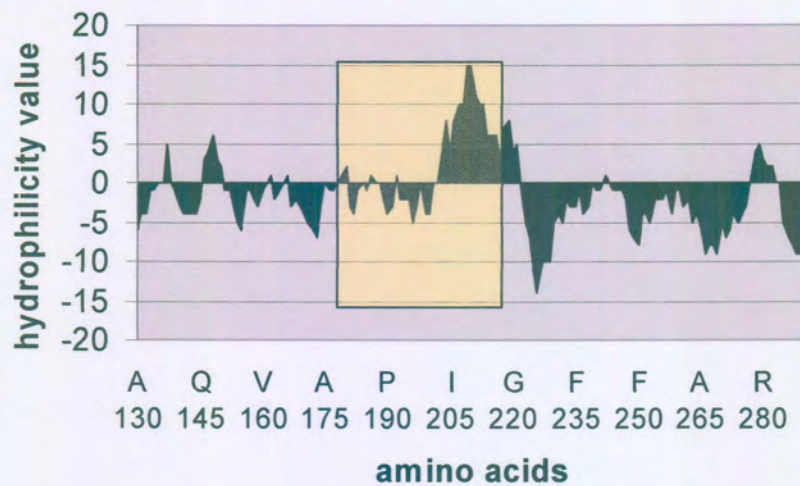


### 3.3.7 Hydrophilicity predictions

The Hopp and Woods predictive method (Hopp and Woods, 1981; Hopp and Woods, 1983) within the ANTHEPROT package (Geourjon *et al.*, 1991; Geourjon and Deléage, 1995) was used to calculate the hydrophilicity plots of chimeric and vector VP7mt177 proteins. This method aims to analyze the constituent amino acid sequences of a peptide chain in order to find the point of greatest local hydrophilicity. Each amino acid is assigned a numerical value (hydrophilicity value), which is repetitively averaged along the peptide chain. The point of highest local average hydrophilicity is assumed to be immediately adjacent to an antigenic determinant or the region having the highest likelihood of antibody binding.

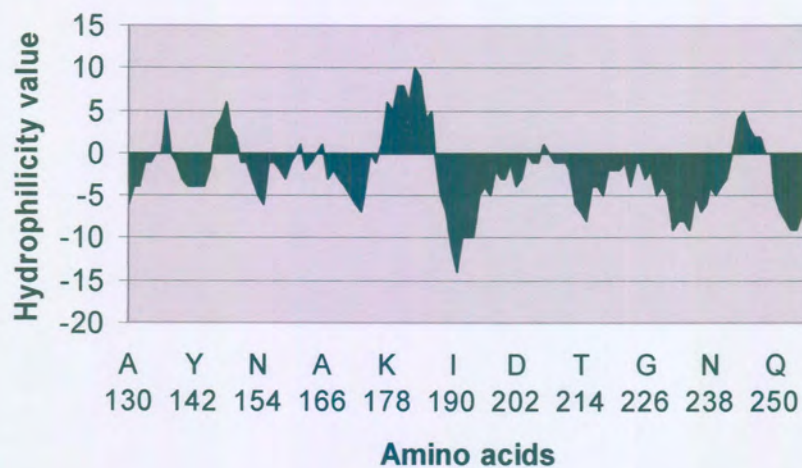
The hydrophilicity plots of a selected region of the chimeric VP7mt177/ epitope A (Figure 3.3.11A) protein and the same portion of the vector VP7mt177 (Figure 3.3.11B) protein are represented in the figures below. Apart from the VP7mt177/epitope A showing a modest increase in the highest hydrophilicity local value in comparison to the vector graph, it would appear that the basic profile of the VP7 protein did not change dramatically with the addition of the insert. This is also supported by the fact that hexagonal crystal structures were still observed with S.E.M. This indicates that these profile changes are not significant enough to disrupt trimer formation and subsequent crystal formation of the VP7 protein.

### VP7mt177VP5a hydrophilicity graph



**A**

### VP7mt177 hydrophilicity graph



**B**

**Figure 3.3.11** **A:** Hydrophilicity profile of a portion of VP7mt177/ EpitopeA.  
The inserted amino acid region, representing epitope A is blocked in yellow.  
**B:** Hydrophilicity profile of a portion of wild type VP7mt177.  
The averaged hydrophilicity values (y-axis) are plotted versus position along the amino acid sequence (x-axis).

### **3.4 Discussion**

Considering that the AHSV VP5 protein was shown to induce neutralizing antibodies (Martinez-Torrecedrada *et al.*, 1999), it was the aim of this study to display the defined epitopes in a particulate system and perform initial analyses of the chimeric proteins for eventual use in immune studies. A novel vaccine delivery system that is being developed at the University of Pretoria was investigated. This approach is based on the expression of AHSV9 VP7 crystalline particles in a baculovirus expression system. The VP5 epitopes were inserted individually as well as simultaneously into the top domain of the VP7 gene at position 177 originally constructed in the pFastbac VP7 mt 177 transfer plasmid (Maree, 2000). The generation of recombinant baculoviruses could potentially allow for the expression of chimeric VP7 crystals that display the VP5 epitopes on its surface.

Fellow students have inserted other defined epitopes into VP7 vectors for immunological display. Ms Daria Rutkowska and Mr Ruan van Rensburg (University of Pretoria) constructed baculovirus recombinants expressing VP7 fusion proteins with 50aa and 105aa inserts into site 177 of the VP7 top domain of vector VP7mt 177 and insertions of up to 250 aa into the VP7 mt144/177/200 vector respectively. The latter vector used by Mr van Rensburg, differs from the vector used in this study by containing three different insertion sites in order to express peptides with different immunological specificities in the same vector. Other display systems being investigated in the department include insertions into the hydrophilic loop at the C-Terminus of AHSV NS1 using a similarly modified pFastbac vector expressing NS1 fusion proteins.

In order to amplify the gene regions expressing the VP5 epitopes by PCR, specific primers were designed that contained the appropriate restriction enzyme sites to facilitate cloning into the transfer plasmid, pFastbac VP7mt177. Three different recombinant transfer plasmids were made, containing each epitope region alone or simultaneously and were confirmed with automated sequencing. Only recombinant baculoviruses that expressed the chimeric

protein VP7 mt177/epitope A was successfully generated. Baculoviruses expecting to express the other two chimeric proteins, VP7mt177/epitope B and VP7mt177/epitopes A+ B failed to do so, reasons could include no recombinant baculoviruses were made (during transposition) or no expression from baculoviruses occurred (during transfection) for some reason. Due to time constraints, transpositions and transfection events for these two recombinant transfer vectors were not repeated or optimized, which creates a need for them to be investigated in the future.

High levels of chimeric protein VP7mt77/epitope A was expressed from recombinant baculoviruses and purified for S.E.M. studies. Sucrose gradient purifications of this chimera indicated that most of the protein sedimented into the gradient pellet and into the lower fractions with a high sucrose content. These results compare to those obtained by Ms Rutkowska and Mr van Rensburg, who found that by lysing the cells on ice in lysis buffer (containing NP-40) the VP7 protein tended to aggregate in the pellet and well as the lower fractions (2-5) of the sucrose gradient after centrifugation.

The S.E.M. results of this study show that the typical crystalline structures were indeed observed and that these chimeric crystals were similar in structure to the hexagonal structures observed with the VP7mt177-vector proteins. The surfaces of the chimeric crystals were uneven, which differs to the rosette surface formation of the vector. This may indicate that the 36 amino acid insertion does not affect the VP7 aggregation pattern to form the hexagonal crystalline lattice, but may only influence the surface structure of the crystal to a small degree. Hydrophilic analysis shows that the profile of chimeric VP7 containing epitope A does not differ significantly from native VP7mt177, confirming why similar crystalline structures were observed. Ms Rutkowska's insertions into pFastbac VP7 mt 177 did not form crystalline structures under S.E.M, but rather formed more rounded and cookie-shaped structures. Mr. van Rensburg's large insertions did not affect the crystal structure; rough, 8um flat crystals of almost circular appearance were seen under S.E.M. He noted that when high concentrations were mounted for S.E.M., web-like tentacles/cables

were observed between the VP7 particles. It is suggested that this attests to the fact that VP7 crystals can tolerate an insertion of up to 250aa without losing its structure, a factor that may be important for vaccine purposes.

This study shows that the chimeric VP7 containing the first VP5 epitope does not interfere with crystalline formation and may be in a suitable configuration to display this epitope to the immune system. As of yet, no attempt has been made to analyze the chimera for its immunological properties. A first priority of further studies would therefore be to confirm the immune recognition of the epitope by Western blotting and/or in an ELISA-based assay. Once immune recognition is confirmed, large quantities of particulate structures may be injected into small animals in a vaccination trial. Injecting this chimera alone or in combination with similarly displayed VP2 epitopes into small animals, followed by ELISA or Western blotting procedures, could confirm the detection of an epitope-specific neutralizing immune responses against AHSV. The detection of such a response would indicate the usefulness of the VP7 particulate presentation system in a vaccine strategy.



# **Chapter 4:**

# **Concluding Remarks**

As described in the literature, the use of sub-unit vaccines can allow for the expression of important epitope regions for its subsequent presentation to the immune system. The recognition of epitope regions found within virus coat proteins have enabled significant immune responses to be mounted against encounters with live viruses (Inumara and Roy, 1987; Roy *et al.*, 1990a; Burrage *et al.*, 1993; Stone-Marshat *et al.*, 1996; Martinez-Torerecuadrada *et al.*, 1996) and so eliminate the chance of death through disease. This is of great importance when considering the AHS disease and being able to control and eradicate the disease and consequent death of infected horses by the use of such vaccines.

The orbivirus capsid consists of the two major proteins VP2 and VP5, of which the VP2 is the main immunodominant, serotype-specific antigen. Considering that the VP5 protein has been shown to elicit a neutralizing response as well as enhance the immune response of VP2, it is of great importance to characterize this protein and gain a thorough understanding of this particular gene and its cognitive gene product.

The main aim of this study was to compare the genetic variation between the VP5 proteins of available field AHSV strains (assumed to be virulent) to that of published vaccine strains likely to be avirulent. This comparison was done to investigate if any amino acid variation found between these strains could be correlated to the virulent phenotype. The strategy included the cloning the various AHSV VP5 genes into a cloning vector, which allowed for sequencing analysis.

The VP5 genes of AHSV field isolates of serotypes 3, 6, 8 and 9 were sequenced and compared to those VP5 sequences already published. The length, base composition and conserved nucleotides of the field isolates sequenced were highly comparable to the laboratory adapted published sequences. Certain regions of VP5 were relatively conserved (79.7-97%) when Clustal alignments of the nucleotide sequences of these serotypes were analysed. The deduced VP5

amino acid sequences of these field serotypes also showed size and molecular weight agreement to those already published.

Field AHSV3 VP5 comparisons to a laboratory adapted counterpart (Filter, 2000) revealed amino acid identities of 97%, with no changes occurring in the proposed amphipatic helices found in the first 40 amino acids (Hassan *et al.*, 2001). AHSV6 VP5 field strain comparisons revealed less similarity, with both field and laboratory adapted strain sequences sharing 94.5% identical amino acids. Notably, the laboratory adapted AHSV6 strain (Williams *et al.*, 1998) had one less amino acid in its VP5 protein sequence. Two amino acid changes were found occurring in the first 40 amino acids between both field and laboratory adapted AHSV6 strains, but the change was synonymous and not likely to be significant. Field AHSV9 showed the least amount of conservation (90.5% amino acid identities) when compared to its laboratory adapted counterpart (du Plessis and Nel, 1997) Similarly, as with the other two serotypes compared, only one synonomous change was observed within the first 40 amino acids of AHSV9 VP5. Since this study provided the first record of an AHSV8 VP5 sequence, no laboratory-adapted sequence was available for direct comparison.

These cumulative results indicate that variation in the probable cytotoxic regions of VP5 could not be correlated to a virulent phenotype in AHSV serotypes 3, 6 and 9. Further comparisons of amino acid variation along the length of these genes revealed no obvious amino acid changes that clearly allowed distinction between field and laboratory adapted strains. Hydrophobic regions within the VP5 are well conserved (75-80%), which is expected considering the important role VP5 plays in the maintenance of viral core structure. Hydrophilic regions are more variable (approximately 65-70%) and could be attributed to the immune pressures that exist upon the virion surfaces. The only hydrophilic region displaying a high degree of conservation (80%) is the amphipatic helix region (first 40 amino acids). This interestingly shows functional constraints on this region, despite it being relatively exposed.

Further comparisons between these field isolates and other published serotypes/groups (such as AHSV4, BTV and EDHV) were also done in this study. AHSV4 was shown to be the most distantly related AHSV serotype when comparing all the sequence data, showing the highest variability (approximate degree of conservation between serotypes: 80-84%). The VP5 of serotype 4 also clustered into a phylogenetically distinct clade apart from the other AHSV serotypes. Despite low amino acid identities between serogroups, all the profiles and physico-chemical predictions were near identical. This supports the suggestions by Oldfield *et al.*, (1991), Iwata *et al.*, (1992) and du Plessis and Nel, (1997) which conclude that the VP5 proteins of AHSV, BTV and EHDV are structurally and presumably functionally very similar. In the future, the next step would be to obtain and compare all the unknown VP5 sequences of the remaining AHSV serotypes and to correlate the data obtained.

In order to broaden the information available up-to-date, the VP5 sequences from those un-characterised AHSV serotypes should be investigated in the future. In this way, all data could be correlated and provide a better understanding of the variability and hence the phylogenetic relationships between and within all the orbivirus serogroups.

Investigating the cytotoxic effects that are assumed to be inherent for the VP5 protein (as described in the literature for BTV) formed part of the study. The strategy involved the cloning of the virulent AHSV4 VP5 protein into an inducible bacterial expression vector that was induced to express the protein within a biological system. This system was employed to investigate any cytotoxic effect that VP5 expression may have on bacterial cells.

The VP5 protein severely retarded cell growth and progressively caused cell death when expressed in bacterial cells. The role of VP5 in being a membrane destabilising protein is well supported and confirms that VP5 is highly cytotoxic, as observed by other authors. Unfortunately the visualization of VP5 proved difficult and it was suggested to raise antibodies against this protein for use in future analyses. These results also confirm the findings by Hassan *et al.*,

(2001) on BTV expressed VP5 that also found VP5 expressed alone was highly cytotoxic and easily degraded following expression.

The actual regions responsible for cytotoxicity in AHSV VP5 is yet to be elucidated, but seems highly probable to be mapped to the two N-terminal amphipathic helices described by Hassan *et al*, (2001) for BTV VP5. In order to investigate this assumption in future studies, deletion mutants containing definite stretches of all regions in VP5 would pinpoint which regions are likely to be responsible for cytotoxicity in VP5.

Another aim in this study was to insert defined VP5 epitopes into a VP7 particulate display system in order to investigate any marked changes in its ability to form crystals. The strategy employed was to construct baculovirus recombinants expressing VP7 chimeric proteins with VP5 epitopes fused into site 177 of the VP7 top domain. Chimeric proteins were isolated using sucrose gradients and visualised using S.E.M.

Considering that the AHSV VP5 protein, in contrast to BTV VP5, showed neutralizing activity (Martinez-Torrecuadrada *et al.*, 1999), it was of interest in this study to insert these epitopes in an epitope presentation system for later immune response investigations. The first epitope (recognised by MAb 10AE12) of AHSV4 VP5 was successfully inserted into a mutant form of the AHSV9 VP7 protein and expressed from baculoviruses in insect cells. Sucrose gradient purifications of this chimera, indicated that most of the protein was found to sediment into the gradient pellet and into the lower fractions. These results compare to similar studies done by fellow students. Resulting chimeric VP7 proteins were observed to aggregate and form hexagonal crystals under the scanning electron microscope. The surface morphology of these chimeric crystals differed slightly to the smooth regular surface of native VP7 crystal structures. These results indicated that this 36 amino acid insertion did not affect the VP7 protein's ability to form crystals.



Chimeric VP7 crystals are proposed to display the inserted epitope from its surface to the immune system. For this purpose, these crystals serve as an epitope display system and could potentially confer both a humeral and a cellular immune response in vaccinated individuals. The next step in future studies would be to amplify this particular construct as well as constructing baculovirus recombinants that express chimeric VP7 fused to the second VP5 epitope for immunological testing in animals. Such constructs, if successful in mounting an immune response in animals, could be utilized in a vaccination strategy with similar constructs displaying the epitopes of VP2 in creating an enhanced immune response against the actual virus in an AHSV challenge.

## **References:**

Arroyo, J., Boceta, M., Gonzalez, M.E., Michel, M., and Carrasco L (1995). Membrane permeabilization by different regions of the human immunodeficiency virus type 1 transmembrane glycoprotein gp41. *J. Virol.* 69 (7), 4095-4102.

Ausubel, F.M., Brent, R., Kingston, R.E., Moore, D.D., Seidman, J.G., Smith, J.A., and Struhl, k. (1989). *Current protocols in Molecular Biology*. (Greene Publishing Associates and Wiley-Interscience, new York).

Beaton, A.R., Rodriguez, J., Krishnamohan Reddy, Y., and Roy, P. (2002). The membrane trafficking protein calpactin forms a complex with bluetongue virus protein NS3 and mediates virus release. *PNAS* 99 (20), 13154-13159.

Birnboim H.C., and Doly J. (1979). A rapid alkaline extraction procedure for screening recombinant plasmid DNA. *Nucleic Acids Res.* 24; 7 (6): 1513–1523

Blackburn, G.M., and Gait, M.J. (1996). *Nucleic Acids in Chemistry and Biology*, second edition (New York, Oxford University Press).

Boger, J., Emini, E.A., and Schmidt, A. (1986). Surface probability profile. An heuristic approach to the selection of synthetic peptide antigens. *Reports on the Sixth International Congress in Immunology (Toronto)* p.250

Brookes, S.M., Hyatt, A.D., and Eaton, B.T. (1993). Characterization of virus inclusion bodies in bluetongue virus-infected cells. *J. Gen. Virol.* 74 (Pt 3), 525-30.

Brown, T.A. (1986). *Gene cloning: an introduction*. (Berkshire; Von Nostrand Reinhold, UK).

Burrage, T.G., Trevejo, R., Stone-Marschat, M., and Laegried, W.W. (1993). Neutralizing epitopes of African Horsesickness Virus Serotype 4 are Located on VP2. *Virol.* 196, 799-803.

Burrage, T.G., and Laegried, W.W. (1994). African horse sickness: pathogenesis and immunity. *Comp. Immun. Microbial. Infect. Dis.* 17; 275-285

Burroughs, J.N., O'Hara, P.S., Smale, C.J., Hamblin, C., Walton, A., Armstrong, R., and Mertens, P.P.C. (1994). Purification and properties of virus particles, infectious subviral particles, cores and VP7 crystals of African horsesickness virus serotype 9. *J. Gen. Virol.* 74, 1849-1857.

Calisher, C.H., and Mertens, P.P.C. (1998). Taxonomy of African horse sickness viruses. *Arch. Virol.* 14, 3-11

Chuma, T., Le Blois, H., Sanchez-Vizcaino, J.M., Diaz-Laviada., and Roy, P. (1992). Expression of the major core antigen VP7 of African horsesickness virus by a recombinant baculovirus and its use as a group-specific diagnostic reagent. *J. Gen. Virol.* 73, 925-931.

Ciccaglione, A.R., Costantino, A., Marcantonio, C., Equestre1, M., Geraci, A., and Rapicetta, M. (2001). Mutagenesis of hepatitis C virus E1 protein affects its membrane-permeabilizing activity. *J. Gen. Virol.* 82, 2243-2250

Cromack, A.S., Blue, J.I., and Gratzek, J.B. (1971). A quantitative ultrastructural study of the development of Blue tongue virus in Madin-Darby Bovine kidney cells. *J. Gen. Virol.* 13, 229-244.

Du Plessis, M., and Nel, L. H. (1997). Comparative sequence analysis and expression of the M6 gene, encoding the outer capsid protein VP5, of African horsesickness virus serotype nine. *Virus Res.* 47, 41-49.

Eaton, B.T., Hyatt, A.D., and White, J.R. (1987). Association of bluetongue virus with the cytoskeleton. *Viol.* 157, 107-16.

Eaton, B.T. and Crameri, G.S. (1989). The site of Bluetongue Virus attachment to glycoporphins from a number of animal erythrocytes. *J. Gen. Virol.* 70, 3347-3353.

Eisenberg, D., Weiss, R.M., and Terwilliger, T.C. (1982). The helical hydrophobic moment: a measure of the amphiphilicity of a helix. *Nature.* 23; 299(5881): 371-4.

French, T.J., and Roy, P. (1990). Synthesis of Bluetongue Virus (BTV) corelike particles by a recombinant baculovirus expressing the two major structural core proteins of BTV. *J. Gen. Virol.* 64, 1530-1536.

Filter, R. D. (2000). Characterisation and co-expression of the two outer capsid proteins of African horsesickness virus serotype 3. MSC dissertation, University of Pretoria, Pretoria.

Fukusho, A., Yu, Y., Yamaguchi, S., and Roy, P. (1989). Completion of the sequence of Bluetongue virus serotype 10 by characterisation of a structural protein, VP6, and a non-structural protein, NS2. *J. Gen. Vir.* 70, 1677-1689.

Garnier, J., Osguthorpe, D.J., and Robson, B. (1978). Analysis of the accuracy and implications of simple methods for predicting the secondary structure of globular proteins. *J Mol Biol.* 25; 120(1): 97-120.

Geourjon, C., Deleage, G., and Roux, B. (1991). ANTHEPROT: an interactive graphics software for analyzing protein structures from sequences. *J Mol Graph.* 9 (3): 188-90, 167.

Geourjon, C., and Deléage G. (1995) a three-dimensional module fully coupled with protein sequence analysis methods. *J Mol Graph.* 13(3): 209-12, 199-200.

Gould AR, Hyatt AD, Eaton BT. (1988) Morphogenesis of a bluetongue virus variant with an amino acid alteration at a neutralization site in the outer coat protein, VP2. *Virology* 165(1), 23-32.

Gould, A.R., and Hyatt, A.D. (1994). The orbivirus genus: diversity, structure, replication and phylogenetic relationships. *Comp. Immun. Microbial. Infect. Dis.* 17, 163-188.

Grubman, M.J., and Lewis, S.A. (1992). Identification and Characterization of the Structural and Nonstructural Proteins of African Horsesickness Virus and determination of the Genome Coding Assignments. *Virology* 186, 444-451.

Han, Z., and Harty, R.N. (2004). The NS3 protein of bluetongue virus exhibits viroporin-like properties. *J. Biol. Chem.* 279 (41), 43092-43097.

Hacket, P.B., Fuch, J.A., and Messing, J.W. (1998). An introduction to recombinant DNA techniques. (California; the Benjamin/Cumming Publishing Company, Ltd).

Hassan, S.S., and Roy, P. (1999). Expression and functional characterization of bluetongue virus VP2 protein: role in cell entry. *J Virol.* 73 (12):9832-42.

Hassan, S.H., Wirblich, C., Forzan, M., and Roy, P. (2001). Expression and Functional Characterisation of Bluetongue Virus VP5 protein: Role in Cellular Permeabilization. *J. Virol.* 75, 8356-8367.

Hewat, E.A. Booth, T.F., Loudon, P.T. and Roy, P. (1992a).a Three-Dimensional Reconstruction of Baculovirus Expressed Bluetongue Virus Core-like Particles by Cryo-Electron Microscopy. *Virology* 189, 10-20.

Hewat, E.A., Booth, T.F., and Roy, P. (1992b). Structure of bluetongue virus particles by cryoelectron microscopy. *J Struct Biol.* 109 (1): 61-9.



Hewat, E.A., Booth, T.F., and Roy, P. (1994). Structure of self-assembled Bluetongue Virus-like particles. *J. Struc. Biol.* 112, 183-191.

Hopp, T.P., and Woods, K.R. (1981). Prediction of protein antigenic determinants from amino acid sequences. *Proc Natl Acad Sci USA.* 78(6): 3824–3828.

Hopp, T.P., and Woods, K.R. (1983). A computer program for predicting protein antigenic determinants. *Mol Immunol.* 20(4): 483-9.

House, J. A. (1998). Future international management of African horse sickness vaccines. *Arch Virol Suppl.* 14: 297-304. Review.

Huisman, H., and Els, H.J. (1979). Characterization of the Tubules associated with the Replication of Three different Orbiviruses. *Virology* 92, 397-406.

Huisman, H., Van der Walt, N.T., Cloete, M., Erasmus, B.J (1987a). Isolation of a capsid protein of bluetongue virus that induces a protective immune response in sheep. *Virology* 157: 172-179.

Huisman, H., Van Dijk, A.A., and Els, H.J. (1987b) Uncoating of Parental Bluetongue Virus to Core and Subcore Particles in infected L. cells. *Virology* 157, 180-188.

Huisman, H., and Van Dijk, A.A. (1990). Bluetongue Virus Structural Components. *Curr.Top. Micro. And Immun.* 162, 21-41.

Hyatt AD, Gould AR, Coupar B, Eaton BT. (1991). Localization of the non-structural protein NS3 in bluetongue virus-infected cells. *J Gen Virol.* 72 (9), 2263-7

Hyatt, A.D., Zhoa, Y., and Roy, P. (1993). Release of bluetongue virus-like particles from insect cells is mediated by BTV nonstructural protein NS3/NS3A. *Virology*. 193, 592-603.

Inumara, S., and Roy, P. (1987). Production and characterization of the neutralization antigen VP2 of Bluetongue virus serotype 10 using a baculovirus expression vector. *Virology*, 157, 472-479.

Ish-Horowicz, D., and Burke, J.F. (1981). Rapid and efficient cosmid cloning. *Nucleic Acids Res.* 10; 9(13):2989-98.

Iwata, H., Hirasawa, T. and Roy, P. (1991). Complete nucleotide sequence of segment 5 of epizootic haemorrhagic disease virus; the outer capsid protein VP5 is homologous to the VP5 protein of bluetongue virus. *Virus Res.* 20 (3), 273-281.

Iwata, H; Chuma, and Roy, P. (1992)a. Characterization of the genes encoding two of the major capsid proteins of epizootic haemorrhagic disease virus indicates a close genetic relationship to bluetongue virus. *J.Gen. Virol.* 73, no. 4, pp. 915-924.

Iwata,H., Yamagawa, M., and Roy, P. (1992)b. Evolutionary Relationships among the Gnat-Transmitted Orbiviruses That cause African Horse Sickness, Bluetongue, and Epizootic Hemorrhagic Disease as Evidenced by their Capsid Protein Sequence. *Virology* 191, 251-261.

Klug, W.S., Cummings, M.R. (1997). *Concepts of Genetics*. 5<sup>th</sup> Edition. (Prentice Hall, New Jersey).

Kyte, J. and Doolittle, R.F. (1982). A simple method for Displaying the Hydropathic Character of a Protein. *J. Mol. Biol.* 157, 105-132.

Laemmli, U.K. (1970). Cleavage of structural proteins during the assembly of the head of bacteriophage T4. *Nature*. 15; 227(5259): 680-5.

Laviada, M.D., Arias, M., and Sánchez-Vizcaino, J. M. (1993). Characterisation of African horsesickness virus serotype 4-induced polypeptides in Vero cells and their reactivity in Western immunoblotting. *J. Gen Virol*. 74, 81-87.

Lecatsas, G. (1968). Electron microscopic study of the formation of Bluetongue virus. *Onderstepoort J. Vet. Res.*35(1), 139-150.

Levy, J.A., Fraenkel-Conrat, H., and Owens, R.A. (1994). *Virology*:3<sup>rd</sup> Edition. (New Jersey, Prentice Hall Inc.).

Louden, P.T., and Roy, P. (1992). Interaction of Nucleic Acids with Core-like and Subcore-like Particles of Bluetongue Virus. *Virology* 191, 231-236.

Luckow, V.A., Lee, S.C., Barry, G.F., and Olins, P.O. (1993). Efficient generation of infectious recombinant baculoviruses by site-specific transposon-mediated insertion of foreign genes into a baculovirus genome propagated in *Escherichia Coli*. *J. Virol*. 67, 4566-4579.

Lymperopoulos, K., Wirblich, C., Brierley, I., and Roy, P. (2003). Sequence specificity in the interaction of Bluetongue virus non-structural protein 2 (NS2) with viral RNA. *J. Biol. Chem*. 278, 31722 -30.

Mandel, M., and Higa A. (1970). Calcium-dependent bacteriophage DNA infection. *J Mol Biol*. 14; 53(1): 159-62.

Maree, S., Durbach, S., and Huismans, H. (1998). Intracellular production of African horsesickness virus core-like particles by expression of the two major core proteins, VP3 and VP7, in insect cells. *J Gen Virol*. 79 (Pt 2):333-7.

Maree, F.F. (2000). Multimeric Protein Structures of African Horse sickness Virus and their use as Antigen Delivery Systems. PHD Thesis, University of Pretoria, Pretoria.

Markotter, W., Theron, J., and Nel, L.H. (2004). Segment specific inverted repeat sequences in bluetongue virus mRNA are required for interaction with the virus non structural protein NS2. *Virus Res* 105, 1-9.

Martínez--Torrecuadrada, J.L., Iwata, H., Venteo, A., Casal, I., and Roy, P. (1994). Expression and Characterization of the Two Outer Capsid Proteins of African Horsesickness Virus: The role of VP2 in Virus Neutralization. *Virology* 202, 348-359.

Martínez--Torrecuadrada, J.L., Diaz-Laviada, M., Roy, P., Sanchez, C., Vela, C., Sanchez-Vizcaino, J. M., Casal, J. I. (1996). Full protection against African horsesickness (AHS) in horses induced by baculovirus-derived AHS virus serotype 4 VP2, VP5 and VP7. *J. Gen. Virology*. 77, (6) , 1211-1221.

Martínez-Torrecuadrada, J. L., Langeveld, J. P. M., Venteo, A., Sanz, A., Dalsgaard, K., Hamilton, W. D. O., Meloen, R. H., and Casal, J. I. (1999). Antigenic Profile of African Horse Sickness Virus Serotype 4 VP5 and Identification of a Neutralizing Epitope Shared with Bluetongue Virus and Epizootic Hemorrhagic Disease Virus. *Virology*, 257 (2), 449-459.

Martínez--Torrecuadrada, J. L., Langeveld, J. P. M., Meloen, R. H., and Casal, J. I. (2001). Definition of neutralising sites on African horse sickness virus serotype 4 VP2 at the level of peptides. *J. Gen. Virol.* 82, 2415-2424.

McMurry, J. and Castellion, M.E. (1996). *Fundamentals of General, Organic, and Biological Chemistry*, second edition. (New Jersey: Prentice Hall, Inc.)

Mellor, P.S. (1994). Epizootiology and vectors of African horse sickness virus. *Comp. Immun. Microbial. Infect. Dis.* 17, 287-296.

Mellor et al., (1998). *Archives of virology supplementum* 14, 337-342

Mellor, P.S., and Boorman, J. (1995). The transmission and geographical spread of African horse sickness and Blue-tongue virus. *Ann. Trop. Med. Parasit.* 89, 1-15.

Mertens, P.P.C., Brown, F., and Sangar, D.V. (1984). Assignment of the genome segments of Bluetongue virus type 1 to the proteins which they encode. *Virology* 135, 207-217.

Mertens, P.P., Pedley, S., Cowley, J., Burroughs, J.N., Corteyn, A.H., Jeggo, M.H., Jennings, D.M., and Gorman, B.M. (1989). Analysis of the roles of bluetongue virus outer capsid proteins VP2 and VP5 in determination of virus serotype. *Virology.* 170(2):561-5.

Mertens, P.P.C., Arella, M., Attoui, H., Belloncik, S., Bergoin, M., Boccardo, G., Booth, T.F., Chiu, W., Diprose, J.M., Duncan, R., Estes, M.K., Gorziglia, M., Gouet, P., Gould, A.R., Grimes, J.M., Hewat, E., Hill, C., Holmes, I.H., Hoshino, Y., Joklik, W.K., Knowles, N., López Ferber, M.L., Malby, R., Marzachi, C., McCrae, M.A., Milne, R.G., Nibert, M., Nunn, M., Omura, T., Prasad, B.V.V., Pritchard, I., Samal, S.K., Schoehn, G., Shikata, E., Stoltz, D.B., Stuart, D.I., Suzuki, N., Upadhyaya, N., Uyeda, I., Waterhouse, P., Williams, C.F., Winton, J.R., Zhou, H.Z., 2000. Reoviridae. In: M.H.V. Van Regenmortel, C.M. Fauquet, D.H.L. Bishop, C.H. Calisher, E.B. Carsten, M.K. Estes, S.M. Lemon, J. Maniloff, M.A. Mayo, D.J. McGeoch, C.R. Pringle, R.B. Wickner (Eds.), *Virus Taxonomy*. In: *Proceedings of the Seventh Report of the International Committee for the Taxonomy of Viruses*. Academic Press, New York, San Diego.

Mizukoshi, N., Sakamoto, K., Iwata, A., Tsuchiya, T., Ueda, S., Apiwatnakorn, B., Kamada, M., and Fukusho, A. (1993). The complete nucleotide sequence of African horsesickness virus serotype 4 (vaccine strain) segment 4, which encodes the minor core protein VP4. *Virus Res.* 28 (3): 299-306.



Old, R.W., and Primrose, S.B. (1995). Principles of Gene Manipulation. 5<sup>th</sup> Edition. (Blackwell Science Ltd, United Kingdom).

Oldfield, S., Hirasawa T., and Roy, P. (1991). Sequence conservation of the outer capsid protein, VP5, of bluetongue virus, a contrasting feature to the outer capsid protein VP2. *J. Gen. Virol.* 72, 449-451.

Parker, J.M.R., Guo, D., and Hodges, R.S., (1986). New hydrophilicity scale derived from high-performance liquid chromatography peptide retention data: Correlation of predicted surface residues with antigenicity and X-ray-derived accessible sites, *Biochem.* 25, 5425-5432

Perbal, B. (1998). A Practical guide to Molecular Cloning. 2<sup>nd</sup> Edition. (John Wiley and Sons, Inc., Canada).

Purdy, M.A., Ritter, G.D. and Roy, P. (1986). Nucleotide sequence of cDNA clones encoding the outer capsid protein, VP5, of bluetongue virus serotype 10. *J. Gen. Virol.* 67 (5), 957-962.

Prasad, B.V.V., Yamaguchi, S., and Roy, P. (1992). Three-dimensional structure of single-shelled Bluetongue Virus. *J. Virol.* 66, 2135-2142.

Rao, C.D., Kiuchi, A., and Roy, P. (1983). Homologous terminal sequences of the genome double-stranded RNAs of bluetongue virus. *J Virol.* 46(2): 378-383.

Riley, J. (2003), Construction of a new peptide insertion site in the top domain of major core protein VP7 of African horsesickness virus. MSC dissertation, University of Pretoria, Pretoria.

Rodriguez, R.L., and Tait, R.C. (1983). Recombinant DNA techniques: an introduction. (Massachusetts; Addison-Wesley publishing company, Inc).

Roitt, I., Brostoff, J., and Male, D. (1998). *Immunology: fifth edition.* (Mosby International Ltd).

Roy, P. (1989). Bluetongue virus genetics and genome structure. *Virus Res.* *13*, 179-206.

Roy, P. (1996). Orbivirus Structure and Assembly. *Virology* *216*, 1-11.

Roy, P., Adachi, A., Urakawa, T., Booth, T.F., and Thomas, C.P. (1990a). Identification of Bluetongue virus VP6 Protein as a nucleic Acid binding Protein and the localization of VP6 in Virus-infected Vertebrate cells. *J. Virology.* *64*, 1-8.

Roy, P., Urakawa, T., Van Dijk, A.A, and Erasmus, B.J. (1990b). Recombinant Virus Vaccine for Bluetongue Disease in sheep. *J. of Virology*, *64*; 1998-2003.

Roy, P., Hirasawa, T., Fernandez, M., Blinov, V.M., and Sanchez-Vixcain Rodrique, J.M. (1991). The complete sequence of the group specific antigen, VP7 of African horsesickness disease virus serotype 4 reveals a close relationship to Bluetongue virus. *J. Gen. Virol.* *72*, 1237-1241.

Roy, P., Mertens, P., and Casal, I. (1994). African Horse Sickness Virus Structure. *Comp. Immun. Microbiol. Infect. Dis.* *17*, 243-273.

Roy, P., Bishop, D. H. L., Howard, S., Aitchison, H., and Erasmus, B. (1996). Recombinant baculovirus-synthesized African horsesickness virus (AHSV) outer-capsid protein VP2 provides protection against virulent AHSV challenge. *J. Gen Virol.* vol. *77*, no. *9*, pp. 2053-2057.

Roy, P., and Sutton, G. (1998). New generation of African horse sickness virus vaccines based on structural and molecular studies of the virus particles. *Arch. Virol. Suppl.* *14*, 177-202.

Sakamoto, K., Mizukoshi, N., Apiwatnakorn, B., Iwata, A., Tsuchiya, T., Ueda, S., Imagawa, H., Sugiura, T., Kamada, M. and Fukusho, A. (1994). The complete sequences of African horsesickness virus serotype 4 (vaccine strain) RNA segment 2 and 6 which encode outer capsid protein. *J. Vet. Med. Sci.* 56 (2), 321-327

Sambrook, J., Fritsch, E.F., and Maniatis, T. (1989). *Molecular Cloning: A laboratory Manual*. (Cold Spring harbor, NY: Cold Spring harbor laboratory press).

Scalen, M., Paweska, J. T., Verskoor, J. A., and van Dijk, A. A. (2002). The protective efficacy of a recombinant VP2-based African horsesickness subunit vaccine candidate is determined by adjuvant. *Vaccine* 20, 1079-1088.

Stone-Marschat, M. A., Moss, S.R., Burrage, T. G., Barber, M. L., Roy, P., and Laegried, W.W. (1996). Immunization with VP2 is sufficient for Protection against Lethal Challenge with African Horsesickness Virus Type 4. *Virology* 220 (1), 219-22.

Strachan, T., and Read, A.P., (1997). *Human Molecular Genetics*. (BIOS Scientific Publishers Limited; Oxford UK.)

Thomas, C.P., Booth, T.F., and Roy, P. (1990). Synthesis of bluetongue virus-encoded phosphoprotein and formation of inclusion bodies by recombinant baculovirus in insect cells: it binds the single-stranded RNA species. *J. Gen. Virol.* 71, 2073-2083.

Urbano, P., and Urbano, F.G. (1994). The *Reoviridae* family. *Comp. Immun. Microbial. Infect. Dis.* 17; 151-161.

Van Niekerk, M., Smit C.C., Fick, W.C., van Staden, V., and Huismans, H. (2001a). Membrane association of African horsesickness virus nonstructural protein NS3 determines its cytotoxicity. *Virology* 279, 499-508.

Van Niekerk, M., van Staden, V., van Dijk, A.A., and Huismans, H (2001b). Variation of African horsesickness virus nonstructural protein NS3 in southern Africa. *J. Virology* 82, 149-158.

Van Rensburg, R. (2004). Construction and structural evaluation of Viral Protein 7 of African horse sickness virus as a particulate, multiple peptide vaccine delivery system. MSC dissertation, University of Pretoria, Pretoria.

Van Staden, V., and Huismans, H. (1991). A comparison of the genes which encode non-structural protein NS3 of different orbiviruses. *J. Gen. Virol.* 72, 1073-1079.

Van Staden, V., Smit C.C., Stoltz, M.A., Maree, F.F., and Huismans, H. (1998). Characterization of two African horse sickness virus non-structural proteins, NS1 and NS3. *Arch. Virol. Suppl.* 14, 251-258.

Verwoerd, D.W., and Huismans, H. (1972). Studies on the *in vitro* and the *in vivo* transcription of the bluetongue virus genome. *Onderstepoort J. Vet. Res.* 359 (4), 185-192.

Verwoerd, D.W., Els, H., de Villiers, E., and Huismans, H. (1972). Structure of the Bluetongue virus capsid. *J. Virol.* 10 (4), 783-794.

Von Heijne, G. (1992). Membrane protein structure prediction. Hydrophobicity analysis and the positive-inside rule. *J. Mol. Biol.* 8, 249-254

Vreede, F.T., and Huismans, H. (1994). Cloning, characterisation and expression of the gene that encodes the major neutralization-specific antigen of African horsesickness virus serotype 3. *J. Gen. Virol.* 75 (12), 3629-3633.

Vreede, F.T., and Huismans, H. (1998). Sequence analysis of the RNA polymerase gene of African horse sickness virus. *Arch. of Viol.* 143, 413-419.

Wade-Evans, A.M., Pullen, L., Hamblin, C., O'Hara, R.S., Burroughs, J.N., and Mertens, P.P.C. (1998). VP7 from African Horse sickness virus serotype 9 protects mice against lethal heterologous serotype challenge. *Arch. of Viol.* 14: 211-9.

Welling, G.W., Weijer, W.J., van der Zee, R., and Welling-Wester, S. (1985). Prediction of sequential antigenic regions in proteins. *FEBS Lett.* 188(2): 215-8

Williams, C. F., Inoue, T., Lucas, A., Zanotto P. M. de A., and Roy, P. (1998). The complete sequence of four major structural proteins of African horse sickness virus serotype 6: evolutionary relationships within and between the orbiviruses. *Virus Res.* 53 (1), 53-73.

Wu, X., Chen, S., Iwata, H., Compans, R.W., and Roy, P. (1992). Multiple Glycoproteins Synthesized by the Smallest RNA Segment (S10) of Bluetongue Virus. *J. Virology* 66, 7104-7112.